ตัวเร่งปฏิกิริยาแคลเซียมออกไซด์ที่มีรูพรุนจากเปลือกหอยแมลงภู่สำหรับการผลิตไบโอดีเซล

นายกรกฎ นิยมสัตย์



วิทยานิพนธ์นี้เป็นส่วนหนึ่งของการศึกษาตามหลักสูตรปริญญาวิทยาศาสตรมหาบัณฑิต
สาขาวิชาเคมี ภาควิชาเคมี
คณะวิทยาศาสตร์ จุฬาลงกรณ์มหาวิทยาลัย
ปีการศึกษา 2557

# POROUS CALCIUM OXIDE CATALYSTS FROM GREEN-MUSSEL SHELLS FOR BIODIESEL PRODUCTION

Mr. Korakot Niyomsat


A Thesis Submitted in Partial Fulfillment of the Requirements
for the Degree of Master of Science Program in Chemistry
Department of Chemistry
Faculty of Science
Chulalongkorn University
Academic Year 2014

| | |
|---|---|
| Thesis Title | POROUS CALCIUM OXIDE CATALYSTS FROM GREEN-MUSSEL SHELLS FOR BIODIESEL PRODUCTION |
| By | Mr. Korakot Niyomsat |
| Field of Study | Chemistry |
| Thesis Advisor | Numpon Insin, Ph.D. |
| Thesis Co-Advisor | Duangamol Tungasmita, Ph.D. |

Accepted by the Faculty of Science, Chulalongkorn University in Partial Fulfillment of the Requirements for the Master's Degree

.....Dean of the Faculty of Science
(Professor Supot Hannongbua, Dr.rer.nat.)

THESIS COMMITTEE

.....Chairman
(Assistant Professor Somsak Pianwanit, Ph.D.)

.....Thesis Advisor
(Numpon Insin, Ph.D.)

.....Thesis Co-Advisor
(Duangamol Tungasmita, Ph.D.)

.....Examiner
(Aticha Chaisuwan, Ph.D.)

.....Examiner
(Associate Professor Sanong Ekgasit, Ph.D.)

.....External Examiner
(Anurak Winitsorn, Ph.D.)

กรกฎ นิยมสัตย์ : ตัวเร่งปฏิกิริยาแคลเซียมออกไซด์ที่มีรูพรุนจากเปลือกหอยแมลงภู่สำหรับการผลิตไบโอดีเซล (POROUS CALCIUM OXIDE CATALYSTS FROM GREEN-MUSSEL SHELLS FOR BIODIESEL PRODUCTION) อ.ที่ปรึกษาวิทยานิพนธ์หลัก: อ. ดร. นำพล อินสิน, อ.ที่ปรึกษาวิทยานิพนธ์ร่วม: อ. ดร. ดวงกมล ตุงคะสมิต, 112 หน้า.

ในงานวิจัยนี้ ได้ศึกษาปฏิกิริยาทรานส์เอสเทอริฟิเคชันของน้ำมันปาล์มบริสุทธิ์ร่วมกับเมทานอลโดยใช้ตัวเร่งปฏิกิริยาที่ได้แปรรูปมาจากเปลือกหอยแมลงภู่เหลือทิ้งเป็นวัตถุดิบ ตัวเร่งปฏิกิริยาถูกสังเคราะห์โดยการเผาโดยตรงของแคลเซียมคาร์บอเนต ($CaCO_3$) บริสุทธิ์ซึ่งเป็นองค์ประกอบหลักของเปลือกหอยแมลงภู่ที่อุณหภูมิ 900 องศาเซลเซียส ($^{o}C$) เป็นเวลา 5 ชั่วโมง ได้ตรวจสอบสมบัติของตัวเร่งปฏิกิริยาที่สังเคราะห์ได้ เช่น ลักษณะทางสัณฐานวิทยา, พื้นที่ผิวจำเพาะและโครงสร้างผลึกโดยใช้เทคนิคการเลี้ยวเบนของรังสีเอ็กซ์ (XRD), ฟูเรียร์ทรานสฟอร์มอินฟราเรดสเปกโทรสโกปี (FTIR), จุลทรรศน์อิเล็กตรอนแบบส่องกราดชนิดฟิลด์อิมิสชัน (FESEM), เทคนิคเอกซ์เรย์โฟโตอิเล็กตรอนสเปกโตรสโกปี (XPS), การวัดพื้นที่ผิวโดยวิธีบรูนัวร์-เอ็มเม็ตต์-เทลเลอร์ (BET) และการวัดการดูดซับ-คายแก๊สไนโตรเจน นอกจากนี้แคลเซียมออกไซด์ (CaO) ถูกเปลี่ยนไปอยู่ในรูปของแคลเซียมไฮดรอกไซด์ ($Ca(OH)_2$) โดยผลที่แสดงจาก XRD ภายหลังที่มีการปรับปรุง CaO โดยใช้วิธีไฮเดรชัน (hydration method) ด้วยน้ำที่ปราศจากไอออนปริมาณเล็กน้อย ปริมาณของตัวเร่งปฏิกิริยา CaO-EGMShell ที่ 4 % และ $Ca(OH)_2$-EGMShell ที่ 3 % โดยน้ำหนักมีความสามารถในการเรงปฏิกิริยาที่ดีภายใต้สภาวะที่เหมาะสมของอัตราส่วนโดยโมลของเมทานอลต่อน้ำมันเท่ากับ 1:6, อุณหภูมิที่ใช้ในการทำปฏิกิริยาเท่ากับ 64 ± 1 $^{o}C$ ที่อัตราการปั่นกวนคงที่ 700 รอบต่อนาที (rpm) สำหรับการสังเคราะห์ไบโอดีเซล อัตราการเปลี่ยนไปไบโอดีเซลมีค่ามากกว่าร้อยละ 98 และปริมาณผลิตภัณฑ์ของไบโอดีเซลมีค่าร้อยละ 97 ได้จากการทำปฏิกิริยาที่ระยะเวลา 2.5 ชั่วโมง นอกจากนี้ตัวเร่งปฏิกิริยา CaO-EGMShell และ $Ca(OH)_2$-EGMShell สามารถนำกลับมาใช้ซ้ำ 5 ครั้ง และ 3 ครั้ง ตามลำดับ โดยไม่มีการเสื่อมสภาพในการเร่งปฏิกิริยาหรือร้อยละอัตราการเปลี่ยนไปเป็นไบโอดีเซลมีค่าสูงกว่าร้อยละ 90 นอกจากนี้ในงานวิจัยนี้ได้ไบโอดีเซลที่มีปริมาณเอสเทอร์สูงกว่าร้อยละ 97 ซึ่งเป็นไปตามมาตรฐานยุโรป EN14103

| | |
|---|---|
| ภาควิชา เคมี | ลายมือชื่อนิสิต ..... |
| สาขาวิชา เคมี | ลายมือชื่อ อ.ที่ปรึกษาหลัก ..... |
| ปีการศึกษา 2557 | ลายมือชื่อ อ.ที่ปรึกษาร่วม ..... |

# # 5571908423 : MAJOR CHEMISTRY
KEYWORDS: BIODIESEL / CALCIUM OXIDE CATALYST / CALCIUM HYDROXIDE CATALYST / GREEN-MUSSEL SHELL / TRANSESTERIFICATION

KORAKOT NIYOMSAT: POROUS CALCIUM OXIDE CATALYSTS FROM GREEN-MUSSEL SHELLS FOR BIODIESEL PRODUCTION. ADVISOR: NUMPON INSIN, Ph.D., CO-ADVISOR: DUANGAMOL TUNGASMITA, Ph.D., 112 pp.

In this research, the transesterification of refined palm oil with methanol was studied using catalysts derived from waste green-mussel shells as a raw material. The catalysts were synthesized by direct calcination of pure $CaCO_3$, a major component of green-mussel shells, at 900 °C for 5 h. The properties of the synthesized catalyst such as morphology, specific surface area and the structure of crystalline phase were characterized using X-ray powder diffractometer (XRD), Fourier transform infrared spectroscopy (FTIR), Field emission scanning electron microscopy (FSEM), Brunauer-Emmett-Teller (BET) surface area analysis and $N_2$ adsorption-desorption measurement. Moreover, the CaO were converted to $Ca(OH)_2$ phase as indicated from the XRD results after the modification of CaO using hydration method in a little amount of deionized water. The 4 wt. % of CaO-EGMShell and 3 wt. % of $Ca(OH)_2$-EGMShell amounts of catalyst showed good catalytic activities under the optimum condition of methanol to oil molar ratio of 1:6, reaction temperature of 64 ± 1 °C at constant speed agitation of 700 rpm for the synthesis of biodiesel. The conversion exceeding 98 % and 97 % yield of biodiesel were obtained when the reaction was carried out for 2.5 h. Furthermore, the CaO-EGMShell and $Ca(OH)_2$-EGMShell catalysts were able to be reused up to 5 and 3 cycles, respectively without deterioration in its activity with the biodiesel conversion above 90 %. Besides, the biodiesels with the ester content of over 97 % in this work are in accordance with the European standard, EN 14103.

| | | | |
|---|---|---|---|
| Department: | Chemistry | Student's Signature | ..... |
| Field of Study: | Chemistry | Advisor's Signature | ..... |
| Academic Year: | 2014 | Co-Advisor's Signature | ..... |

# ACKNOWLEDGEMENTS

This dissertation would not have been accomplished without the considerable assistance of the following persons and organizations:

I would like to express my sincerest gratitude and appreciation to my advisors Dr. Numpon Insin and my co-advisors, Dr. Duangamol Tungasmita for their excellent supervision, inspiring guidance and encouragement throughout this research. Especially, I would like to extend my appreciation to Assist.Prof. Dr. Somsak Pianwanit, Assoc.Prof. Dr. Sanong Ekgasit, Dr. Aticha Chaisuwan and Dr. Anurak Winitson for serving as chairman and members of thesis committee, respectively.

The author wishes to express his thankfulness to all people in the associated institutions for their kind assistance and collaboration.

I would like to give my special thanks to the funding support from the 90th Anniversary of Chulalongkorn University Fund (Ratchadaphiseksomphot Endowment Fund).

Finally, I would like to give a heartfelt thanks to my family for their love, support, empathetic and encouragement throughout graduate study.

**CONTENTS**

Page

THAI ABSTRACT ..... iv

ENGLISH ABSTRACT ..... v

ACKNOWLEDGEMENTS ..... vi

CONTENTS ..... vii

LIST OF TABLES ..... xii

LIST OF FIGURES ..... xiv

LIST OF ABBREVIATIONS ..... 1

CHAPTER I INTRODUCTION ..... 2

1.1 Statement of Problems ..... 2

1.2 Objectives ..... 4

1.3 Scopes of this research ..... 4

CHAPTER II THEORY AND LETERATURE REVIEWS ..... 6

2.1 Transesterification reaction ..... 6

2.2 Natural calcium carbonate ($CaCO_3$) sources for the synthesis of CaO as catalysts ..... 6

2.3. Important benefits of natural calcium oxide derived from waste shells. ..... 8

2.4 Mechanism of transesterification reaction using CaO as catalyst ..... 11

2.4.1 In the systems without water ..... 11

2.4.2 In the system with the addition of a small quantity of water ..... 12

2.5 Literature review ..... 16

CHAPTER III EXPERIMENTAL ..... 19

3.1 Instruments ..... 19

Page

3.1.1 The instruments for characterization and analysis $CaCO_3$-precursor and CaO catalyst from waste green-mussel shell.....19

3.1.2 The instruments for analysis of the synthesized biodiesel.....20

3.2 Materials and chemicals.....20

3.3 Experimental process.....22

3.3.1 Preparation calcium carbonate from green-mussel shell (GMShell) ...22

3.3.2 Preparation calcium carbonate from green-mussel shell after purification ($CaCO_3$-EGMShell).....22

3.3.3 Preparation calcium carbonate by co-precipitate method ($CaCO_3$-CoGMShell).....23

3.4 Synthesis of CaO catalyst from $CaCO_3$-precursor.....24

3.5 Pretreatment of CaO catalyst for high active catalytic activity.....24

3.6 Characterization of $CaCO_3$-percursor and CaO catalyst.....24

3.7 Synthesis and characterization of the biodiesel products.....25

3.7.1 Optimization for the synthesized CaO catalyst from different $CaCO_3$-precursor in transesterification reaction.....25

3.7.2. Effect of calcination time.....26

3.7.3 Effect of amount of CaO catalyst.....26

3.7.4 Effect of mole ratio of oil to methanol.....27

3.7.5 Effect of reaction temperature.....27

3.7.6 Effect of agitation speed.....27

3.7.7 Effect of reaction time.....27

3.7.8 Effect of water loading amount.....28

3.7.9 Reusability of CaO catalyst.....28

Page

3.7.10 Comparison of catalytic activity of CaO catalysts from different $CaCO_3$-precursors....29

3.8 Characterization of synthesized biodiesels....29

3.8.1 Proton nuclear magnetic resonance ($^1$H-NMR) analysis....29

3.8.2 Gas chromatography (GC) technique....30

3.8.2.1 Determination of ester content in biodiesel by using EN14103....30

3.8.2.2 Determination of glycerin (EN14105)....31

CHAPTER IV RESULTS AND DISCUSSION....32

4.1 Processing for preparation of $CaCO_3$ precursors....32

4.1.1 Elimination of organic matter on green mussel shell surface....32

4.1.2 Purification of green mussel shell surface after eliminating impurities....33

4.2 Characterization of $CaCO_3$ precursor and CaO catalyst using green mussel shells as raw material....34

4.2.1 Fourier transforms infrared (FTIR) spectroscopy....34

4.2.2 X-ray powder diffraction (XRD)....39

4.3. Percent yield (% yield) of $CaCO_3$-precursors and CaO catalysts....42

4.4 The basic strength of CaO catalysts as investigated using various Hemmett indicators....43

4.4 Surface properties of CaO-EGMShell catalyst from green-mussel shell....45

4.5 Adsorption-desorption isotherms of catalysts from green-mussel shell....47

4.6 Morphological studies using FESEM technique....49

Page

4.6.1 FESEM images of $CaCO_3$-precursor from natural and eliminated residue on surface of green-mussel shell .....49

4.6.2 FESEM images of CaO from natural after elimination of residues on surface of green-mussel shell after calcination at 900 °C for 5 h.....50

4.7 Physical properties of refined palm oil .....51

4.8 Influences of parameters on catalytic activity of CaO catalysts in transesterification.....52

4.8.1 Effect of optimized conditions for synthesis of biodiesel using different types of CaO catalysts.....52

4.8.2 Effect of calcination temperature of CaO-EGMShell catalyst.....54

4.8.3 Effect of calcination time of CaO-EGMShell catalyst .....56

4.8.4 Effect of amount of CaO catalyst loaded on % conversion.....57

4.8.5 Effect of methanol to oil molar ratio on % conversion .....59

4.8.6 Effect of reaction temperature on % conversion .....60

4.8.7 Effect of water loaded on % conversion.....61

4.8.8 Effect of agitation speed on % conversion .....63

4.8.9 Effect of reaction time on % conversion.....65

4.8.10 Reusability of CaO-EGMShell catalyst .....66

4.9 The chemical properties of the synthesized biodiesel using CaO-EGMShell catalyst.....69

4.10 Physical properties of modified $Ca(OH)_2$ from CaO precursor.....70

4.11 FESEM images of modified CaO-EGMShell catalyst .....71

4.12 Transmission electron microscopy (TEM).....72

4.13 Catalyst activity of $Ca(OH)_2$-EGMShell catalyst in transesterification .....73

Page

4.13.1 Effect of amount of $Ca(OH)_2$-EGMShell catalyst loaded on % conversion....73

4.13.2 Effect of methanol to palm oil molar ratio on the synthesis of biodiesel....75

4.13.3 Effect of reaction temperature on % conversion....76

4.13.4 Effect of agitation speed on % conversion....78

4.13.5 Effect of reaction time on % conversion....79

4.13.6 Reusability of $Ca(OH)_2$-EGMShell catalyst....80

4.13.7 Comparison of catalytic activities in transesterification of different catalysts....83

4.14 The chemical properties of the synthesized biodiesel using $Ca(OH)_2$-EGMShell catalyst....84

CHAPTER V CONCLUSION....85

5.1 Conclusion....85

5.2 Suggestion....86

REFERENCES....87

VITA....112

## LIST OF TABLES

**Table 2.1** Heterogeneous catalysts derived from different natural resources in the transesterification of different oils to biodiesel.....9

**Table 2.2** Heterogeneous catalysts derived from different natural resources in the transesterification of different oils to biodiesel (continued) .....10

**Table 3.1** List of characterization and analytical instruments.....19

**Table 3.2** List of instruments .....20

**Table 3.3** List of chemicals.....20

**Table 3.4** List of chemicals (continued).....21

**Table 3.5** The GC condition for determination ester content in synthesized biodiesel according EN 14103 method.....30

**Table 3.6** The GC conditions for the determination of glycerol residue content in synthesized biodiesel according to the EN 14105 method.....31

**Table 4.1** Comparison of % yield $CaCO_3$-precursor.....42

**Table 4.2** Comparison of % yield of CaO from different $CaCO_3$-precursor after calcination under 900 $^{o}$C for 5 h.....42

**Table 4.3** List of Hammett indicators used as references in this work .....43

**Table 4.4** The results of basic strength of CaO-GSMShell catalyst determined by Hammett indicator method .....44

**Table 4.5** The results of basic strength of the CaO-EGSMShell catalyst determined by Hammett indicator method.....44

**Table 4.6** Surface properties of adsorbents using BET method. .....45

**Table 4.7** The BET surface area of CaO catalyst from previous reports .....46

**Table 4.8** Properties of refined palm oil used in the present study .....51

**Table 4.9** Effect of amount of catalyst loaded on the yield of production ...58

**Table 4.10** The optimal condition for biodiesel production .....69

**Table 4.11** Properties of the synthesis biodiesel production .....69

**Table 4.12** Physical property of $Ca(OH)_2$ catalyst .....70

**Table 4.13** Effect of quantity of $Ca(OH)_2$-EGMShell catalyst on the yield of production .....74

**Table 4.14** Effect of methanol to oil molar ratio on the yield of production ..76

**Table 4.15** The yield of production of the reused $Ca(OH)_2$-EGMShell catalyst 81

**Table 4.16** Surface properties of $Ca(OH)_2$-EGMShell catalyst .....81

**Table 4.16** Surface properties of $Ca(OH)_2$-EGMShell catalyst (continued) .....82

**Table 4.17** Analyses of the biodiesel obtained at the optimal condition .....84

**Table 4.18** Properties of the synthesis biodiesel production .....84

**Table B1** Value of free fatty acids contain in refined palm oil. ..... 103

**Table B2** Saponification value of refined palm oil..... 104

## LIST OF FIGURES


**Figure 2.1** Hierarchical structures (5 levels) of the abalone nacre from nano, micro, meso to the structural length scales. .....7

**Figure 2.2** Dissociation pressure and temperature of $CaCO_3$. .....8

**Figure 2.3** A mechanism for CaO-catalyzed transesterification. .....11

**Figure 2.4** Mechanism between triglyceride and methanol in transesterification using CaO as catalyst .....12

**Figure 3.1** Apparatus set-up for the synthesis of biodiesel. .....25

**Figure 4.1** Green mussel shells (A) before and (B) after removal of impurities with 1 % w/v NaOH solution using a hydrothermal method. .....32

**Figure 4.2** Green mussel shells (A) before and (B) after treated with 0.5 M HCl solution. .....33

**Figure 4.3** Powders of green mussel shells (A) before and (B) after treated with 0.5 M HCl solution. .....33

**Figure 4.4** FTIR spectra of green mussel shells (A) $CaCO_3$-GMShell and (B) $CaCO_3$-EGMShell. .....34

**Figure 4.5** FTIR spectra of treated green mussel shells (A) $CaCO_3$-EGMShell and (B) CaO-EGMShell. .....35

**Figure 4.6** FTIR spectra of products from $CaCO_3$-precursor after calcination 900°C for 5 h (A) CaO-GMShell from $CaCO_3$-GMShell, (B) CaO-EGMShell from $CaCO_3$-EGMShell and (C) commercial CaO as standard. .....36

**Figure 4.7** FTIR spectra of (A) treated CaO-EGShell and (B) commercial $Ca(OH)_2$ as standard. .....37

**Figure 4.8** FTIR spectra of (A) Natural residue of organic matrix and (B) residue of CaO-EGMShell after calcination at 900 °C for 5 h. .....38

**Figure 4.9** XRD patterns for (A) $CaCO_3$-GMShell and (B) $CaCO_3$-EGMShell from green-mussel shell.....39

**Figure 4.10** XRD patterns of $CaCO_3$-EGMShell from green-mussel shells that were calcined at different temperatures from 600 to 1000 $^{o}$C.....40

**Figure 4.11** XRD patterns of (A) CaO-EGMShell (B) Commercial $Ca(OH)_2$ used as standard and (C) $Ca(OH)_2$ from CaO-GMShell.....41

**Figure 4.12** Adsorption isotherm of $CaCO_3$-EGMShell when P: Pressure, $P_0$: Pressure saturated. .....47

**Figure 4.13** Adsorption isotherm of CaO-EGMShell when P: Pressure, $P_0$: Pressure saturated. .....48

**Figure 4.14** Adsorption isotherm of $Ca(OH)_2$-EGMShell when P: Pressure, $P_0$: Pressure saturated. .....48

**Figure 4.15** SEM images of (A).and (B) $CaCO_3$-GMShell; and (C) and (D) $CaCO_3$-EGShell. .....49

**Figure 4.16** SEM images of (A).and (B). $CaCO_3$-GMShell and (C) and (D) $CaCO_3$-EGMShell after calcination at 900 $^{o}$C for 5 h.....50

**Figure 4.17** A photograph of refined palm oil from the Olein co, th. Thailand used as a raw material.....51

**Figure 4.18** Effect of different types of CaO catalysts on the conversion of palm oil under the reaction condition of methanol to oil molar ratio; 12:1, reaction temperature, 64 ± 1 $^{o}$C, reaction time of 0-4 h and constant agitation speed at 500 rpm.....52

**Figure 4.19** Effect of calcination temperature on the conversion of palm oil using CaO-GMShell catalyst with the reaction condition of methanol to oil molar ratio of 12:1, reaction temperature of 64 ±1 $^{o}$C, reaction time of 2 h and agitation speed at 500 rpm.....54

**Figure 4.20** The powdery solid products after calcination at (A) 600 °C, (B) 700 °C, (C) 800 °C, (D) 900 °C and (E) 1000 °C. .....55

**Figure 4.21** Effect of calcination time on conversion of palm oil using CaO-GMShell catalyst. Reaction condition were 10 wt. % catalyst, methanol to oil molar ratio of 12:1, reaction temperature at 64 ± 1 °C, reaction time for 2 h and agitation speed at 500 rpm. .....56

**Figure 4.22** Effect of amount of catalyst loaded on conversion of palm oil using CaO-EGMShell catalyst. Reaction condition of methanol to oil molar ratio of 6:1, reaction temperature of 64 ± 1 °C, reaction time of 2 h and agitation speed at 500 rpm. .....57

**Figure 4.23** Effect of methanol to oil molar ratio on conversion of palm oil using CaO-EGMShell catalyst. Reaction condition were 4 wt. % catalyst, reaction temperature at 64 ± 1 °C, reaction time for 2 h and agitation speed at 500 rpm. .....59

**Figure 4.24** Effect of reaction temperature on conversion of palm oil by using CaO-EGMShell catalyst. Reaction condition were 4 wt. % catalyst, methanol to oil molar ratio of 6:1, reaction time for 2 h and agitation speed at 500 rpm. .....61

**Figure 4.25** Effect of amount of water loaded on conversion rate of palm oil using CaO-GMShell catalyst. Reaction condition were 4 wt. % catalyst, methanol to oil molar ratio of 6:1, reaction temperature at 64 ± 1 °C, reaction time for 2 h and agitation speed at 500 rpm. .....62

**Figure 4.26** Effect of agitation speed on conversion rate of palm oil using CaO-GMShell catalyst. Reaction condition were 4 wt. % catalyst, methanol to oil molar ratio of 6:1, reaction temperature at 64 ± 1 °C, reaction time for 2 h. .....63

**Figure 4.27** Photograph of the mixtures of product and CaO-EGMShell catalyst after the reaction finished (A) before and (B) after the separation of CaO-EGMShell catalyst. .....64

**Figure 4.28** Effect of reaction time on conversion rate of palm oil by using CaO-EGMShell catalyst. Reaction condition were 4 wt. % catalyst, methanol to oil molar ratio of 6:1, reaction temperature of 64 ± 1 $^{o}$C and constant agitation speed at 700 rpm. .....65

**Figure 4.29** Effect of reusing of catalyst on conversion of palm oil using CaO-GMShell catalyst. Reaction condition were 4 wt. % catalyst, methanol to oil molar ratio of 6:1, reaction temperature at 64 ± 1 $^{o}$C, reaction time for 2 h and agitation speed at 700 rpm. .....67

**Figure 4.30** FESEM images of (A) and (B) fresh CaO-EGMShell catalyst, (C) and (D) reused CaO-EGMShell catalyst for 4 cycles. .....68

**Figure 4.31** XRD patterns of (A) CaO-EGMShell (B) Commercial $Ca(OH)_2$ used as standard and (C) $Ca(OH)_2$ from CaO-GMShell. .....70

**Figure 4.32** FESEM images of (A) and (B) Fresh CaO-EGMShell catalyst, (C) and (D) $Ca(OH)_2$-EGMShell catalyst.....71

**Figure 4.33** TEM images of (A) and (B) fresh CaO-EGMShell catalyst; (C) and (D) $Ca(OH)_2$-EGMShell catalyst.....72

**Figure 4.34** Effect of amount of catalyst loaded on % conversion of palm oil using $Ca(OH)_2$-EGMShell catalyst. Reaction condition were methanol to oil molar ratio of 6:1, reaction temperature of 64 ± 1 $^{o}$C, reaction time of 2.5 h and agitation speed at 700 rpm. .....73

**Figure 4.35** Effect of methanol to oil molar ratio on conversion rate of palm oil using $Ca(OH)_2$-EGMShell catalyst. Reaction condition were 3 wt. % catalyst, reaction temperature of 64 ± 1 $^{o}$C, reaction time of 2.5 h and agitation speed at 700 rpm. .....75

**Figure 4.36** Effect of reaction temperature on conversion of palm oil using $Ca(OH)_2$-EGMShell catalyst. Reaction condition were 3 wt. % catalyst, methanol to oil molar ratio of 6:1, reaction temperature of 64 ± 1 °C, reaction time of 2.5 h and agitation speed at 700 rpm. ....77

**Figure 4.37** Effect of agitation speed on conversion of palm oil using $Ca(OH)_2$-EGMShell catalyst. Reaction condition were 3 wt. % catalyst, methanol to oil molar ratio of 6:1, reaction temperature of 64 ± 1 °C, reaction time of 2.5 h. ....78

**Figure 4.38** Effect of reaction time on conversion of palm oil using $Ca(OH)_2$-EGMShell catalyst. Reaction condition were 3 wt. % catalyst, methanol to oil molar ratio of 6:1, reaction temperature of 64 ± 1 °C and agitation speed at 700 rpm. ....79

**Figure 4.39** Effect of reusing of catalyst on conversion rate of palm oil using $Ca(OH)_2$-EGMShell catalyst. Reaction condition were 3 wt. % catalyst, methanol to oil molar ratio of 6:1, reaction temperature of 64 ± 1 °C and agitation speed at 700 rpm. ....80

**Figure 4.40** SEM image of A), B) fresh $Ca(OH)_2$-EGMShell catalyst and C), D) reused $Ca(OH)_2$-EGMShell catalyst at cycle 5 after separated from the reaction mixtures....82

**Figure 4.41** Comparison of catalyst activites with the reaction condition of 3 wt. % catalyst, methanol/oil molar ratio of 6:1, reaction temperature of 64 ± 1 °C and agitation speed of 700 rpm for 2.5 h. ....83

**Figure A1** $^1$H-NMR spectrum of triglyceride from refined palm oil. ....97

**Figure A2** $^1$H-NMR spectrum of fatty acid methyl ester (FAME) from refined palm oil. ....98

**Figure A3** GC chromatogram of 37 FAME stand. ....99

**Figure A4** GC chromatogram of palm oil methyl ester. ..... 100

**Figure A5** GC chromatogram of standard for EN 14105 methid. ..... 101

**Figure C1** Mechanism between triglyceride and methanol in transesterification using CaO-EGMshell as catalyst. ..... 109

**Figure C2** Mechanism between triglyceride and methanol in transesterification using $Ca(OH)_2$-EGMshell as catalyst. ..... 110

## LIST OF ABBREVIATIONS

| | |
|---|---|
| XRD | X -ray powder diffraction |
| BET | Brunauer-Emmett-Teller method |
| GC | Gas chromatography |
| FT-IR | Fourier-transform infrared spectroscopy |
| TGA | Thermogravimetric analysis |
| wt. % | Percent by weight |
| % yield | Percent yield |
| % conversion rate | Percent conversion rate |
| h | Hour (s) |
| $^{\circ}$C | Degree Celsius |
| P | Pressure |
| mL | Milliliter |
| g | Gram |
| V | volume |
| $cm^{-1}$ | unit of wave number |
| EN | European Standards |
| ASTM | American Standard Test Method |
| FFA | Free fatty acid |
| FAME | Free Fatty Acid Methyl Esters |
| FID | Flame Ionization Detector |
| RMP | Revolution per minute |
| µL | Microliter |
| NMR | Nuclear Magnetic Resonance |
| XPS | X-ray photoelectron spectroscopy |
| nm | Nanometer |
| Å | Angstrom |

# CHAPTER I

# INTRODUCTION

## 1.1 Statement of Problems

Nowadays, the energy crisis is considered as one of the most important problems worldwide. One approach for solving this problem has been focused on the reduction of using petroleum from natural sources and replacing it by using other alternative energy sources such as $H_2$ [1, 2], biomass [3], solar energy [4], wind energy [5] and hydropower or water energy [6, 7], etc. Furthermore, biodiesel [8-10], an alternative to petroleum-based fuel, is one of the most interesting alternative fuels that can be conveniently produced from renewable sources. Other than renewable sources, the advantages of biodiesel are preponderant lubricity, high flash point, high cetane number, less free aromatics and sulfur compounds in composition, high biodegradability, environmental friendly, and lower emissions carbon dioxide ($CO_2$) as greenhouse gases and particulate matter. Generally, biodiesel is currently synthesized from vegetable oils [11] and animal fats [12], which contain triglyceride as essential components. Transesterification, so-called alcoholysis [13], is the process widely used for the production of biodiesel from triglyceride with alcohols of small molecules, such as methanol, ethanol and other alcohols with short carbon chains.

The transesterification process requires acids or bases in forms of homogenous or heterogeneous catalyst to promote the reactions. In industries, sodium hydroxide (NaOH) and potassium hydroxide (KOH) in the form of homogenous base catalysts were commonly used for producing biodiesel because of quickly completed reaction at short time and lower temperature [14]. However, the problem of the process using these catalyst systems is that it generates a large of wastewater from washing process to remove homogenous catalysts in product mixture layers at separation and purification process of biodiesel product [15] and non-reusability of this catalyst after the reaction finished. To avoid these restrictions of this catalyst system, several heterogeneous catalysts have been employed in the transesterification such

as magnesium oxide (MgO) [16], calcium oxide (CaO) [17], zinc (II) oxide (ZnO) [18] and hydrotalcites [19]. The benefits of heterogeneous base catalysts are that they have higher catalytic efficiency, easily separation, and decrease in the amount of water used for purification of biodiesel. Moreover, these catalysts can be reused for several cycles.

CaO is easily generated by using calcium carbonate ($CaCO_3$), calcium nitrate ($Ca(NO_3)_2$), calcium hydroxide ($Ca(OH)_2$), calcium acetate ($(CH_3COO)_2Ca$) and calcium oxalate ($Ca(COO)_2$) as raw materials [11]. $CaCO_3$, an environmentally-friendly, is major source for the production of CaO. In Thailand $CaCO_3$ are abundant in form of natural rocks such as lime stone and animal skeleton as egg shells, oyster shells, green-mussel shells, mollusk shells and bones.

The abundant of green mussel shells and high purity source of calcium carbonate are two major advantages that lead us to be interested in study the catalytic properties of calcium oxide produced by green-mussel shells. The green mussel shells were found in several areas of Thailand and, in fact, sea food industries in Thailand produce waste green-mussel shell of several tons [20, 21] a day. Besides, green mussel shell are $CaCO_3$ source of high purity. Therefore, $CaCO_3$ from the green mussel shells are used to produce CaO using directly calcination at high temperature as shown in Equation (1) [22] below,



$$CaCO_{3\,(s)} \xrightarrow{\Delta} CaO_{(s)} + CO_{2\,(g)} \quad (1)$$

The advantages of CaO are high basicity, high surface area, low solubility in methanol easy separation from the system, and low cost. Recently, many researchers studied CaO catalysts using waste mollusk skeleton as raw materials to produce biodiesel [23].

In this research, we focus on synthesized and modified CaO from green-mussel shell, wasted from food industry, using direct calcination at high temperature. Then, CaO was used as a catalyst to synthesis biodiesel from refined palm oil and methanol via transesterification reaction. The physical properties of natural and after calcination of green mussel shell were investigated by characterizations using various techniques including Fourier transform infrared spectroscopy (FTIR), X-ray Powder

Diffraction (XRD), Field-Emission Scanning Electron Microscopy (FESEM), Transmission Electron Microscopy (TEM) and $N_2$ adsorption-desorption measurement. In this study, we would like to demonstrate that the advantages of synthesized CaO catalyst from green-mussel shell are not only the reduction in the cost of imported commercial CaO catalyst and biodiesel production, but also the decrease in environmental problems of a large quantities of wastes from food industries too.

## 1.2 Objectives

The objectives of this research are follows;

1.2.1 To prepare and characterize $CaCO_3$ and CaO catalyst from green-mussel shells.

1.2.2 To investigate the effects of CaO catalyst for produce biodiesel production by transesterification in various conditions in the synthesis biodiesel such as methanol to oil moleratio, amount of CaO catalyst, reaction temperature, reaction time, speed of agitation and number of reusability cycle of the catalysts.

1.2.3 To study the chemical components of biodiesel produced.



## 1.3 Scopes of this research

The CaO catalyst from green mussel shell was synthesized using direct calcination and carried out in transesterification for produce biodiesel. The experimental procedures were carried out as follows;

1.3.1 Survey literatures review and study the previous research works.

1.3.2 Prepare the $CaCO_3$-precursor for synthesis CaO catalyst from green-mussel shell by direct calcination method at high temperature.

1.3.3 Characterization of natural green-mussel shell, $CaCO_3$-precursor and CaO using various techniques as following below.

1.3.3.1 X-ray powder diffraction (XRD)

1.3.3.2 Fourier transform infrared spectroscopy (FT-IR)

1.3.3.3 Thermogravimetric and differential thermal analysis (TG/DTA)

1.3.3.4 Field emission scanning electron microscopy (FESEM)

1.3.3.5 Transmission electron microscopy (TEM)

1.3.3.6 Surface area analysis and $N_2$ adsorption-desorption measurement

1.3.4 Evaluation of the efficient catalyst (catalytic activity) on conversion rate and yield of the FAME obtained from transesterification of refined palm oil with methanol under various parameters of synthesis conditions.

1.3.5 Characterization of % conversion rate of biodiesel production using a Proton nuclear magnetic resonance ($^1H$ *NMR*) spectroscopy

1.3.6 Characterization of % fatty acid methyl esters (FAMEs) and % yield of biodiesel production by using gas chromatography (GC)

1.3.7 Analysis and summarization of the results and writing thesis

# CHAPTER II

# THEORY AND LETERATURE REVIEWS

## 2.1 Transesterification reaction

Transesterification or alcoholysis is the reaction of triglycerides from vegetable oil or fat from animal reacted with short chain or low molecular weight of alcohol such as methanol and ethanol by employing acid or base catalysts. A mol of triglyceride transformed to 3 mol of fatty acid alkyl esters (FAAE) and 1 mol of glycerol as by-product after the reaction finished. This transesterification reaction is shown in Scheme 2.1.

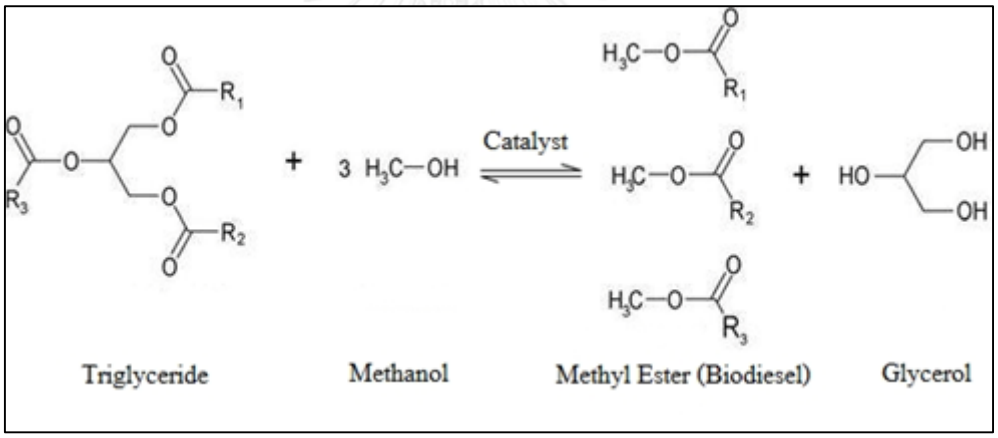


**Scheme 2.1** Transesterification reaction between triglyceride and methanol

## 2.2 Natural calcium carbonate ($CaCO_3$) sources for the synthesis of CaO as catalysts

Mollusk exoskeletons are an abundant $CaCO_3$ source in the forms of aragonite and calcite with excellent fracture strength and fracture toughness, which are attributed to their unique microstructures. The main composition of mollusk exoskeletons shell, such as green mussel shell, is of 95 to 99 percentage of $CaCO_3$ such as aragonite and calcite crystalline forms and 0.1 to 5 percentage of protein film

or organic matter content such as chitin and conchiolin, as the protein binders and covering on its surface [24]. The protein fiber, chitin and conchiolin in mollusk shell structures were consisted of β-(1-4)-linked N-acetyl-D-glucosamine subunits forming a linear homopolymer, and according to some researchers, it is one of those biopolymers identified in the organic parts of the mollusk shells which play an important role in the crystal orientation of mollusk shells [25]. The Figure 2.1 showed the components in microstructures of shells.

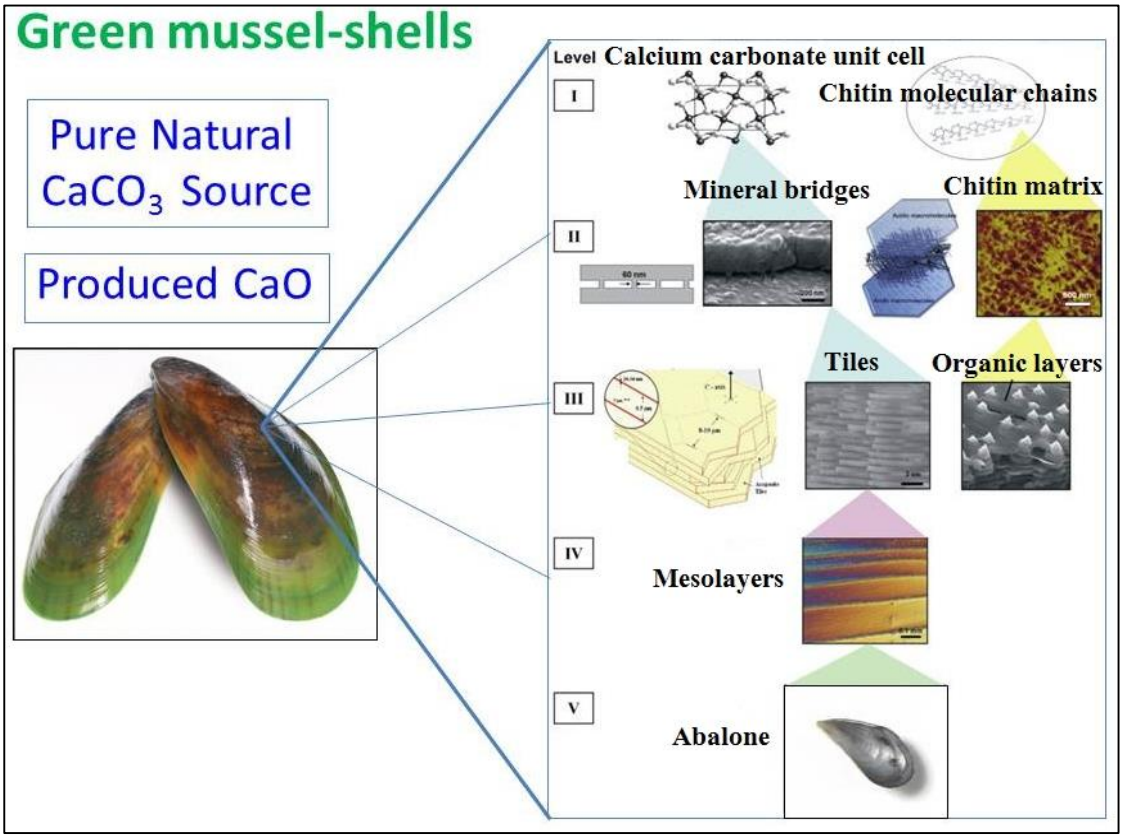


**Figure 2.1** Hierarchical structures (5 levels) of the abalone nacre from nano, micro, meso to the structural length scales. [25]

**2.3. Important benefits of natural calcium oxide derived from waste shells.**

The advantages of heterogeneous catalyst are that they can be easily removed after the reaction was finished by separation, which reducing amount of wastewater in the pretreatment step for the purification of biodiesel production, and the catalyst can be reused for several cycles. Calcium oxide as heterogeneous base catalyst has been widely used for producing biodiesel via transesterification. The benefits of CaO catalyst that have been observed are such as high surface area and basicity, lower solubility in such alcohol as methanol, ethanol and propanol, high porosity and low cost. Moreover, CaO catalysts showed the high catalytic activity in transesterification and easily separated from the biodiesel production process. CaO can be produced from $CaCO_3$ sources by direct calcination or thermal decomposition at high temperature as showed in (Eq.(2.1)) [26].

$$CaCO_3\,(s) \xrightarrow[\Delta]{} CaO\,(s) + CO_2\,(g) \qquad (2.1)$$

Generally, The CaO required high temperature for direct calcination to release the carbon dioxide ($CO_2$) gas and little adsorbed moisture. The relation between temperature and phase transformation was depicted in Figure 2.2.

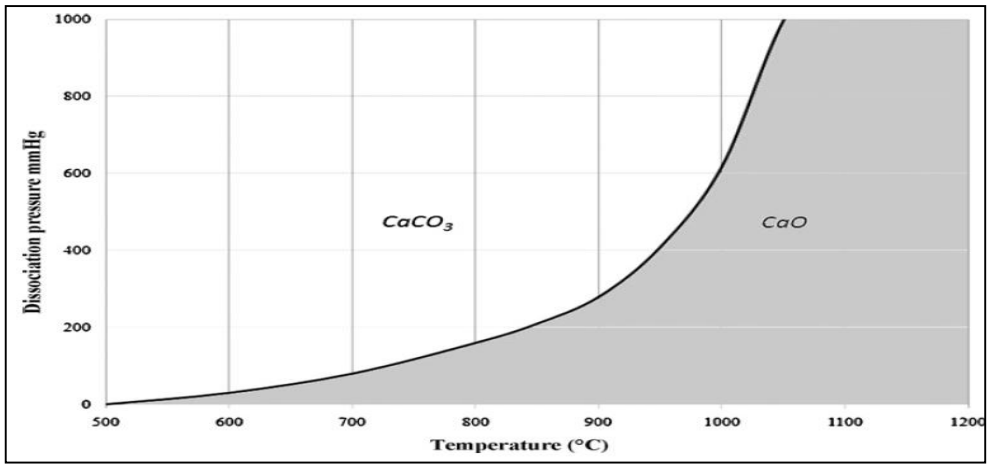


**Figure 2.2** Dissociation pressure and temperature of $CaCO_3$. [27]

Normally, the CaO was produced using calcium salt sources such as calcium hydroxide ($Ca(OH)_2$), calcium nitrate ($Ca(NO_3)_2$) and $CaCO_3$ by thermal decomposition at high temperature. Moreover, CaO can be generated from waste of organisms such as animal bones, seaweed, sea shells (oyster, mud crab shell, green-mussel shell and cuttlebone) and eggshells using a direct calcination. Recently, several researchers have investigated and studied $CaCO_3$ sources from natural and waste shell to produce CaO used as catalysts for transesterification. Pervious works of this area of research are shown in Table 2.1 and 2.2.

**Table 2.1** Heterogeneous catalysts derived from different natural resources in the transesterification of different oils to biodiesel [23]

| **Biodiesel feedstock** | **Source of catalyst** | **Temperature (°C) and time (h) for calcination** | **Catalyst amount (wt.%)** | **Y/C (%)** |
|---|---|---|---|---|
| Mustard oil | Waste shell of *T. striatula* | 600-900, 4 | 3 | 93.3(Y) |
| Soybean oil | Waste eggshell | 200-1000, 2 | 3 | >95(Y) |
| Palm olein oil | Waste cockle shell | 900, 2 | 2.2-7.8 | >97(Y) |
| Palm olein oil | Waste shells of mollusk and egg | 800, 4 | 10 | >90(Y) |
| R.T. = Reaction temperature, Y = Yield, C = Conversion | | | | |

**Table 2.2** Heterogeneous catalysts derived from different natural resources in the transesterification of different oils to biodiesel (continued) [23]

| **Biodiesel feedstock** | **Source of catalyst** | **Temperature (° C) and time (h) for calcination** | **Catalyst amount (wt.%)** | **Y/C (%)** |
|---|---|---|---|---|
| Waste frying oil | Clamshell (*M. meretrix*) | 900, 2.5 or 3.5 | 3 | >89 (Y)<br>>97 (C) |
| Soybean oil | Oyster shell | 100-1000, 3 | 5.86-34.14 | >70(Y) |
| Palm olein oil | Industrial waste shells of egg, golden apple snail and *meretrix venus* | 700-1000, 0.5-8 | 10 | >90(Y) |
| Rapeseed oil | Biont shell | 200-700 | 3 | 97.5(Y) |
| Chinese tallow oil | Waste freshwater mussel shell | 200-1000, 4 | 5 | >90(Y) |
| Soybean oil | Waste fish scale | 600-1000, 2 | 1-5 | 97.73(Y) |
| Palm olein oil | Waste mud crab shell | 900, 2 | 5 | *NM* |
| *Pongamia pinnata* | Chicken eggshells | 900, 2 | 2.5 | 95(Y)<br>97.43(C) |
| R.T. = Reaction temperature, Y = Yield, C = Conversion | | | | |

## 2.4 Mechanism of transesterification reaction using CaO as catalyst

### 2.4.1 In the systems without water

The mechanism of transesterification reaction with CaO catalyst has been investigated by several researchers [27]. The Figure 2.3 showed one of well-supported mechanism for this reaction.

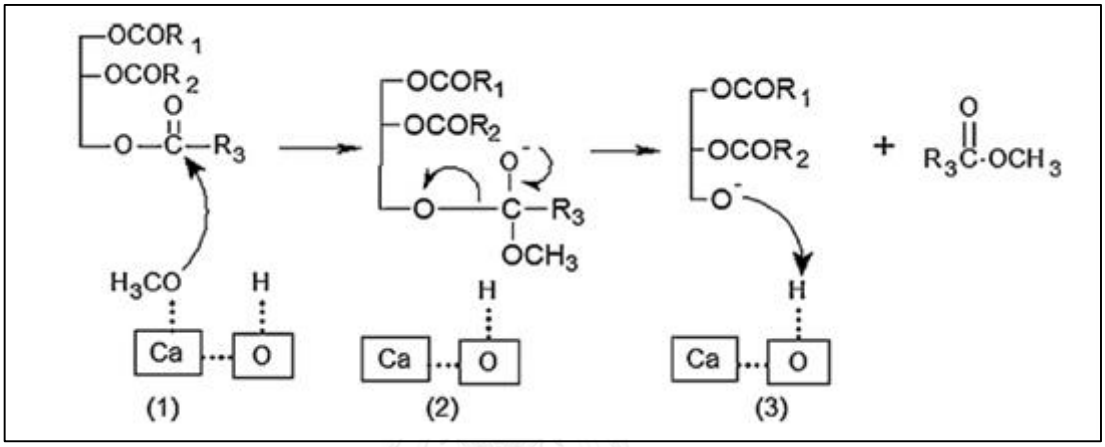


**Figure 2.3** A mechanism for CaO-catalyzed transesterification.

In the first step, the methoxide ion attached on the surface of CaO catalyst attacks the carbonyl carbon atom of triglyceride molecules from oil and transform triglyceride to a new intermediate molecule with the tetrahedral carbons as the second step. Next, the intermediate molecules continuously rearrange their structures before converting to a methyl ester and a diglyceride anion. Then, the diglyceride anion is protonated by a proton on the surface of CaO catalyst and converts to diglyceride molecule. Finally, three moles of methyl ester and a mole of glycerol were obtained after one mole of triglyceride was continuously attacked with methoxide ion for three cycles in role. Kouzu et al. [28] examined CaO catalyst in the transesterification reaction using triglyceride and methanol in detail. First, the methoxide anion was generated using CaO as a solid base catalyst reacting with methanol. Then, the methoxide anion attached to the carbonyl carbon group of triglyceride and converted to alkoxycarbonyl intermediate. Then, alkoxycarbonyl

intermediate underwent the rearrangement of its formation, the FAME and diglyceride anion were obtained. Finally, the diglyceride anion was protonated by a proton on CaO surface and converted to monoglyceride. The mechanism showed in Figure 2.4.

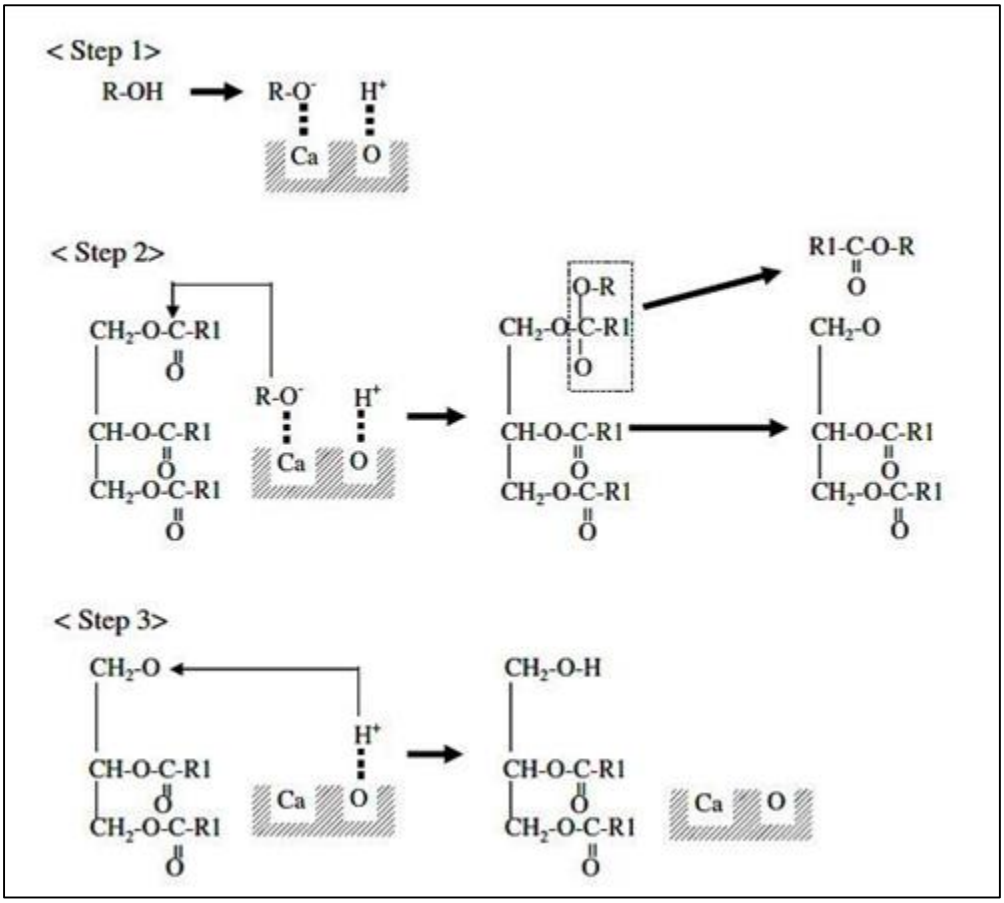


**Figure 2.4** Mechanism between triglyceride and methanol in transesterification using CaO as catalyst

### 2.4.2 In the system with the addition of a small quantity of water

Liu *et al.* [29] studied by experimental and proposed the mechanism of transesterification in excess CaO catalyst with small amount of water. The surface of CaO heterogeneous base catalyst acted as a basic site. Therefore, on the CaO surface, the $O^{2-}$ extracted a proton ($H^+$) from water ($H_2O$) molecules and transformed into hydroxide ($OH^-$) intermediate deposited on CaO surface. Moreover, the chemical

reaction between $O^{2-}$ and $H_2O$ easily generated OH- group in the system as shown in (Eq. (2.2)).

2.2

As soon as methanol was added into the system, the $OH^-$ group got protonated from $CH_3OH$ and converted to a methoxide anion ($CH_3O^-$) and $H_2O$ as by-product. Besides, the $CH_3O^-$ group is a representative of expeditiously basic and has high catalytic activity as showed in Eq. (2.3).

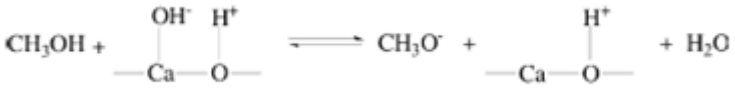

2.3

Also, the other possible pathway was proposed as the $O^{2-}$ group on the surface of CaO catalyst can be protonated by the hydroxyl (OH) group of methanol and converts to $CH_3O^-$ group in the system. The new $OH^-$ group was deposited on CaO surface as shown in Eq. (2.4).

2.4

Then, the glycerol as by-product from the transesterification was generated by $CH_3O^-$ reacting with a triglyceride molecule in oil. In the first step, $CH_3O^-$ attacked the carbonyl carbon (-C=O) atom in triglyceride and converted to an intermediate molecule with tetrahedral carbon. The mechanism was proposed in Eq. (2.5).

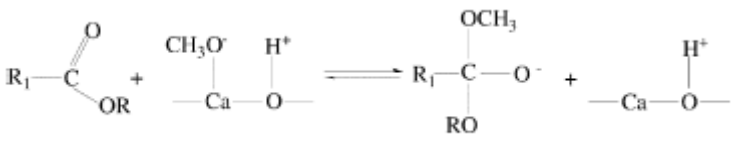

(2.5)

For the next step, tetrahedral intermediate molecule was protonated by the $OH^-$ group on the surface of CaO catalyst as shown in Eq. (2.6).

(2.6)

In addition, the $CH_3O^-$ generated by the tetrahedral intermediate also reacted with methanol in the system as well (shown in (Eq. (2.7)).

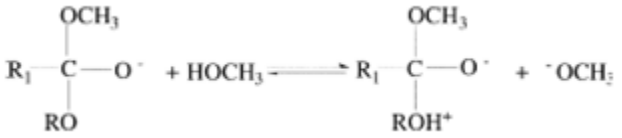

(2.7)

In the final step, the tetrahedral intermediate underwent the rearrangement of its structure and transformed into the fatty acid methyl esters (FAME) or biodiesel and glycerol as by-product after the reaction finished as shown in (Eq. (2.8)).

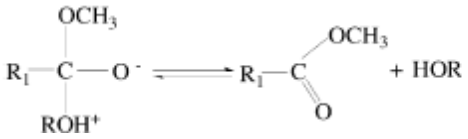

(2.8)

The overall mechanism of transesterification reaction can be concluded by (Eq. (2.9). The long chain alkyl group were represented by the symbols of R1, R2 and R3.

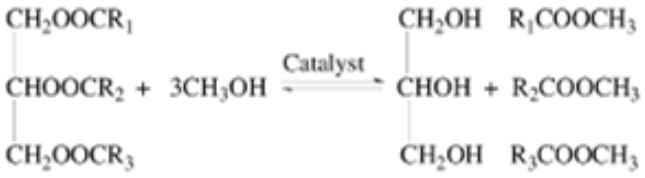

(2.9)

In this case, the hydroxide anions were easily generated using a little amount of water reacting with CaO catalyst, and more methoxide anions as real catalyst in transesterification reaction were promoted. The observation when amount water of no more than 2.8 % wt. (depending on soybean oil weight) was loaded to methanol in the system, the rate of reaction can be increasingly accelerated and the yield of FAME was improved in short time. However, if excess amount of water of more than 2.8 % wt. is loaded in methanol, the water tended to hydrolyze FAMEs and converted them to free fatty acids in this system as shown in (Eq. (2.10)). Then, the free fatty acids can react with base catalyst and generated soaps as products from saponification reaction, a side reaction in this system as shown in Eq. (2.11) [30].

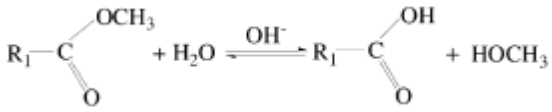

(2.10)

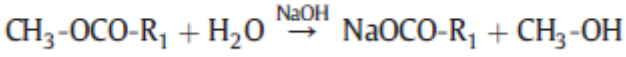

(2.11)

**2.5 Literature review**

In 2009, Nakatani *et al*.[31] investigated the catalysts from powdery calcium carbonate ($CaCO_3$) of oyster shells. In this case, the $CaCO_3$ converted to CaO after calcination at temperature above 700 $^{o}$C and acted as catalysts in the transesterification of soybean oil. The optimized condition for biodiesel production was determined under the amount of catalyst of 25 wt. % and 5 h for reaction time. Under this condition, the biodiesel yield of 73.8 % was collected with 98.4 wt. % of high purity.

In 2011, Boro *et al.* investigated effects of calcination temperature for the synthesis of CaO between 600 and 900 $^{o}$C. The results from BET surface area analysis examined that the shells calcined at temperature ranging from 700 to 900 $^{o}$C showed higher surface area and pore volume than the shells calcined under 600 $^{o}$C. The biodiesel was synthesized by employing optimal condition of 3.0% wt of catalyst with methanol to oil ratio of 1:9 for 6h, and 93.3 % yield biodiesel was obtained.

In 2011, Boey *et al*. [32] synthesized heterogeneous catalysts using cockle shell as raw materials and calcination at 900 $^{o}$C for 2h. The 4.9 wt. % of catalyst carried out in the transesterification between refined palm olein and methanol under the optimum condition of 0.54:1 methanol/oil mass ratio. The maximum of 99.1 percentage purity of the starting content in synthesized biodiesel was obtained and the catalyst was reusable under the optimal condition of this reaction.

In 2011, Hu *et al.* [33] studied the CaO derived from waste freshwater mussel shells (FMS) using a calcination-impregnation-activation method. The FMS was calcined at 900 $^{o}$C and cleaned up with water before calcination at 600 $^{o}$C, and the newly formed CaO crystals were obtained. The results showed that the yield of above 90 % was obtained under optimal condition of 5 wt. % of catalyst, methanol to oil molar ratio of 12:1 at 70 $^{o}$C for 1.5 h.

In 2012, Nair *et al*. [34] studied the production of biodiesel from transesterification of wasted frying oil (WFO) with methanol using diverted heterogeneous catalyst of clamshells (*Mereterix mereterix*). The differrent catalytic

activities of catalyst from clamshells showed in the transesterification for reduce reaction time after the clamshells were calcined at 1173 K for 3.5 h. The results indicated that the higher activity of catalyst was observed when 3.0 g catalysts with methanol to oil molar ratio of 6.03:1 at 333 K for 3 h were used, resulting in high yield and high conversion of biodiesel of 97 % and 89 %, respectively.

In 2014, Boro *et al*. [35] studied and prepared heterogeneous catalyst using barium chloride ($BaCl_2$) doped with transformed CaO from waste shells of *Turbonilla striatula* in transesterification for biodiesel production. The CaO was doped with Ba from $BaCl_2$ by varying the amount of Ba from 0.5 to 1.5 wt. % and the catalyst were used in transesterification of waste cooking oil (WCO) with methanol. Under the condition of 1 wt. % of catalyst, methanol to oil molar ratio of 6:1 at 65 $^{o}$C for 3 h, the maximum conversion more than 98 % was obtained.

In 2015, Lee *et al*. [36] produced biodiesel via transesterification reaction of palm oil with methanol using derived CaO catalysts from waste obtuse horn shells (*C. Obtusa*). The 86.75 % of conversion was obtained under optimum condition at methanol to oil ratio of 12:1, 5 wt. % of catalyst for reaction time of 6 h. Besides, for the reusability of this catalyst, it can be reused up to three times with conversion of higher than 70 % after the third cycles.

In 2015, Li *et al.* [37] investigated solid base catalyst using waste carbide slag as raw materials. The waste carbide slag calcined at 650 $^{o}$C was used as a catalyst in the transesterification between soybean oil and methanol. The base catalyst exhibited high yield of fatty acid methyl ester (FAME) of 91.3 % under the condition of catalyst to oil mass ratio of 1.0 wt. %, methanol/oil molar ratio of 9:1 at 65 $^{o}$C for 30 minutes.

In 2015, Sirisomboonchai *et al*. [38] studied transesterification of waste cooking oil (WCO) with methanol using calcined waste scallop shells as a catalyst. The XRD results showed that after scallop shells were calcined at 1000 $^{o}$C for 2 h, the CaO was obtained. For the CaO catalyst from calcined waste scallop shell has higher activity than commercial grade CaO, therefore, 86 % yield of biodiesel fuel was found when optimal reaction condition were methanol to oil molar ratio of 6:1, 5 wt. % of catalyst,

reaction temperature at 64 °C, and reaction time of 2 h. In addition, the catalyst was reused for 4 cycles; while % yield of biodiesel reduced by 20 % due to the conversion of CaO catalyst to Ca-glyceroxide formation on its surface.

All the research mentioned above expressed that the derived CaO catalyst prepared from waste shells exhibited high catalytic activity in transesterification for the production of biodiesel under the optimum reaction. Moreover, the benefits of these catalysts are low cost and environmental friendly. For there are many seafood industries in Thailand resulting in a lot of waste shells from food industries, especially green mussel shells, an environmental pollution problem from these wastes currently exist. The study of CaO catalyst from green mussel shells can be in part reducing these problems and will be discussed in the next chapters.

# CHAPTER III

# EXPERIMENTAL

In this research, the waste green-mussel shells were used as raw materials for preparation of $CaCO_3$-precursors and CaO catalyst. CaO was synthesized from pure $CaCO_3$-precursor using direct calcination at high temperature and used as heterogeneous basic catalyst in the transesterification of refined palm oil with methanol. The experimental section was divided into two parts.

**Part I** : Synthesis and characterization of $CaCO_3$-precursor and CaO catalysts from green-mussel shells.

**Part II** : Synthesis and characterization of biodiesel production by using CaO as base catalyst via transesterification reaction in various conditions of controlled parameters.

## 3.1 Instruments

### 3.1.1 The instruments for characterization and analysis $CaCO_3$-precursor and CaO catalyst from waste green-mussel shell

The instruments used for analysis and characterization $CaCO_3$ and CaO catalyst from green mussel shell source were shown in Table 3.1 below.



**Table 3.1** List of characterization and analytical instruments

| Instruments | Manufacture : Model |
|---|---|
| Fourier transform infrared spectroscopy (FT-IR) | Impact 410 (Nicolet) |
| X-ray powder diffraction spectrometer (XRD) | DMAX2200/Ultima$^+$ (Rigaku) |
| Field emission scanning electron microscope (FESEM) | JSM-7001F |
| Transmission electron microscope (TEM) | JEM-2100 (JOEL) |
| Surface area analyzer | BELSORP-mini (BEL japan) |

### 3.1.2 The instruments for analysis of the synthesized biodiesel

The instruments used for analysis and characterization biodiesel were shown in Table 3.2 below.

**Table 3.2** List of instruments

| Instruments | Manufacture : Model |
|---|---|
| Fourier transform infrared spectroscopy (FT-IR) | Impact 410 (Nicolet) |
| Proton nuclear magnetic resonance ($^{1}H$ *NMR*) and Carbon-13 nuclear magnetic resonance ($^{13}C$ *NMR*) spectroscopy | Bruker |
| Gas chromatography (GC) | CP-3800, Varian |

## 3.2 Materials and chemicals

1. Green mussel shell of *Perna viridis Linneaus* was collected from Numpu market, Chathaburi Thailand

2. All chemicals in this research are listed in the Table 3.3-3.4 as shown below;

**Table 3.3** List of chemicals

| Chemicals | Suppliers |
|---|---|
| Sodium hydroxide (NaOH) | Merck (pellet for analysis) |
| Hydrochloric acid (HCl) | Lab scan (AR grade) |
| Hydrogen peroxide ($H_2O_2$) | Merck (pellet for analysis) |
| Methanol ($CH_3OH$) | Sigma-Aldrich (99.9999%) |
| n-Hexane | Carlo erba |
| Chlorofrom-d | Merck |
| Methyl heptadecanoate | Aldrich |
| *N*-Methyl-*N*-(trimethylsilyl) trifluoroacetamide (MSTFA) | Aldrich |
| (S)-(-)-1,2,4-Butanetriol | Supelco |
| Tricaprin internal Standard | Supelco |

**Table 3.4** List of chemicals (continued)

| Chemicals | Suppliers |
|---|---|
| 1,3-diolein | Supelco |
| Monoolein | Supelco |
| Glyceryl Trioleate | Supelco |
| 1-oleoyl-rac-glycerol | Supelco |
| Heptane anhydrous | Sigma-Aldrich |
| 37 Component FAME Mix (10 mg/mL) in methylene chloride | Supelco |
| Bromophenol blue | Supelco |
| Methyl red | Merck |
| Phenol red | Merck |
| Phenolphthalein | Merck |
| Indigo carmine | Fluka |
| Bromothymol blue | Merck |
| Neutral red | Fluka |
| 2,4-Dinitroaniline | Aldrich |
| 4-nitroaniline | Aldrich |

**Part I** : Synthesis and characterization of $CaCO_3$-precursor and CaO catalyst from green-mussel shells.

**3.3 Experimental process**

The $CaCO_3$-precursors were prepared from green mussel shells as raw material using different processes before CaO catalysts were synthesized following the methods below.

**3.3.1 Preparation calcium carbonate from green-mussel shell (GMShell)**

100 g of green-mussel shells were cleaned to remove residues such as lipids, sand, and other interference substances on their surfaces by scraping and washing thoroughly with 25 milliliter (mL) of hot deionized (DI) water at 80-90 $^{o}$C for 3 times and the samples were dried to remove excess water at 105 $^{o}$C in electric oven until reaching a constant weight. Then, dried samples were crushed with mortar and selectively obtained samples of particle sizes about 100 mesh using a metal sieve. Finally, the powdery samples were kept in a desiccator for protecting of sample from absorbing moisture in air. For reference, we named these samples as GMShell for cleaned-natural green-mussel shell.

**3.3.2 Preparation calcium carbonate from green-mussel shell after purification ($CaCO_3$-EGMShell)**



The green-mussel shells of 100 g were cleaned up for removing of impurities on its surface with 25 mL of hot water for 3 times. Next, 100 mL of 1 % w/v sodium hydroxide (NaOH) solution was added into cleanly treated shell samples in a 500 mL beaker for 1 h and the reaction mixture was refluxed at 80-85 $^{o}$C for 30-60 min to eradicate the organic matter and remaining proteins binder on green-mussel shell surfaces. After reaction finished, the shell samples were completely changed from green to brown color on their top surface, and protein film and other residues in solution were entirely removed. The shell-sample were washed repeatedly with DI water until pH near neutral. Next, samples were immaculately treated with 50 mL of 0.5 M hydrochloric acid (HCl) solution for 30 second, brown pigment of impurity protein on top surface was removed, and this process was repeated once again. Then, the

samples were thoroughly washed with DI water until pH near neutral and the white shell-sample with high brightness were obtained. Finally, the bright shell-samples were dried in oven at temperature of 105 °C to remove excess water for overnight or until the samples reached constant weight. Then, dried samples were crushed with mortar and selectively obtained samples of particle sizes about 100 mesh using a metal sieve. The powdery samples were kept in a desiccator with the name labeled as $CaCO_3$-EGMShell.

### 3.3.3 Preparation calcium carbonate by co-precipitate method ($CaCO_3$-CoGMShell)

About 10 g of the pure $CaCO_3$-EGMShell in 3.3.1.2 were digested with 100 mL of 1 M HCl solution, and the reaction mixture were slowly stirred in fume hood to remove carbon dioxide ($CO_2$) gas from this process. The reaction was continued until $CaCO_3$-EGMShell sample were completely dissolved in solution, followed by equation (3.1) [39] below.

$$CaCO_{3\,(s)} + 2\,HCl_{\,(aq)} \rightarrow CaCl_{2\,(aq)} + CO_{2\,(g)} + H_2O_{\,(l)} \qquad (3.1)$$

Then, The solution were filtrated through No.1 filter papers to eliminate impurities from protein film in porous structures of $CaCO_3$. The clear solution was neutralization with 100 mL of 2 M of NaOH solution. The solution was collected into a 250 mL volumetric flask, and DI water was added in the solution until the total volume of 250 mL was reached. The flask was swirled periodically to mix the solution, and this solution was labeled as a solution. Next, 250 mL of 0.1 M sodium carbonate ($Na_2CO_3$) solution was added into a 500 mL clean beaker of solution A by single drop co-precipitation method and continuously stirred using a magnetic stirrer. Then, a small amount of white solid was slowly precipitated from mixture. Finally, the white precipitate was separated using a suction filter, and the white solid were kept in electric oven at 105 °C until reaching a constant weight. The sample was labeled as $CaCO_3$-CoEGMShell.

### 3.4 Synthesis of CaO catalyst from $CaCO_3$-precursor

Five grams of milled $CaCO_3$-precursor were added into an alumina ceramic crucible and direct calcined in an electric furnace at various temperatures ranging from 600, 700, 800, 900 and 1000 $^{o}$C for 5 h. Then, aggregated white solid were obtained and crushed by using mortar. Finally, the powdery white solid were kept in an electric desiccator in order to be protected from a little moisture and carbon dioxide ($CO_2$) in air.

### 3.5 Pretreatment of CaO catalyst for high active catalytic activity

Five grams of the CaO catalysts after calcination at 800-1000 $^{o}$C (from 3.4) were dispersed in 5 mL of DI water in a 25 mL beaker and constantly stirred for 5 minutes. Then, the mixture was filtered using Whatman No.4 filter paper. Next, soaked sample was dried at 105 $^{o}$C in an electric oven for 2.5 h until obtaining constant weight. Finally, the white solid was crushed and kept in electric desiccator.

### 3.6 Characterization of $CaCO_3$-percursor and CaO catalyst

From the main objectives of this research, CaO catalyst was synthesized from natural green-mussel shells using direct calcination at high temperature. Therefore, the physical and chemical properties of $CaCO_3$ and CaO catalyst, before and after calcined, were investigated using Fourier transform infrared spectroscopy (FTIR), X-ray powder diffraction (XRD), X-ray photoelectron spectroscopy (XPS), transmission electron microscopy (TEM), and scanning electron microscopy (SEM). Moreover, the specific surface area, total pore volume and average pore diameter of catalysts were determine using Brunauer-Emmett-Teller (BET) method from $N_2$ adsorption-desorption isotherms. Basic strengths (H_) of catalysts were examined using Hammett indicator method.

**Part II** : Synthesis and characterization of biodiesel production by using CaO as base catalysts via transesterification reaction using various parameter for synthesis conditions

### 3.7 Synthesis and characterization of the biodiesel products

Parameters studied for synthesized biodiesel from refined palm oil and methanol using CaO catalyst in transesterification reaction

#### 3.7.1 Optimization for the synthesized CaO catalyst from different $CaCO_3$-precursor in transesterification reaction

The CaO catalysts from $CaCO_3$-EGMShell**,** after calcined at temperature 600, 700, 800, 900 and 1000 $^{o}$C for 5 h, were used for synthesizing of biodiesel under conditions of 10.0 % wt CaO catalyst (based on palm oil weight) and about 3.42 g methanol (methanol to oil mole ratio as 1:12.) The reaction mixture was loaded into a 25 mL three-necked round bottom flask and refluxed at 60 $^{o}$C for 2 h. Next, 10.0 g refined palm oil was added into the system. Then, the mixture was constantly stirred at 500 rpm while refluxed at 64 ± 1 $^{o}$C for 2 h. The instrument set up was shown in Figure.3.1.



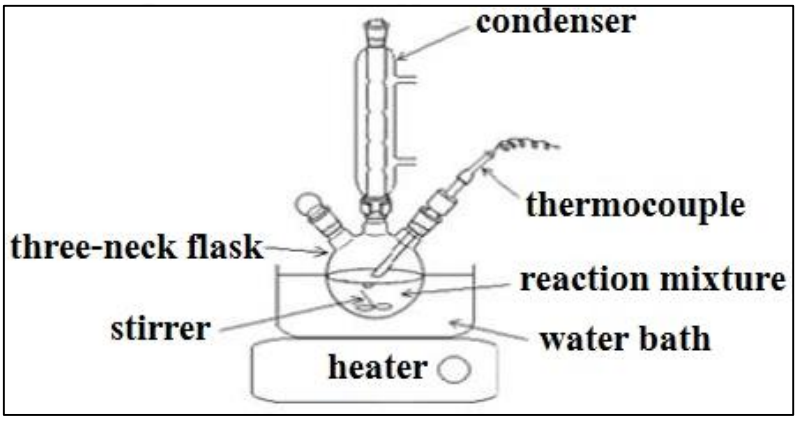


**Figure 3.1** Apparatus set-up for the synthesis of biodiesel.

After reaction finished, the three-necked round bottom flask was put in an ice-bath for 10 minute in order to decrease the temperature for stopping the reaction. Then, the mixture was separated by centrifugation at 4000 rpm for 10 minutes. According to the reaction equation in Chapter 2, the top layer contained little methanol residue, the middle layer mainly contained fatty acid methyl ester (FAME) or biodiesel products, and the bottom layer contained mixture between glycerol and CaO catalyst. Finally, the middle layer was separated and other residue was removed for purification. The purified middle layer was subjected to determine the % conversion rate from triglycerides of palm oil converted to FAMEs using proton nuclear magnetic resonance ($^1$H-NMR) analysis.

### 3.7.2. Effect of calcination time

The calcined CaO catalysts with highest % conversion rate were studied the effects of calcination time by varying the time for calcination as 0, 1, 2, 3, 4 and 5 h. For this study, about 10 g of CaO catalysts obtained from various time for calcination were loaded and refluxed with methanol following the same condition as in 3.7.1. Finally, the biodiesel production was subjected into $^1$H-NMR for the calculation of % conversion rate.

### 3.7.3 Effect of amount of CaO catalyst

The condition for synthesis of biodiesel in this step was 10.0 g refined palm oil with amounts of CaO catalysts of 1, 2, 3, 4 and 5 wt. % (based on palm oil weight). For the synthesis, the CaO catalysts of different weights were refluxed with 3.42 g methanol (methanol to oil mole ratio of 1:12) at 60 $^{\circ}$C for 2h. Next, 10.0 g of refined palm oil were added into the systems. Then, the mixture was refluxed at 64 ± 1 $^{\circ}$C and constantly stirred at 500 rpm for 2 h. After reaction finished, the impurities and by-products were separated from biodiesel following the method in 3.7.1. The % conversion rates were determined by $^1$H-NMR.

### 3.7.4 Effect of mole ratio of oil to methanol

Biodiesel production was synthesized by various methanol to oil mole ratio for using ratio equal form 3:1, 6:1, 9:1, 12:1 and 15:1. The CaO catalysts of different weights were refluxed with methanol at 60 °C for 2h. Next, 10.0 g of refined palm oil was added into the systems. Then, the mixture was refluxed at 64 ± 1 °C and constantly stirred at 500 rpm for 2 h. After reaction finished, the impurities and by-products were separated from biodiesel following the method in 3.7.1. The % conversion rates were determined by $^{1}$H-NMR.

### 3.7.5 Effect of reaction temperature

The effects of reaction time for synthesis biodiesel were studied by varying the reaction temperatures as 35, 40, 45, 50, 55, 60, 65 and 70 °C. In the synthesis, CaO catalysts were refluxed with methanol in a 25 mL three-necked round bottom flask at 60 °C and constant stirring at 500 rpm for 2 h. Next, refined palm oil of about 10.0 g was added into the system and continuously refluxed at different temperature parameters. Then, the reaction was stopped after 2 h and a three-necked round bottom flask was transferred into an ice bath for 5 minutes. Finally, the middle layer of biodiesel products was separated and purified using identical condition as in 3.7.1 before calculation of % conversion rate with $^{1}$H-NMR.

### 3.7.6 Effect of agitation speed

The conditions with the best $^{1}$H-NMR results from 3.7.1, 3.7.2, 3.7.3, 3.7.4 and 3.7.5 were used to synthesize biodiesel with various agitation speeds as 0, 100, 300, 500, 700, 900 and 1100 rpm. The transesterification reaction was done following the method mentioned in 3.3.5.1. After the reaction was finished, purified biodiesel products was determined the % conversion rate by $^{1}$H-NMR.

### 3.7.7 Effect of reaction time

The experiment for the synthesis of biodiesel in this step was to study the variation resulting from the different reaction times as 30, 60, 90, 120, 150, 180 and 210 minutes; while other parameters was chosen according to the best results from 3.7.1, 3.7.2 and 3.7.3, 3.7.4, 3.7.5, and 3.7.6. First, CaO catalysts were refluxed with

methanol in a 250 mL three-necked round bottom flask at 60 °C for 2 h with constant stirring. After 2 h, about 100.0 g refined palm oil was slowly loaded into the systems. Next, about 10 mL of the homogenous mixture was sampled out every 30 min using a volumetric pipette until the reaction time reaching 210 min. All, samples were centrifuged and removed impurity following the methods in 3.7.1. Finally, purified biodiesel products were analyzed using $^{1}$H-NMR for the calculation of % conversion rate of all samples from the reaction.

**3.7.8 Effect of water loading amount**

For the synthesis process, the effects of water loading were studied by adding various amounts of water as 0, 1, 2, 3 and 4 wt. % (based on catalyst weight.) Biodiesel was synthesized by transesterification reaction using the best conditions for $^{1}$H-NMR results from 3.7.1 to 3.7.7. The mixture of CaO catalyst, methanol and various amount of water was refluxed at 60 °C for 2 h. Then, about 10.0 g refined palm oil were added into the mixture and refluxed at 64 °C at constant speed agitation for 2 h. Finally, the purified biodiesel was analyzed using $^{1}$H-NMR for calculation of % conversion rate.

**3.7.9 Reusability of CaO catalyst**

For the reusability of CaO catalysts, the transesterification was repeated many times with the used CaO catalyst. After the Cycle 1 of biodiesel synthesis was finished, the CaO catalyst was isolated from the reaction mixture by centrifugation at 4,000 rpm for 10 minute. Next, 2 mL of n-hexane was loaded into a centrifuge tube to dissolve and eliminate such residues as triglycerides from refined palm oil, soaps and a little amount of catalyst by washing and shaking the mixture for 5 minutes. Then, hexane was removed, and 1 mL pure methanol was added into a centrifuge tube to dissolve and remove glycerol byproduct. The mixture was shaken and centrifuged at 4000 rpm for 10 minutes. Next, methanol was removed and cleaned CaO catalyst was obtained. Finally, the cleaned CaO catalyst was dried in an oven at 105 °C until reaching constant weight.

### 3.7.10 Comparison of catalytic activity of CaO catalysts from different $CaCO_3$-precursors

All CaO catalysts from different $CaCO_3$-precursors after calcined at 900 $^{o}$C, were selected for synthesis of biodiesel using the best condition from $^{1}$H-NMR results from 3.7.1 to 3.7.7. All synthesized and purified biodiesels were compared based on % conversion rate calculated using $^{1}$H-NMR data.

### 3.8 Characterization of synthesized biodiesels

3.8.1 Proton nuclear magnetic resonance ($^{1}$H-NMR) analysis

The biodiesels containing fatty acid methyl esters (FAMEs) or the middle layer products were subjected to determine % conversion rate from triglyceride of palm oil converting to FAMEs by using $^{1}$H-NMR analysis. The calculation was done following Equation (3.2) [40] shown below.

$$\% \text{ Conversion rate} = [(2A_{Me})/ (3A_{CH2})] \times 100 \%, \quad (3.2)$$

Where $A_{Me}$ is the integration of the area under the curve at 3.6-3.7 ppm, which is corresponding to the methoxy protons of the FAMEs or biodiesel, and $A_{CH2}$ is the integration of the area under the curve at 2.2-2.3 ppm, which is corresponding to $\alpha$-methylene protons from triglycerides in the starting oil.

For analysis using $^{1}$H-NMR, about 5 mg of synthesized biodiesel was dissolved in chloroform-d ($CDCl_3$) as an internal standard. Next, the homogenous mixture was subjected to NMR tube and loaded into a spectrometer (Bruker model ACF200) operating at 400 MHz. The $^{1}$H-NMR data were analyzed by processing with MestReNova software.

### 3.8.2 Gas chromatography (GC) technique

#### *3.8.2.1 Determination of ester content in biodiesel by using EN14103*

For the best condition for synthesis of biodiesel or the condition of which % conversion rate was higher than other conditions as calculated using $^{1}$H-NMR results, the biodiesel product was characterized using a gas chromatography (GC) to determine the ester content in the products. The chromatography was carried out using a CP-3800 Varian connected with OmegaWax column. For GC analysis, the sample was preparation by following European standard method EN14103. The purified synthesized biodiesel samples of approximately 250 mg (± 0.5 mg) and 200 µL MSTFA were added into a 20 mL vial using a micropipette. The mixtures were shaken vigorously for 20 minutes at room temperature. Next, 5 mL of methyl heptadecanoate as an internal standard solution (prepared by dissolving 500 mg methyl heptadecanoate in n-heptane 50 mL) was added into the mixture. The mixture was shaken continuously for 10 minutes. Approximately 1 µL of homogenous solution in volume was injected under conditions in Table 3.5.

**Table 3.5** The GC condition for determination ester content in synthesized biodiesel according EN 14103 method

| Parameter | Condition |
|---|---|
| Column | OmegaWax-column 30m, ID 0.25 mm, 0.25 µm film thickness |
| Injector temperature | 250 °C |
| Detector | Flame ionization (FID) |
| Detector temperature | 250 °C |
| Column oven | 50 °C (hold 1 min), rate of 4 °C/min to 220 °C and rate of 10 °C/min to 230 °C |
| Carrier gas | $N_2$ gas |
| Split ratios | 1:100 |
| Flow rate | 1.2 mL/min |
| Volume injected | 1 µL |

*3.8.2.2 Determination of glycerin (EN14105)*

The European standard method EN 1405 was used in determination of total glycerol, free glycerol, monoglyceride, diglyceride and triglyceride as residue contents in the synthesis of biodiesel. Standard mixtures and internal standard solutions were prepared according to the following methods. First, 100 mg (± 0.1 mg) of each clean synthesized biodiesel sample and 200 µL of MSTFA were loaded in a 20 mL vial by using a micropipette, and the mixture was shaken vigorously for 20 minutes. Next, 80 µL of the Internal Standard No.1 (1,2,4-Butanetriol) and 100 µL of the Internal Standard No.2 (Tricaprin) were added into a vial using a micropipette. The mixture was homogenized by continuous shaking at room temperature for 15-20 minutes. Then, approximately 8 mL of heptane were added in to the homogenous solution, and 1 µL of the mixture was injected into a GC using the instrumental conditions as described in Table 3.6 for analysis according to the EN 14105 method.

**Table 3.6** The GC conditions for the determination of glycerol residue content in synthesized biodiesel according to the EN 14105 method

| Parameter | Condition |
|---|---|
| Column | Metal column 10 m, 0.32 µm, ID 0.25 mm |
| volume Injected | 1 microliter (µL) |
| Detector | Flame ionization (FID), 380 $^{o}$C |
| Temperature | 100 $^{o}$C (1 min) – 15 $^{o}$C / min to 370 $^{o}$C |
| Carrier gas | $N_2$ gas, Constant Flow 3.5 mL / min |
| Column Oven | 50 $^{o}$C (hold 1 min), to 180 $^{o}$C at 15 $^{o}$C / min to 230 $^{o}$C at 7 $^{o}$C / min and to 370 $^{o}$C (5 min) at 10 $^{o}$C / min |

# CHAPTER IV

# RESULTS AND DISCUSSION

In this research, we focused on the preparation of $CaCO_3$-precursor ($CaCO_3$-EGMShell) and CaO (CaO-EGMShell) catalysts from wasted green mussel shells using direct calcination method at high temperature. The CaO catalyst was used in transesterification reaction for synthesis biodiesel under optimal condition by varying factors such as amount of CaO catalyst, methanol to oil molar ratio, reaction temperature, reaction time and agitation speed. Finally, the reusability of catalyst was investigated by using the catalysts repeatedly under the optimal condition.

## 4.1 Processing for preparation of $CaCO_3$ precursors

### 4.1.1 Elimination of organic matter on green mussel shell surface

The impurities such as sand, lipid, barnacle, and organic matter on green mussel shell surface were remove using a hydrothermal method in 1 % w/v NaOH solution at 80 $^{o}$C for 45 min. The results clearly indicated that about 9-10 wt. % (depending on the weights of shells) of impurities were easily removed under this condition. The physical property of green mussel shells were compared between the ones before and after removal of impurities as shown in Figure 4.1

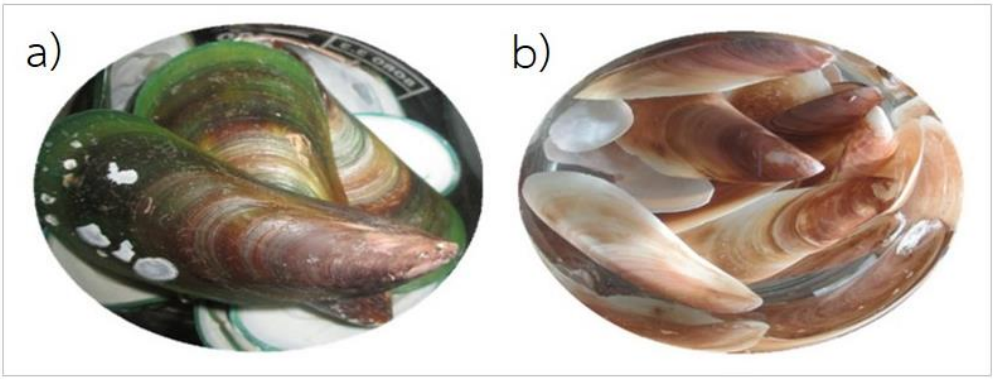


**Figure 4.1** Green mussel shells (A) before and (B) after removal of impurities with 1 % w/v NaOH solution using a hydrothermal method.

### 4.1.2 Purification of green mussel shell surface after eliminating impurities

In this experiment, pure $CaCO_3$ was prepared as raw materials. The brown pigment residues on green mussel shells were removed by washing with 10 mL of a 0.5 M HCl solution. Finally, the white shells of about 98.75 % yield of final products were obtained. This method showed that the shell weight was decreased about 1-2 wt. % only after using the 0.5 M HCl solution. The reason for the weight loss was likely due to the loss of $CaCO_3$, which is the main component of green mussel shells. When $CaCO_3$ from shells reacted with the HCl solution, it was converted to carbon dioxide ($CO_2$) following Equation 4.1.

$$CaCO_{3\,(s)} + 2\,HCl_{(aq)} \longrightarrow CaCl_{2\,(aq)} + CO_{2\,(g)} + H_2O_{(l)} \quad (4.1)$$

Figures 4.2 and 4.3 showed the physical appearances of the shells comparing the ones before and after purification by acid treatment.

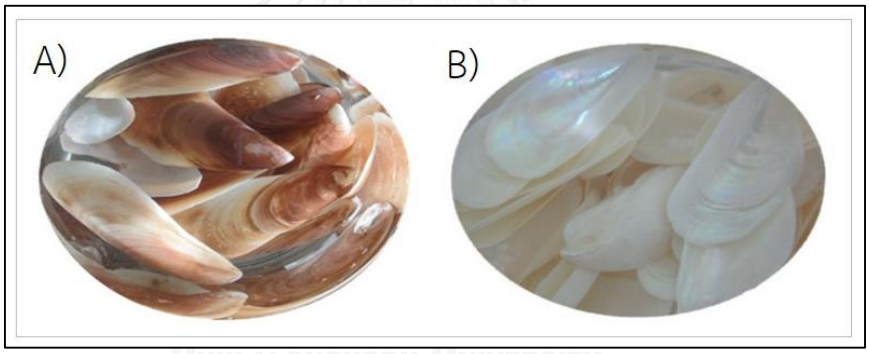




**Figure 4.2** Green mussel shells (A) before and (B) after treated with 0.5 M HCl solution.

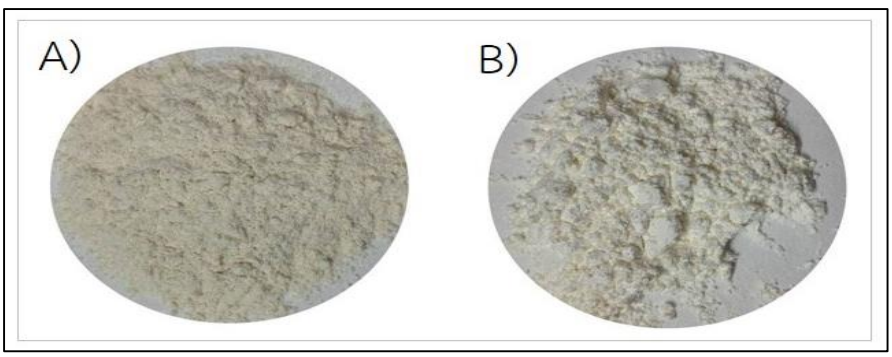


**Figure 4.3** Powders of green mussel shells (A) before and (B) after treated with 0.5 M HCl solution.

## 4.2 Characterization of $CaCO_3$ precursor and CaO catalyst using green mussel shells as raw material

### 4.2.1 Fourier transforms infrared (FTIR) spectroscopy

Functional groups on $CaCO_3$-GMShell and $CaCO_3$-EGMShell, derived $CaCO_3$-precursor from green mussel shells, were characterized using a FTIR technique. The similar FTIR patterns of $CaCO_3$-GMShell and $CaCO_3$-EGMShell were presented in Figure 4.4. The asymmetric stretching for carbonate ($CO_3^{2-}$) group was observed at 1473.85 $cm^{-1}$. This major absorption band belongs to $CO_3^{2-}$ group of $CaCO_3$, [41] the main content of green-mussel shells. Besides, the other absorption bands of the $CO_3^{2-}$ group were observed at 864.62 and 713.85 $cm^{-1}$. The sharp absorption band at 864.62 and 713.85 $cm^{-1}$ are attributed to the out-of-plane and in-plane vibration modes, respectively [42]. In addition, the characteristic peak of C=O Stretching was observed at 1784.62 $cm^{-1}$ which belongs to $CO_3^{2-}$ group from $CaCO_3$ Finally, the absorption bands around 2498-3436 $cm^{-1}$ (2498.46, 2526.15, 2550.77, 2849.23, 2926.15 and 3436.92 $cm^{-1}$) are due to characteristic peaks of the C-H, N-H, and O-H bonds [43] from organic matrix as impurities from green mussel shells. .

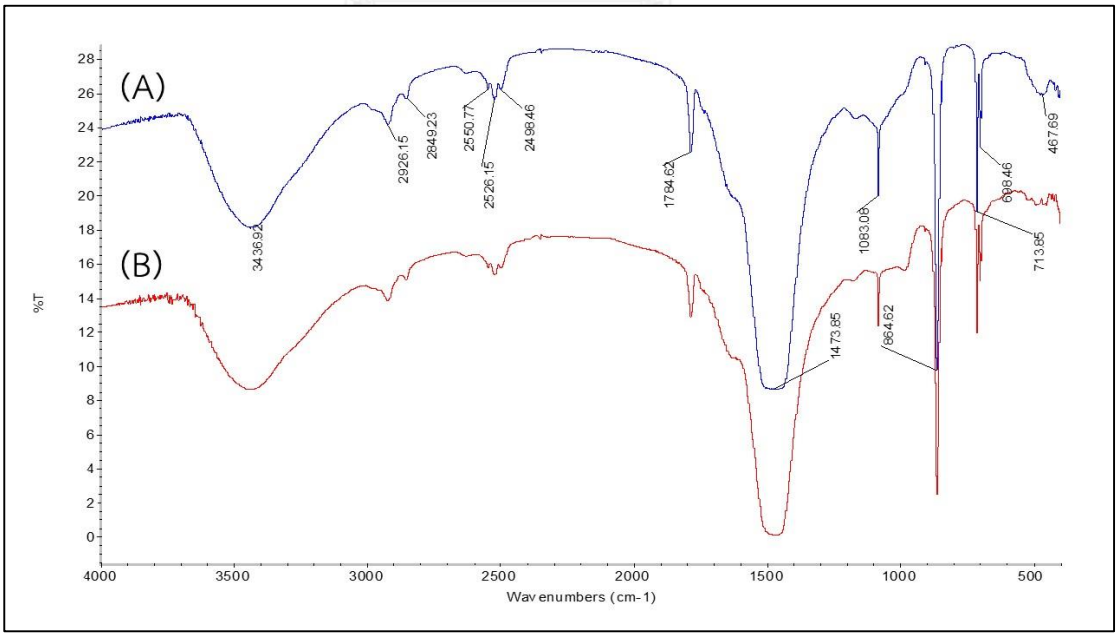


**Figure 4.4** FTIR spectra of green mussel shells (A) $CaCO_3$-GMShell and (B) $CaCO_3$-EGMShell.

The $CaCO_3$-precursors ($CaCO_3$-GMShell and $CaCO_3$-EGMShell) were then calcined at 900 °C in an electric furnace for 5 h. During the calcination, the $CaCO_3$ slowly decomposed and converted to CaO and $CO_2$. After calcination finished, the new absorption band appeared at 3636.92 $cm^{-1}$, which is a characteristic peak assigned to the formation of basic Hydroxyl group (-OH) from the adsorption of a little amount of water molecules in air on CaO surface[44]. Moreover, the intensity of absorption band at 3436.92 and 1473.85 $cm^{-1}$ from $CaCO_3$-precursor in Figure 4.5 (A) decreased, indicating the evidence of $CO_3^{2-}$ group decomposition as the $CaCO_3$ mass reduced [45, 46].

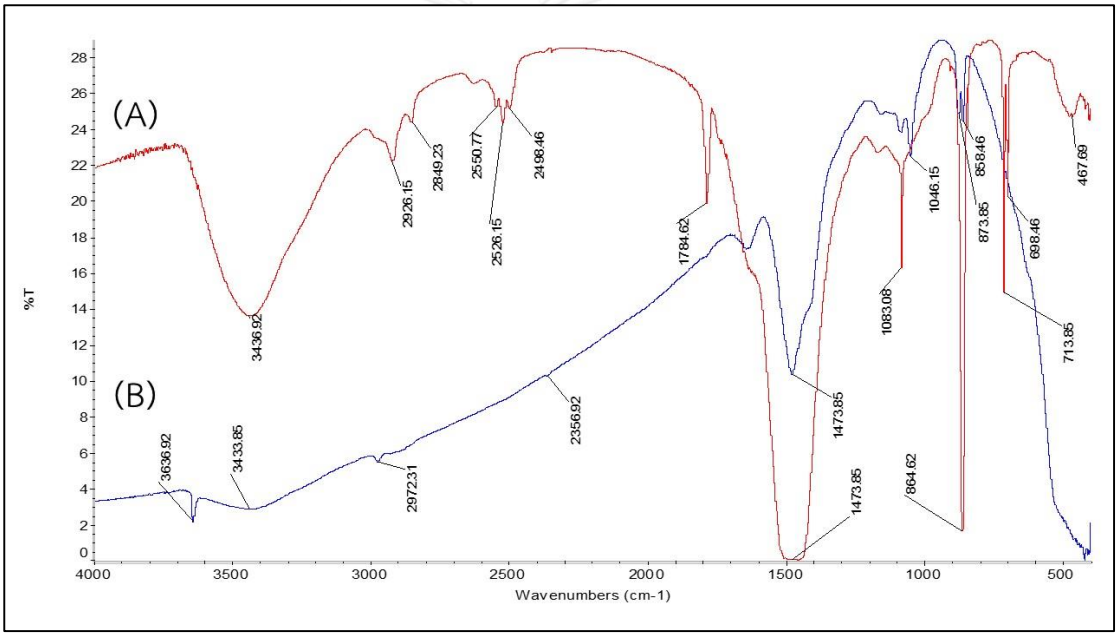


**Figure 4.5** FTIR spectra of treated green mussel shells (A) $CaCO_3$-EGMShell and (B) CaO-EGMShell.

The crystalline products from $CaCO_3$-GMShell and $CaCO_3$-EGMShell after calcination at 900 °C for 5 h were characterized by comparing with an FTIR spectrum of commercial CaO as standard. The results in Figure 4.6 indicated the absorption bands of the both products from $CaCO_3$-GMShell and $CaCO_3$-EGMShell after calcination were corresponded with similar spectrum to CaO standard. Therefore, both crystalline products from calcined $CaCO_3$-GMShell and $CaCO_3$-EGMShell were assigned as CaO phase.

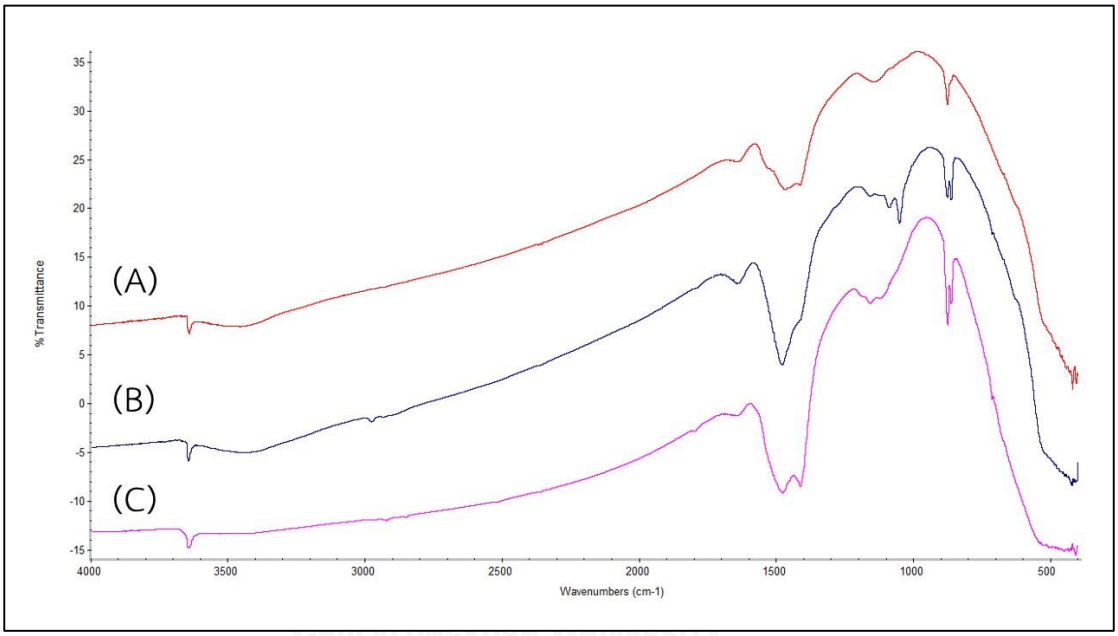


**Figure 4.6** FTIR spectra of products from $CaCO_3$-precursor after calcination 900°C for 5 h (A) CaO-GMShell from $CaCO_3$-GMShell, (B) CaO-EGMShell from $CaCO_3$-EGMShell and (C) commercial CaO as standard.

The CaO-EGShell was treated with DI water for removing of residues deposited on its surface using a wet impregnation method. The results from FTIR in Figure 4.7 indicated that both absorption spectra from modified CaO-EGShell and commercial calcium hydroxide ($Ca(OH)_2$) had similar FTIR patterns. The sharp absorption band at 3640 $cm^{-1}$ is a characteristic band of hydroxyl group (-OH) from $Ca(OH)_2$. Therefore, this result can be preliminary confirmed that the CaO-EGMShell (CaO form) was converted to $Ca(OH)_2$ form after the CaO-EGMShell was impregnated with a little amount of DI water.

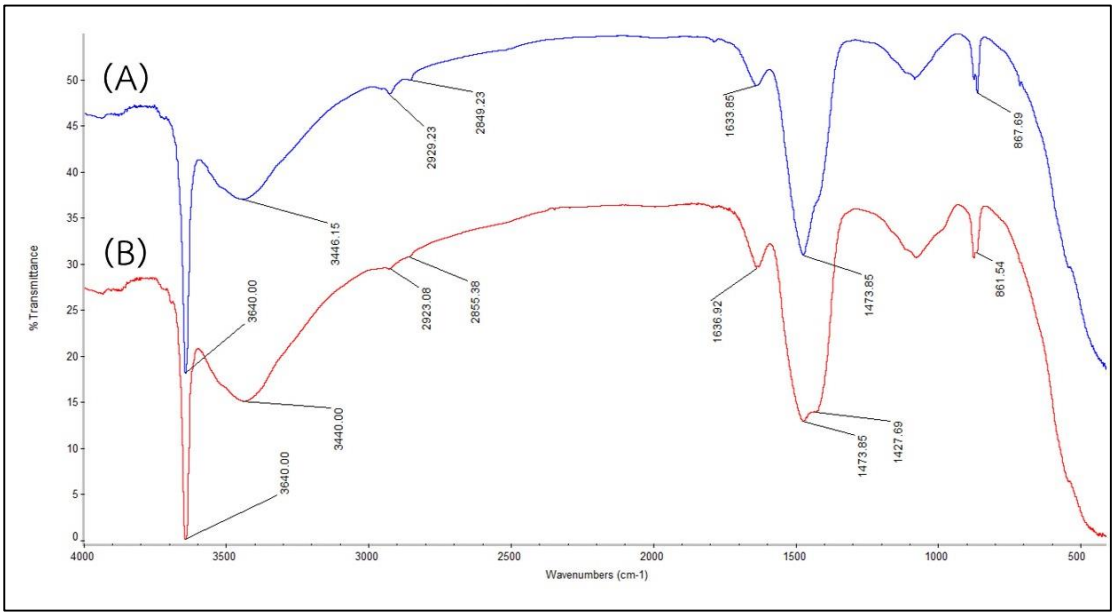


**Figure 4.7** FTIR spectra of (A) treated CaO-EGShell and (B) commercial $Ca(OH)_2$ as standard.

Moreover, the organic matrix as residues from green-mussel shell were investigated using FTIR. FTIR spectra of the natural organic matrix [47, 48] from green-mussel shell (before calcination) and residue of organic matrix content in CaO-EGMShell (after completely digested mineral from CaO) were compared in order to confirm residue content in CaO-EGMShell after calcination at 900 $^{o}$C for 5 h. The results indicated that both of the absorption bands are in similar patterns, then it can be concluded that a little amount of organic matrix as impurities were stilled in CaO-EGShell structure even after calcination at 900 $^{o}$C. The absorption bands of natural organic matrix (before calcination) at 1636.92, 1483.08 and 1243.08 cm$^{-1}$ were identified as the characteristic peaks of amides due to acetyl group content in $\alpha$-chitin molecules [49, 50]. Besides, the characteristic peaks of amides due to acetyl group were observed after calcination at the absorption at around 1630.77, 1446.15 and 1169.23 cm$^{-1}$. The FTIR result were showed in Figure 4.8

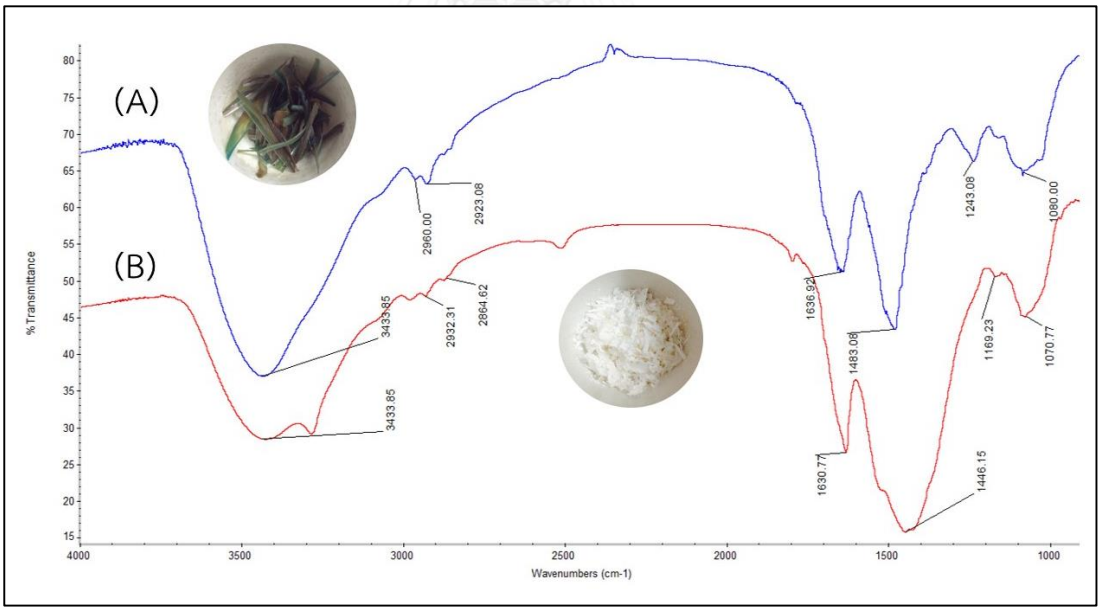


**Figure 4.8** FTIR spectra of (A) Natural residue of organic matrix and (B) residue of CaO-EGMShell after calcination at 900 $^{o}$C for 5 h.

### 4.2.2 X-ray powder diffraction (XRD)

The crystalline structures of $CaCO_3$-GMShell and CaO-EGMShell were characterized using X-ray powder diffraction. Both samples presented the similar XRD patterns as shown in Figure 4.9 Both of the XRD patterns showed the peaks at 2 Theta (2θ) of 26.282, 27.301, 31.179, 33.198, 36.158, 37.955, 38.611, 45.951, 48.514, 50.335, 52.485, 53.078 and 66.095. The patterns were corresponded with XRD pattern of the Joint Committee on Powder Diffraction Standards (JCPDS) of No. 41-1475 of the aragonite ($CaCO_3$) structure with characteristic peaks at 26.282, 31.179, 33.198, 37.955 and 52.485.

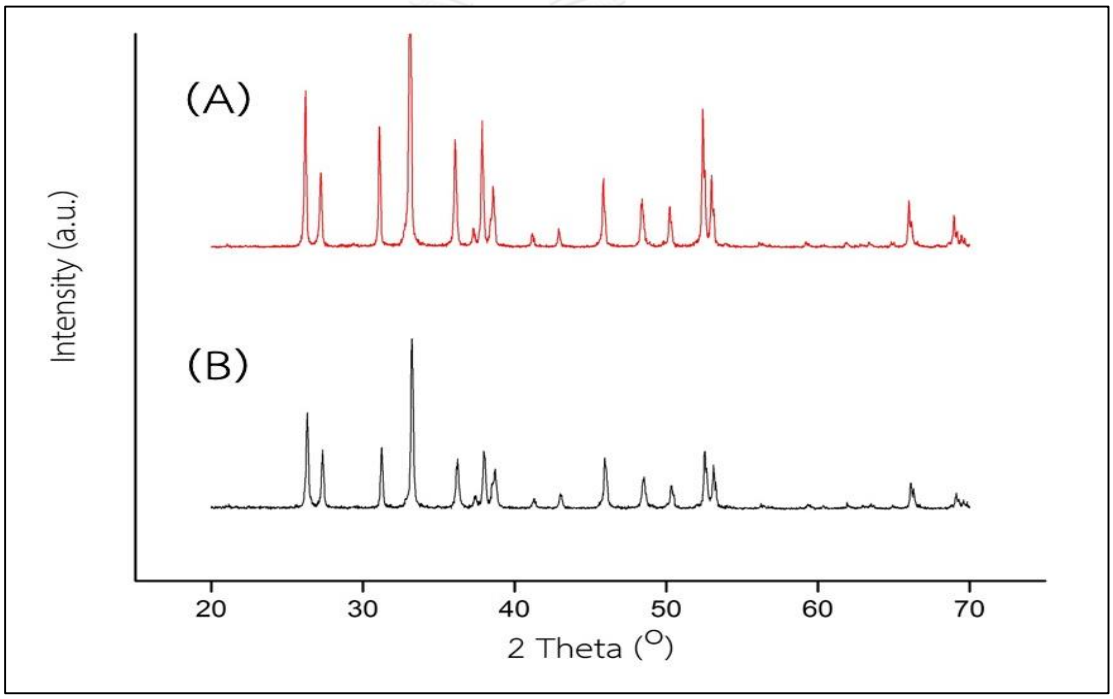


**Figure 4.9** XRD patterns for (A) $CaCO_3$-GMShell and (B) $CaCO_3$-EGMShell from green-mussel shell.

The $CaCO_3$-EGMShell (pure $CaCO_3$ after eliminated protein binders) was used to investigate the optimum condition for the temperature of calcination. The XRD results were shown in Figure 4.10

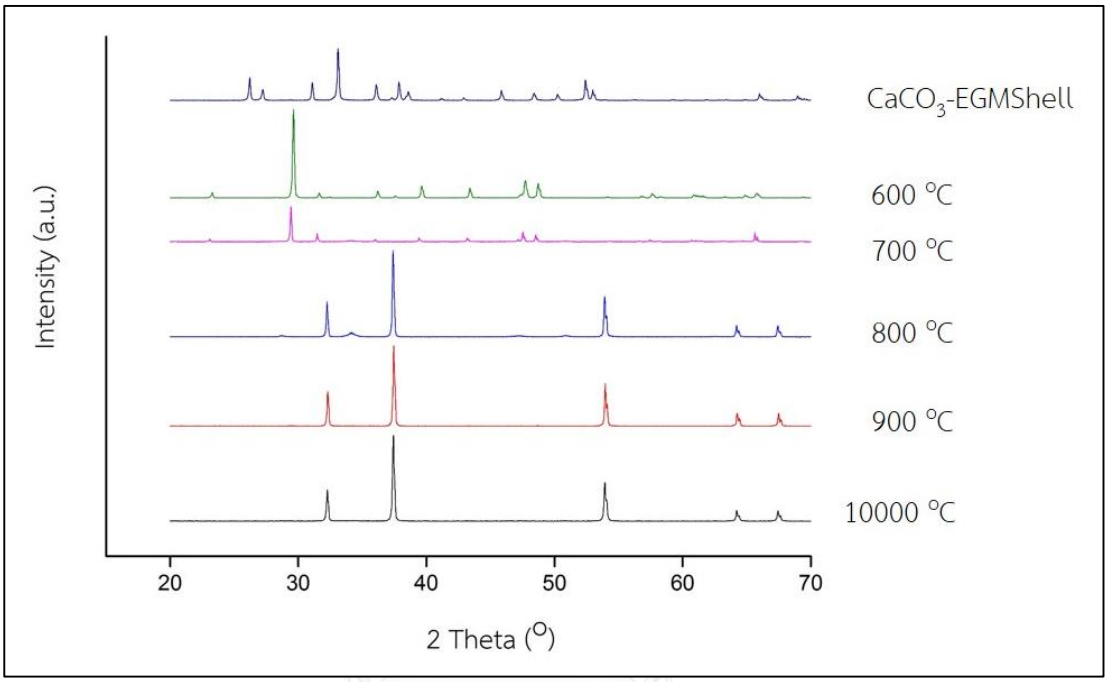


**Figure 4.10** XRD patterns of $CaCO_3$-EGMShell from green-mussel shells that were calcined at different temperatures from 600 to 1000 °C.

The calcite ($CaCO_3$) crystalline structure was obtained as the peaks corresponding with the JCPDS of No. 86-0174 were observed when $CaCO_3$-EGMShell was calcined at 600 and 700 °C. The peaks at 2θ of 29.480, 36.056, 39.497, 43.253, 47.579 and 48.579 were identified as the characteristic peaks of calcite. At above 800°C, the highest peak at 37.382 was observed and identified to the CaO crystalline phase. Therefore, we can conclude that the $CaCO_3$-EGMShell as aragonite and calcite (at 600 and 700 °C) phases completely converted to CaO phase at or above 800 °C. Besides, the smooth base lines of the XRD pattern at 900 °C implied that the impurities were removed comparing with the XRD pattern at 800 °C. These results from XRD indicated

that the $CaCO_3$-EGMShell can be completely converted to CaO under the temperature of calcination at above 800 °C. Moreover, the CaO-EGMShell at 900 °C were modified by wet impregnation with DI water, the XRD results were shown in Figure 4.11.

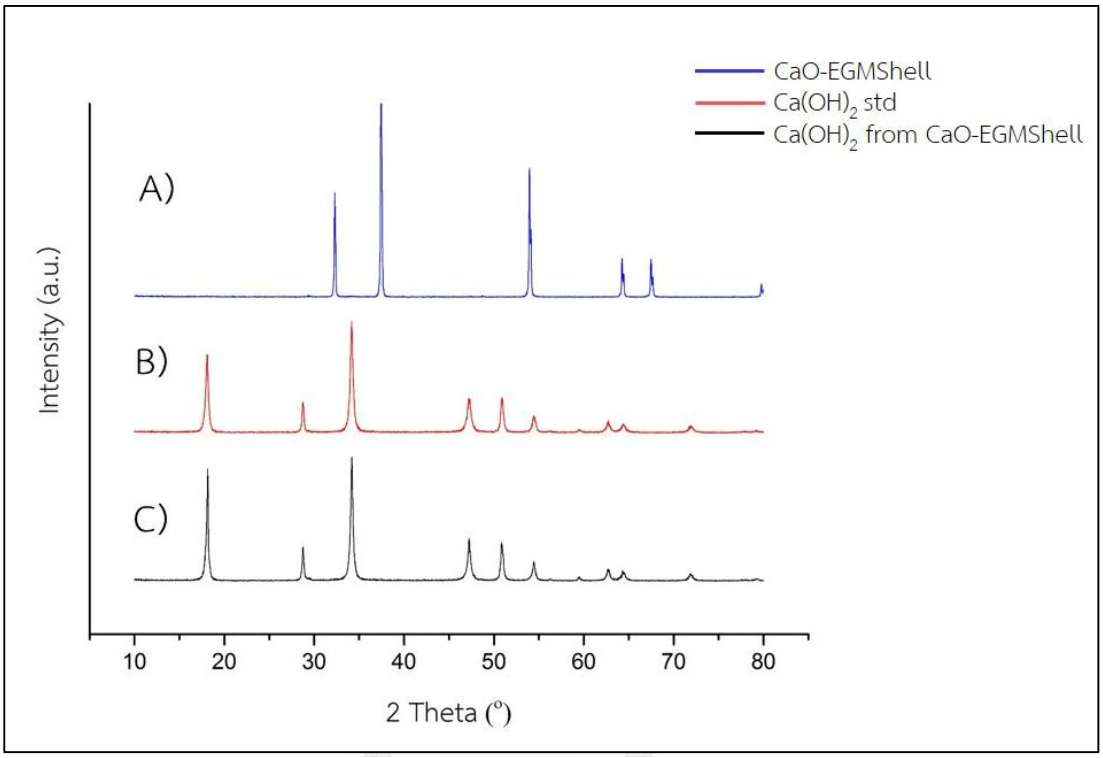


**Figure 4.11** XRD patterns of (A) CaO-EGMShell (B) Commercial $Ca(OH)_2$ used as standard and (C) $Ca(OH)_2$ from CaO-GMShell.

The XRD pattern of $Ca(OH)_2$ from CaO-EGMShell in Figure 4.11 (B) is similar to the XRD pattern of the commercial $Ca(OH)_2$. The peaks were observed at $2\theta$ of 28.741, 34.180, 47.219, 50.860, 54.401, 62.698 and 64.379, with the highest peak at 34.180 is the characteristic peak of $Ca(OH)_2$ as comparing with JCPDS of No.81-2040 (calcium hydroxide). The results can lead to the conclusion that the CaO-EGMShell transformed to $Ca(OH)_2$ phase when the CaO-EGMShell was modified using wet impregnation method.

### 4.3. Percent yield (% yield) of $CaCO_3$-precursors and CaO catalysts

Table 4.1 show the determination of percent yield of $CaCO_3$-precursors such as $CaCO_3$-GMShell and $CaCO_3$-EGMShell using different synthesis conditions such as including removal of protein residues with NaOH solution and cleaning up for eliminating of impurities with low concentration of HCl solution. The % yield of $CaCO_3$-GMShell and $CaCO_3$-EGMShell of 99.23 and 91.05 % were obtained, respectively.

**Table 4.1** Comparison of % yield $CaCO_3$-precursor

| Samples | Weight of $CaCO_3$-precursors | | | % Yield (%) |
|---|---|---|---|---|
| | Original (g) | Not-Purification (g) | Purification (g) | |
| $CaCO_3$-GMShell | 100.60 ± 0.27 | 99.83 ± 0.12 | - | 99.23 ± 0.27 |
| $CaCO_3$-EGMShell | 100.44 ± 0.21 | 99.64 ± 0.35 | 90.72 ± 0.55 | 91.05 ± 0.66 |

The results in Table 4.2 indicated that the high % yield of CaO was depended on the high purity $CaCO_3$-precursor then. The maximum of 99.34 % yield of CaO-EGShell was obtained when the $CaCO_3$-EGMShell was used as precursor because the $CaCO_3$-EGMShell had lower impurities than $CaCO_3$-GMShell.



**Table 4.2** Comparison of % yield of CaO from different $CaCO_3$-precursor after calcination under 900 °C for 5 h.

| Sample | Weight. (g) | Weight[b] (g) | % Yield[a] (%) |
|---|---|---|---|
| $CaCO_3$-GMShell | 5.0025 ± 0.0014 | 2.7459 ± 0.0064 | 98.07 ± 0.23 |
| $CaCO_3$-EGMShell | 5.0030 ± 0.0108 | 2.7816 ± 0.0800 | 99.34 ± 0.30 |

[a]In Comparison with theoretical CaO weight (2.80 g)

[b]After calcination and $CaCO_3$ converted to CaO phase

**4.4 The basic strength of CaO catalysts as investigated using various Hemmett indicators**

The basic strength of CaO-GMShell and CaO-EGMShell were determined using the Hammett indicator method [51-53]. The basic strength of CaO catalyst can be investigated with the color changing in indicators of different basic strength. The Table 4.3 showed the pKa and changes of color of the indicators used as references in this work.

**Table 4.3** List of Hammett indicators used as references in this work [51, 54-56]

| No. | Chemicals | $pK_a$ ($H_-$) | Color changed |
|---|---|---|---|
| 1 | Bromophenol blue | $H_-$ = 4.0 | Yellow to Blue |
| 2 | Methyl red | $H_-$ = 4.2 | Red to Yellow |
| 3 | Neutral red | $H_-$ = 6.8 | Red to Yellow |
| 4 | Bromothymol blue | $H_-$ = 7.2 | Yellow to Blue |
| 5 | Phenol red | $H_-$ = 7.4 | Yellow to Red |
| 6 | Phenolphthalein | $H_-$ = 9.8 | Colorless to Pink |
| 7 | Indigo carmine | $H_-$ = 12.2 | Blue to Yellow |
| 8 | 2,4-Dinitroaniline | $H_-$ = 15.0 | Yellow to Mauve |
| 9 | 4-nitroaniline | $H_-$ = 18.4 | Yellow to Orange |

As illustrated in Tables 4.4 and 4.5, the Hammett indicator test indicated that the samples had higher basic strength after calcination at or above 800 $^{o}$C comparing to the sample using low temperature for calcination. This result can be confirmed using XRD as the samples showed CaO phase. CaO-EGMShell can change the color of indigo carmine ($H_-$ = 12.2) from blue to yellow and 2,4-dinitroaniline ($H_-$ = 15.0) from yellow to orange but failed to change the color of 4-nitroaniline ($H_-$ = 18.4). Therefore, the basic strength of CaO-EGMShell was in the range of $12.2 < H_- < 15.0$ in accordance with the commercial CaO. This result showed that when the temperature of calcination increased, basic strength increased. Besides, the CaO-GMShell ($9.8 < H_- < 12.2$) had lower basic strength than CaO-EGMShell at 900 $^{o}$C as shown in Table 4.4.

**Table 4.4** The results of basic strength of CaO-GSMShell catalyst determined by Hammett indicator method

| Sample | Changes of Hammett indicators | | | | | | | | | Basic strength (H_) |
|---|---|---|---|---|---|---|---|---|---|---|
| | 1 | 2 | 3 | 4 | 5 | 6 | 7 | 8 | 9 | |
| $CaCO_3$- GMShell | x | x | x | x | x | x | x | x | x | 4.0 < H_ (no color change) |
| CaO-GMShell 600 °C | √ | √ | √ | x | x | x | x | x | x | 6.8 < H_ < 7.2 |
| CaO-GMShell 700 °C | √ | √ | √ | √ | √ | x | x | x | x | 7.4 < H_ < 9.8 |
| CaO-GMShell 800 °C | √ | √ | √ | √ | √ | √ | x | x | x | 9.8 < H_ < 12.2 |
| CaO-GMShell 900 °C | √ | √ | √ | √ | √ | √ | x | x | x | 9.8 < H_ < 12.2 |
| CaO-GMShell 1000 °C | √ | √ | √ | √ | √ | √ | √ | x | x | 12.2 < H_ < 15.0 |
| Commercial CaO | √ | √ | √ | √ | √ | √ | √ | x | x | 12.2 < H_ < 15.0 |

√ = Color change observed, x= no color change observed

**Table 4.5** The results of basic strength of the CaO-EGSMShell catalyst determined by Hammett indicator method

| Samples | Changes Hammett indicators | | | | | | | | | Basic strength (H_) |
|---|---|---|---|---|---|---|---|---|---|---|
| | 1 | 2 | 3 | 4 | 5 | 6 | 7 | 8 | 9 | |
| $CaCO_3$- EGMShell | x | x | x | x | x | x | x | x | x | 4.0 < H_ (no color change) |
| CaO-EGMShell 600 °C | √ | √ | √ | x | x | x | x | x | x | 6.8 < H_ < 7.2 |
| CaO-EGMShell 700 °C | √ | √ | √ | √ | √ | x | x | x | x | 7.4 < H_ < 9.8 |
| CaO-EGMShell 800 °C | √ | √ | √ | √ | √ | √ | x | x | x | 9.8 < H_ < 12.2 |
| CaO-EGMShell 900 °C | √ | √ | √ | √ | √ | √ | √ | x | x | 12.2 < H_ < 15.0 |
| CaO-EGMShell 1000 °C | √ | √ | √ | √ | √ | √ | √ | x | x | 12.2 < H_ < 15.0 |
| Commercial CaO | √ | √ | √ | √ | √ | √ | √ | x | x | 12.2 < H_ < 15.0 |

√ = Color change observed, x= no color change observed

### 4.4 Surface properties of CaO-EGMShell catalyst from green-mussel shell

The physical properties of CaO-EGMShell catalysts from green mussel shell after calcination at different temperatures ranging from 800-1000 °C for 5 h were examined using Brunauer-Emmett-Teller (BET) method for determination of specific surface area, total pore volume and average pore size diameter. The results were shown in Table 4.6.

**Table 4.6** Surface properties of adsorbents using BET method.

| Catalysts | Surface properties | | |
|---|---|---|---|
| | BET surface area ($m^2/g$) | Total pore volume ($cm^{-1}/g$) | Average Pore Diameter (Å) |
| [b]$CaCO_3$-EGMShell | 29.12 | $5.15 \times 10^{-2}$ | 70.1 |
| CaO-EGMShell 800 °C | 2.49 | $1.05 \times 10^{-2}$ | 169.3 |
| CaO-EGMShell 900 °C | 7.67 | $2.16 \times 10^{-2}$ | 112.4 |
| CaO-EGMShell 1000 °C | 0.47 | $6.10 \times 10^{-3}$ | 527.0 |

The surface area, pore volume and pore diameter of various adsorbents were determined using the nitrogen adsorption isotherms at 77 K. From the results in Table 4.6, the CaO-EGMShell converted by the calcination of $CaCO_3$-EGMShell at 900 °C for 5 h had the highest of BET surface area, total pore volume and average pore diameter. The pore diameter analysis showed that the catalysts were classified as the mesoporous material type as their pore diameters were in the range of 20-500 Å [57]. Therefore, calcination temperature at 900 °C were used to synthesis other CaO using different $CaCO_3$-precursor. Moreover, the surface properties of the delivered CaO from previous researches is presented in Table 4.6 for comparison with the BET results of CaO-EGMShell using green-mussel shell after calcination at 900 °C for 5 h in this work.

**Table 4.7** The BET surface area of CaO catalyst from previous reports

| Researchers | CaO Source | Calcination time (h) | Temperature of calcination (°C) | BET surface area ($m^2/g$) |
|---|---|---|---|---|
| Boro J. *et al.* [22] | *Turbonilla striatula* shell | 4 | 900 | 8.36 |
| Hu S. *et al.* [33] | Freshwater mussel | 5 | 900 | 1.50 |
| Vujicic DJ. *et al.* [58] | commercial CaO | - | 900 | 4.30 |
| Obadiah, A. *et al.* [59] | waste animal bone | - | 200 -1000 | 3.03 |
| Nair P. *et al.* [34] | Mereterix mereterix | 2.5 | 900 | 2.60 |
| Choudhury H.A. *et al.* [60] | Commercial CaO | 3 | 900 | 7.11 |
| This research | Green-mussel shell | 5 | 900 | 7.67 |

From Table 4.7, CaO from different sources exhibited the BET surface area in the range from 1.5 to 8.36 $m^2/g$. In this work, the BET surface area of CaO (CaO-EGMShell) was comparable with the results from research of Choudhury H.A [60] and Boro J. [22] as the BET surface area of CaO-EGMShell was investigated as in range of around 7 to 8 $m^2/g$.

## 4.5 Adsorption-desorption isotherms of catalysts from green-mussel shell

The nitrogen adsorption-desorption isotherms for $CaCO_3$-EGMShell, CaO-EGMShell and $Ca(OH)_2$-EGMshell from purified $CaCO_3$ of green-mussel shells were presented in the Figure 4.13, 4.14 and 4.15, respectively. All samples exhibited type IV isotherms, which are a character of mesoporous materials according to IUPAC classification. Moreover, the hysteresis loops were observed at high relative pressures, confirming the mesoporous characters according with previous works from Yoosuk (2010) [61] and Lertpanyapornchai (2015) [62].

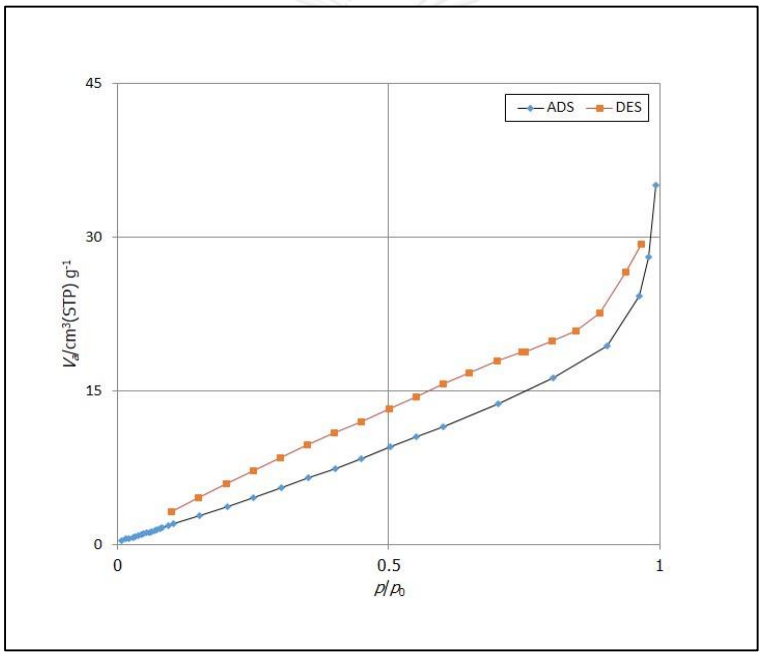


**Figure 4.12** Adsorption isotherm of $CaCO_3$-EGMShell when P: Pressure, $P_0$: Pressure saturated.

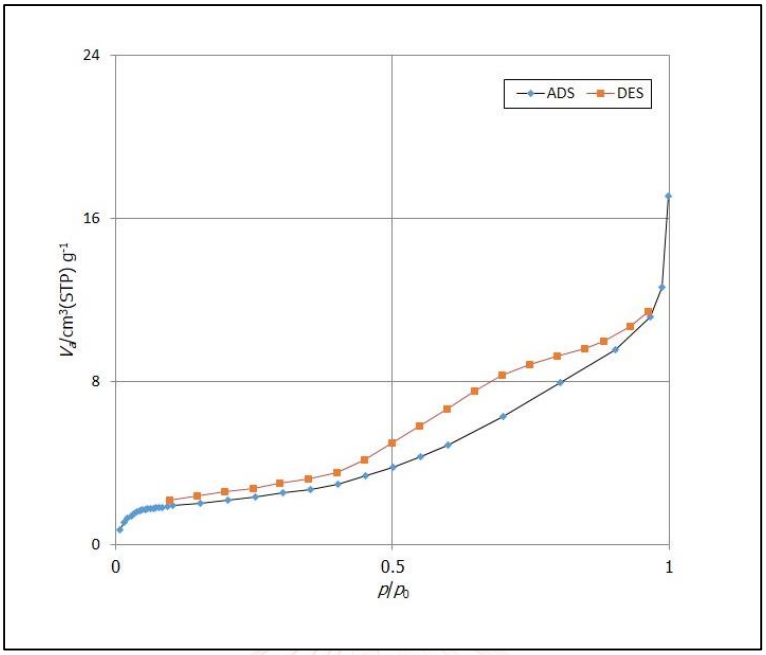


**Figure 4.13** Adsorption isotherm of CaO-EGMShell when P: Pressure, $P_0$: Pressure saturated.

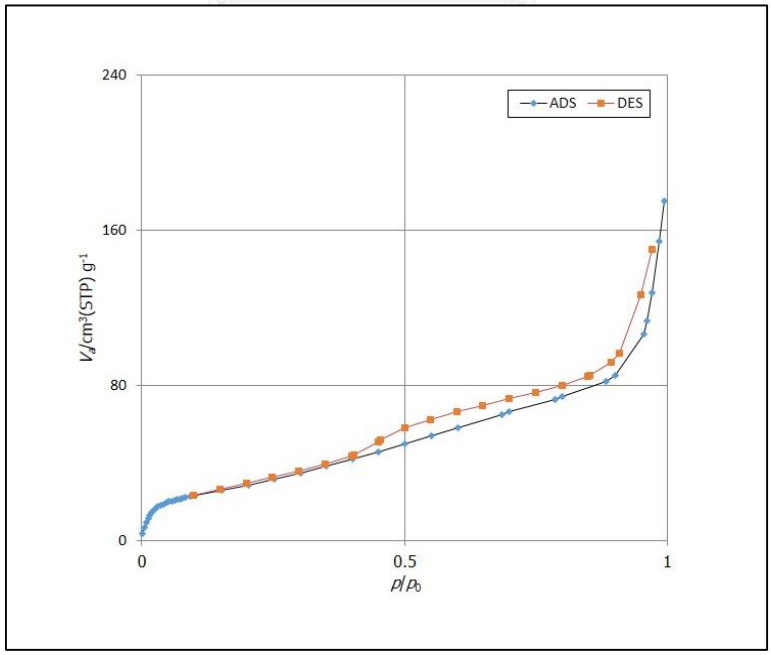


**Figure 4.14** Adsorption isotherm of $Ca(OH)_2$-EGMShell when P: Pressure, $P_0$: Pressure saturated.

## 4.6 Morphological studies using FESEM technique

### 4.6.1 FESEM images of $CaCO_3$-precursor from natural and eliminated residue on surface of green-mussel shell

The morphology of $CaCO_3$-GMShell as $CaCO_3$-precursor after removal of impurities on the surfaces of green-mussel shells were investigated using FESEM. From the results in Figure 4.15, it was observed that there were different surface patterns of the both samples. Figure 4.15 of (A) and (B) showed the multilayer, which is a typical layered architecture [63] of the layered nacres from effect of organic matrix deposited on surface of green-mussel shells. Then, the surface of natural green-mussel shells were obtained in the form of multilayer of nacre layers [64, 65]. The several single and aggregated sheets of $CaCO_3$-GMShell as $CaCO_3$-precursor after impurity elimination with NaOH solution were observed in Figure 4.15 (C) and (D). After the organic matrix were removed using the NaOH solution, different morphological patterns in comparison to (A) and (B) in Figure 4.15 were obtained.

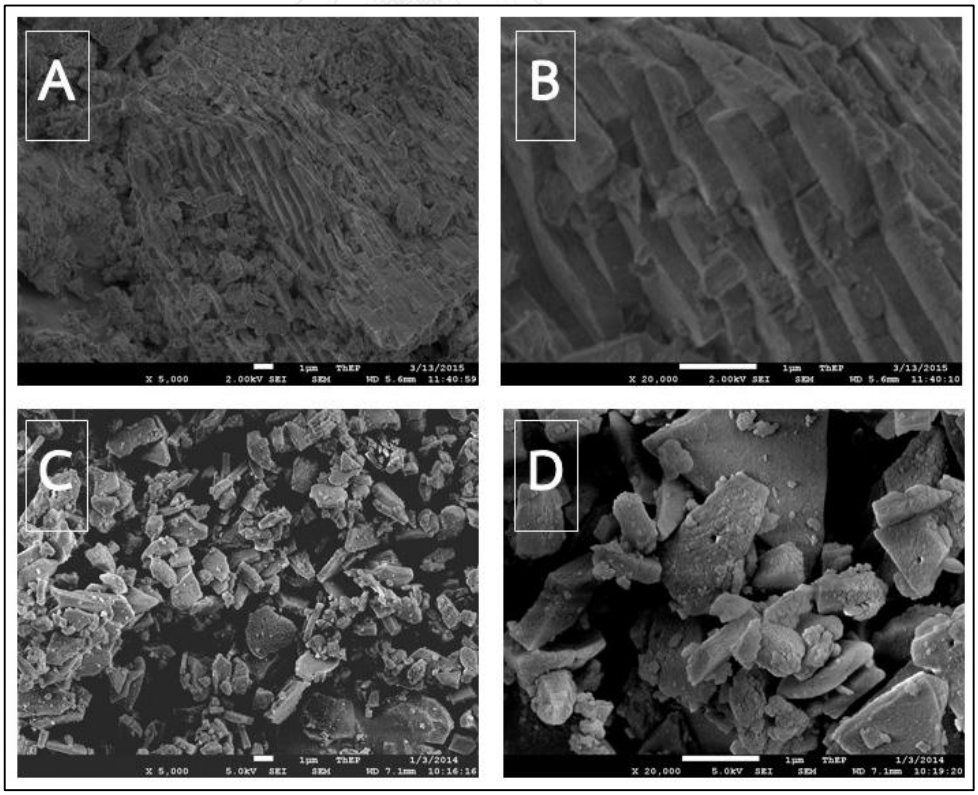


**Figure 4.15** SEM images of (A).and (B) $CaCO_3$-GMShell; and (C) and (D) $CaCO_3$-EGShell.

**4.6.2 FESEM images of CaO from natural after elimination of residues on surface of green-mussel shell after calcination at 900 °C for 5 h**

The morphological fractures of $CaCO_3$-GMShell and $CaCO_3$-EGMShell were observed in different patterns before and after calcination at 900 °C for 5 h. The microstructures and sheets of $CaCO_3$-precursor were transformed significantly in that there were a reduction in sizes and changes of morphologies. Then, the porous and slit structures appeared on their surfaces because high temperature from direct calcination and long calcination time can induce the decrease in sizes and morphologies into the form of microstructures and unique sheet structures [66]. The results were shown in the Figure 4.16.

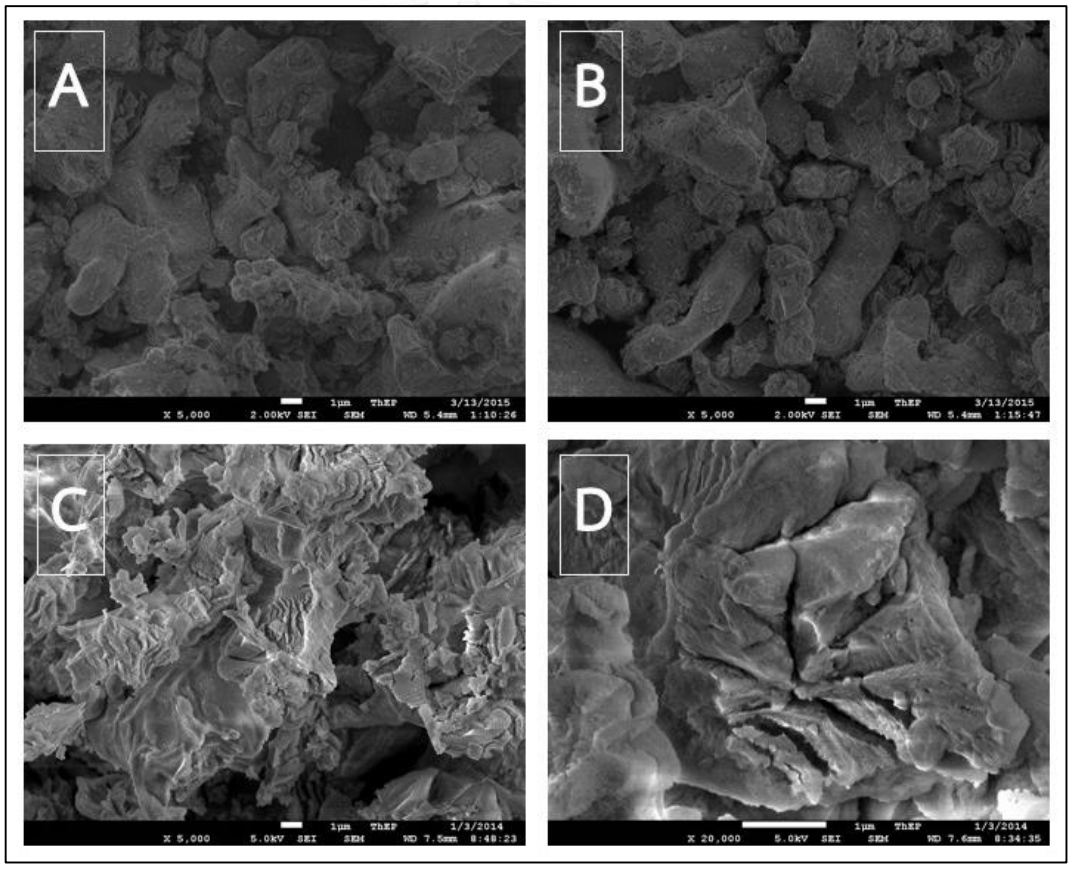


**Figure 4.16** SEM images of (A).and (B). $CaCO_3$-GMShell and (C) and (D) $CaCO_3$-EGMShell after calcination at 900 °C for 5 h.

### 4.7 Physical properties of refined palm oil

The refined palm oil from the Olein co, th., Thailand (figure 4.17) was used as a raw material for producing biodiesel. The physical properties of refined palm oil were investigated to find saponification value (SN), % free fatty acid (FFA) and molecular weight. The results were shown in Table 4.8.

**Figure 4.17** A photograph of refined palm oil from the Olein co, th. Thailand used as a raw material.



**Table 4.8** Properties of refined palm oil used in the present study

| Properties | Value | Unit |
|---|---|---|
| Saponification value | 196.59 ± 0.5 | mg KOH/g of oil |
| Free fatty acid | 0.69 ± 0.1 | % |
| Molecular weight | 856.10 ± 1.2 | g/mol |

The transesterification was used to synthesize biodiesel. In this experimental method, the parameters such as amount of catalyst loaded, methanol to oil molar ratio, reaction temperature, reaction time and speed of agitation were adjusted to investigate to optimized conditions for the synthesis of biodiesel using synthesized CaO catalyst from green-mussel shell.

### 4.8 Influences of parameters on catalytic activity of CaO catalysts in transesterification

#### 4.8.1 Effect of optimized conditions for synthesis of biodiesel using different types of CaO catalysts

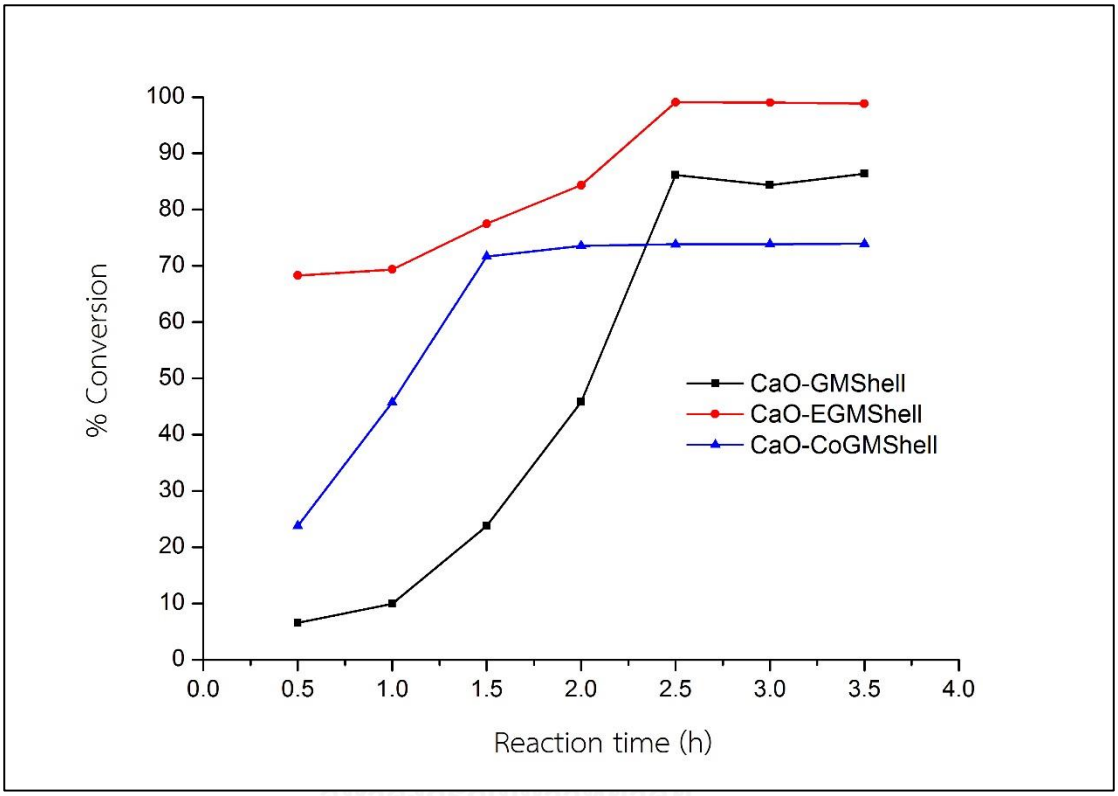




**Figure 4.18** Effect of different types of CaO catalysts on the conversion of palm oil under the reaction condition of methanol to oil molar ratio; 12:1, reaction temperature, 64 ± 1 °C, reaction time of 0-4 h and constant agitation speed at 500 rpm.

The catalyst activities of different CaO were compared under the identical condition for synthesis biodiesel via tranesterification reaction. The condition used is that amount of catalyst loaded of 10 wt. % (base on oil weight), methanol to oil molar ratio of 12:1, reaction temperature of 64 ± 1 °C for 2 h at constant speed agitation of 500 rpm. The different types of CaO catalyst including CaO-GMShell from $CaCO_3$-GMShell, CaO-EGMShell from $CaCO_3$-EGMShell and CaO-CoGMShell from $CaCO_3$-CoGMShell were used as catalysts for comparing their effects on catalytic activity. The

highest conversion of biodiesel from 0.5 h after reaction finished at 3.5 h were obtained when CaO-EGMShell was used as catalyst. Then, the catalytic activities of different CaO catalysts were concluded as shown in the trend line in Figure 4.18.

CaO-EGMShell was cleaned up to remove organic matrix on green-mussel shells surface with NaOH and HCl solutions. Then, the surface of CaO-EGMShell had active basic sites (clear surface). When the triglyceride from oil and methanol reacted on surface of CaO-EGMShell during reaction, the CaO-EGMShell was more active than CaO-GMShell (the sample without pretreated of its surface). In addition, the CaO-EGMShell was compared with CaO-CoGMShell in transesterification under the same condition and it was found that the CaO-EGMShell tended to be more stable in methanol than CaO-CoGMShell. This result was likely because of the effects of a small amount of organic matrix binding in its porous structure and surface. To confirm this prediction, the organic matrix in CaO-EGMShell after digestion with HCl solution was investigated by FTIR and found in accordance with the previous work [67]. Therefore, CaO-EGMShell has higher stability than CaO-CoGMShell (the sample without organic matrix and regenerated by co-precipitation) as the percent conversion rate in biodiesel synthesis of the two catalysts were compared in this experimental section. Moreover, higher surface area is one of the important factors observed in this reaction. The highest surface area of CaO-EGMShell (7.67 $m^2/g$) was obtained in comparison with CaO-GMShell (3.33 $m^2/g$) and CaO-CoGMShell (5.59 $m^2/g$.) These results indicated that high surface area of catalyst can promote the rate of the reaction more than catalyst with low surface area leading to the high percent conversion of biodiesel production [68] under the same condition.

In conclusion for this experiment, the CaO-EGMShell were chosen for synthesis of biodiesel for the next experiment because not only the highest % conversion were obtained in 0.5 to 2.5 h when compared with CaO-GMShell and CaO-CoGMShell, but also the high stability from a small amount of protein binders remained in inside catalyst pores and on surfaces as investigated by FTIR technique.

### 4.8.2 Effect of calcination temperature of CaO-EGMShell catalyst

In this experiment, the CaO-GMShell catalyst generated from various calcination temperatures were studied for their catalytic activities. The studies were done by loading the catalyst in the transesterification under the condition of 10 wt. % catalyst; methanol to oil molar ratio of 12:1, reaction temperature of 64 ± 1 °C for 2 h at 500 rpm. The results were indicated in Figure 4.19.

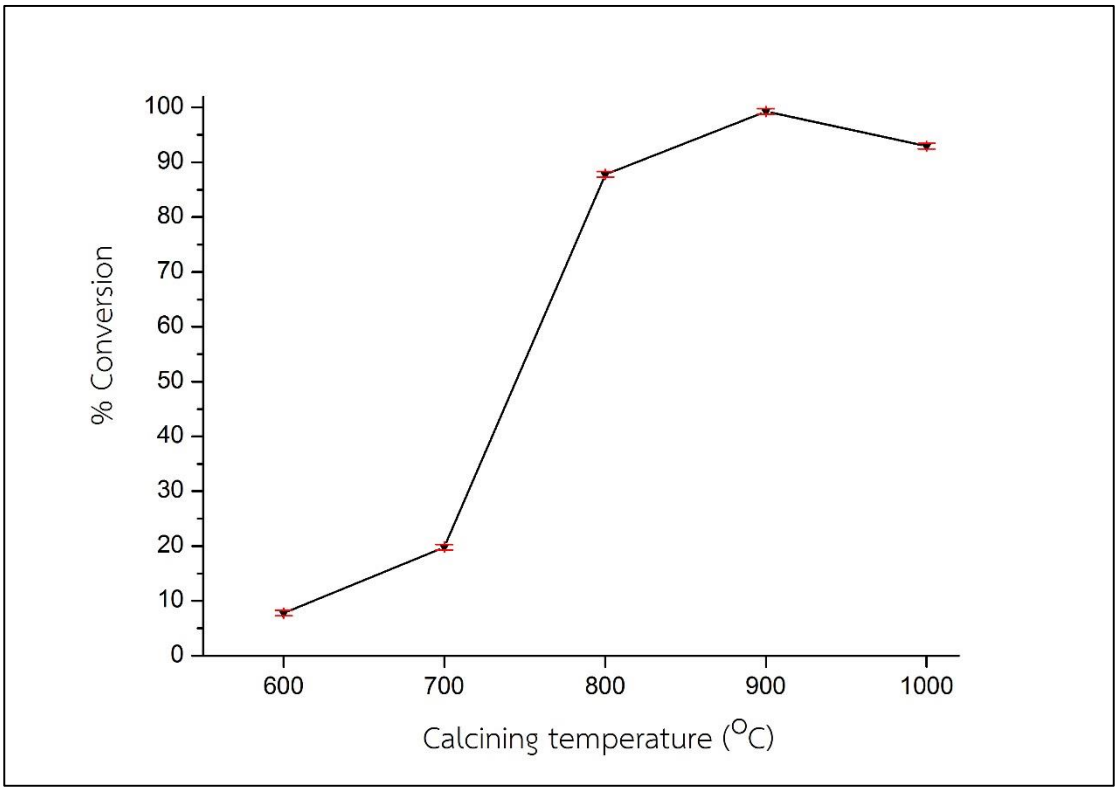


**Figure 4.19** Effect of calcination temperature on the conversion of palm oil using CaO-GMShell catalyst with the reaction condition of methanol to oil molar ratio of 12:1, reaction temperature of 64 ± 1 °C, reaction time of 2 h and agitation speed at 500 rpm.

The maximum conversion of palm oil of 99.25 % was obtained when $CaCO_3$-GMShell were calcined under temperature of 900 °C for 5 h. The XRD results indicated that the $CaCO_3$ from green-mussel shells completely converted to CaO above temperature for calcination of 800 °C [69-71]. Moreover, the % conversion of palm oil

was depended on with the basicity of catalyst, high basicity should help converting triglyceride to fatty acid methyl esters (FAME) better than the catalyst with low basicity. The CaO-EGMShell catalyst calcined above 800 °C showed the higher % conversion because the catalyst in form CaO have more basic strength than the calcite form (at 600 and 700 °C).

Besides, the highest specific surface area of CaO-GMShell were the one calcined at 900 °C. This is likely due to the organic matrix and impurities of $CaCO_3$-precursors were completely eliminated when calcined above 800 °C. The results in Figure 4.20 showed the black and light gray of powdery solid, likely due to the fact that the residues from a little amount of organic matrix cannot be removed at lower temperature, which was obtained after calcination at 600 and 700 °C, respectively. Moreover, the residues were easily eliminated and cleanly white powdery solid were obtained at above 800 °C.

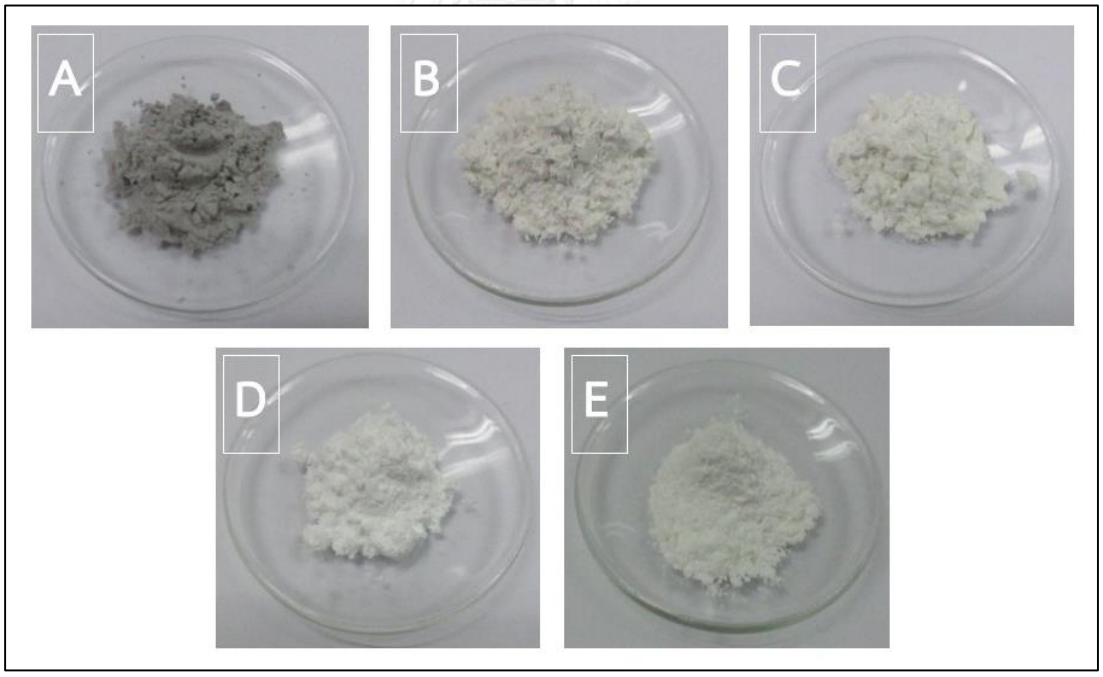


**Figure 4.20** The powdery solid products after calcination at (A) 600 °C, (B) 700 °C, (C) 800 °C, (D) 900 °C and (E) 1000 °C.

### 4.8.3 Effect of calcination time of CaO-EGMShell catalyst

The influence of calcination time was investigated by varying time for calcination of green-mussel shell from 1 to 6 h. In this experiment, CaO-EGMShell samples from difference calcination times were used as catalyst in transesterification with methanol to oil molar ratio of 12:1 at 64 ± 1 °C for 2 h for synthesis of biodiesel. As the results shown in Figure 4.21, the percent conversion of palm oil increased from 8.04 to 97.21 % when using the range of calcination time from 1 to 5 h. Besides, the percent conversion was dropped after calcination for 6 h was used in this experiment. This observation might due to the effect of aggregation of particles from the powdery solid of CaO-EGMShell after calcination for 6 h leading to the decrease in surface area.

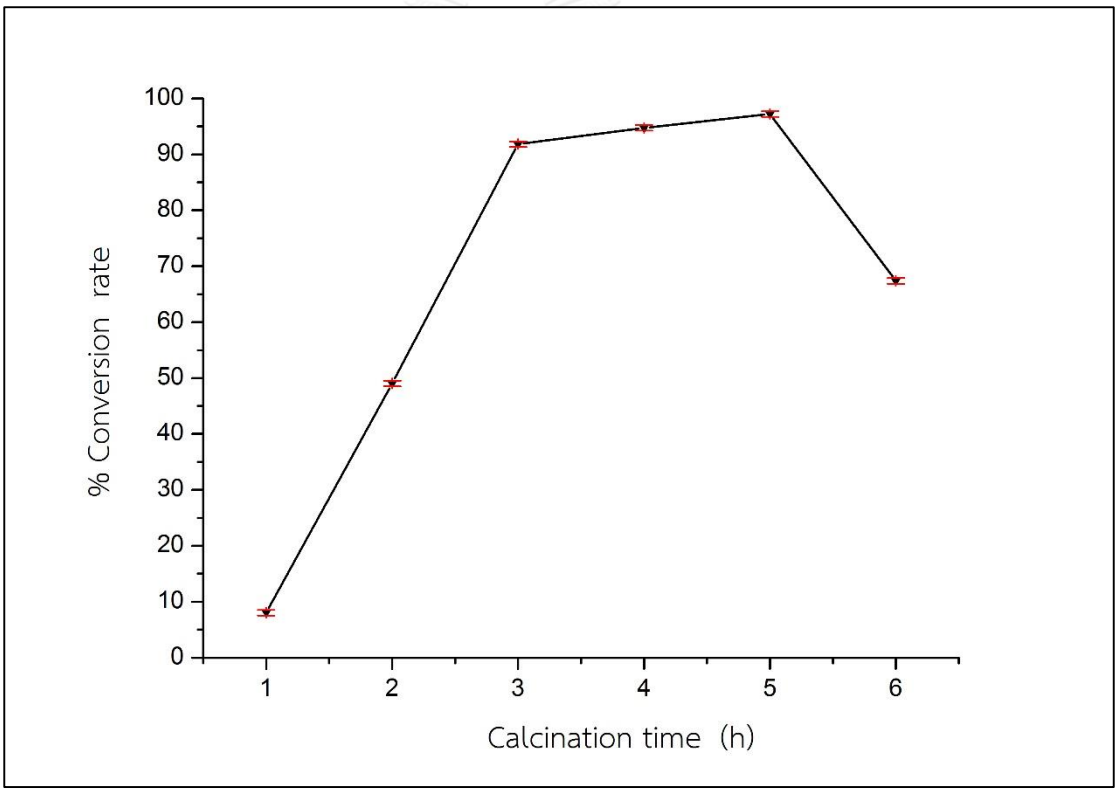


**Figure 4.21** Effect of calcination time on conversion of palm oil using CaO-GMShell catalyst. Reaction condition were 10 wt. % catalyst, methanol to oil molar ratio of 12:1, reaction temperature at 64 ± 1 °C, reaction time for 2 h and agitation speed at 500 rpm.

### 4.8.4 Effect of amount of CaO catalyst loaded on % conversion

The varying amount of CaO-EGMShell catalyst was loaded from 0.5 to 4.5 wt. % (based on refined palm oil weight) for synthesis of biodiesel under the condition of methanol to oil molar ratio of 6:1, reaction temperature of 64 ± 1 °C at constant agitation speed at 500 rpm for 2 h. The results were presented in Figure 4.22.

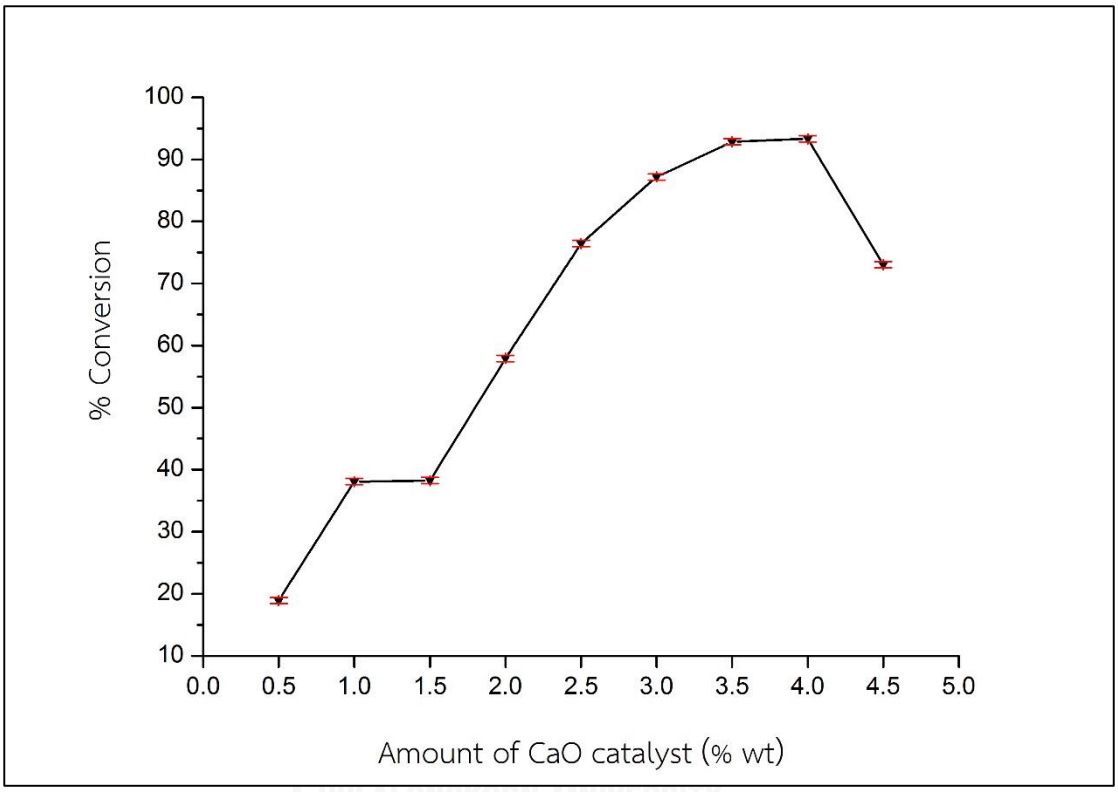




**Figure 4.22** Effect of amount of catalyst loaded on conversion of palm oil using CaO-EGMShell catalyst. Reaction condition of methanol to oil molar ratio of 6:1, reaction temperature of 64 ± 1 °C, reaction time of 2 h and agitation speed at 500 rpm.

From the results presented in Figure 4.22, the maximum conversion of 93.31 % was obtained when 4 wt. % CaO-EGMShell catalyst was used. The results can be explained that when the amount of catalyst increased, the contact surface area of catalyst increase, and the triglyceride molecules can react with methoxide ion on its surface more [36, 55]. Therefore, the % conversion of biodiesel was depended on the

amount of contact surface. The probability of generation of methoxide ion as nucleophile on catalyst surface were increased when the contact surface increased.

The important role of the methoxide ion was that it can attack the carbonyl group of triglyceride during in the reaction before converting to FAME and by-products [72] such as diglyceride, monoglyceride and glycerol when the reaction completely finished. Besides, the effect of mass transfer from excess amount of catalyst to the reactants, refined palm oil and methanol, were observed as the decrease in % conversion after the amount of catalyst loaded over 4 % wt. In this experiment, 96.65 % yield of biodiesel was obtained. Then, the optimal condition for synthesis of biodiesel was used 4 % wt of CaO-EGMShell catalyst loading in the reaction as the result shown in Table 4.9.

**Table 4.9** Effect of amount of catalyst loaded on the yield of production

| **Catalyst** | **Amount of catalyst loaded (wt. %)** | **Yield (%)** |
|---|---|---|
| CaO[a] | 1.0 | 98.77 |
| | 2.0 | 96.50 |
| | 3.0 | 97.79 |
| | 4.0 | 96.65 |
| | 4.5 | 90.34 |

Reaction condition[a]: Methanol to oil molar ratio,6:1, temperature, 64 ± 1 $^{o}$C, time, 2 h.

### 4.8.5 Effect of methanol to oil molar ratio on % conversion

The molar ratio of methanol to oil is a significant factor for synthesis biodiesel. Theoretically, 3 mol of alcohol was required in the transesterification to react with 1 mol triglyceride and given 3 mol fatty acid methyl ester and 1 mol glycerol after the reaction finished. In this experiment, methanol to oil molar ratio was varied from 3:1 to 15:1 under the condition with fixed parameters of amount of catalyst at 4 wt. %, reaction temperature of 64 ± 1 °C at 500 rpm for 2 h. The results displayed in the Figure 4.23.

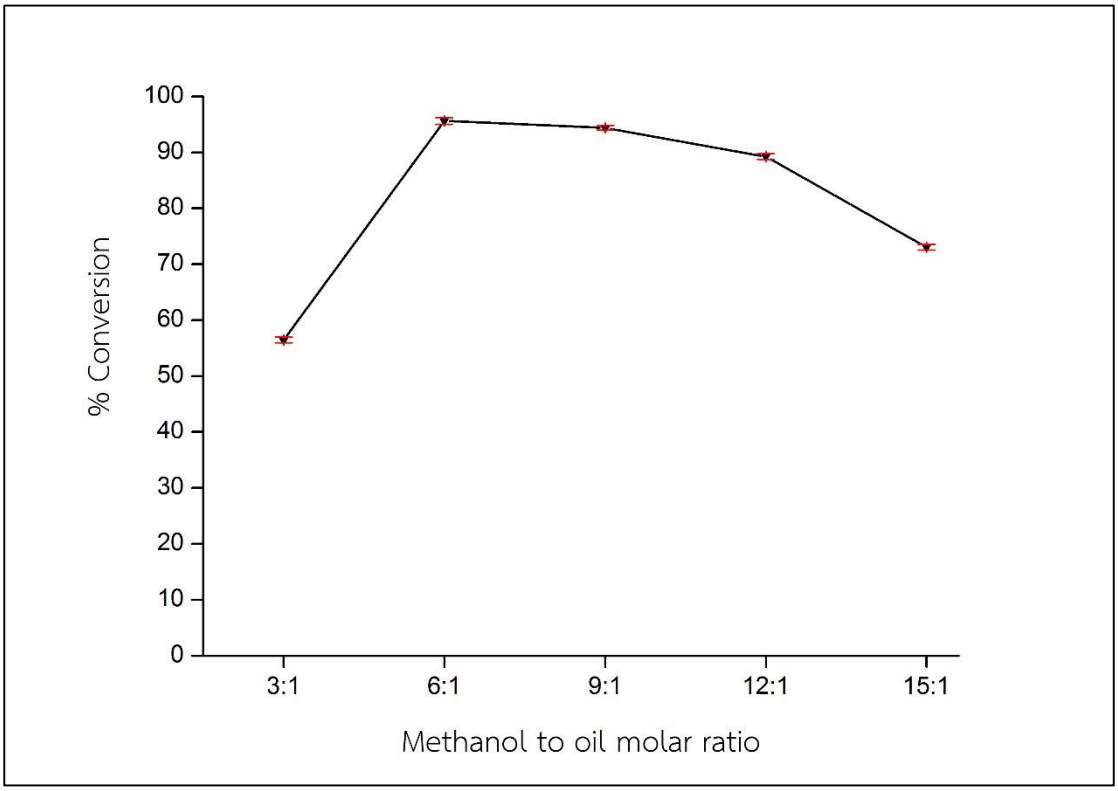


**Figure 4.23** Effect of methanol to oil molar ratio on conversion of palm oil using CaO-EGMShell catalyst. Reaction condition were 4 wt. % catalyst, reaction temperature at 64 ± 1 °C, reaction time for 2 h and agitation speed at 500 rpm.

The maximum percent conversion of 95.62 % was observed when 6:1 methanol molar ratio was used. This results can be described that the excess methanol under ratio of 6:1 cannot drive the transesterification reaction forward and shifted the

equilibrium for triglyceride to FAME and glycerol completely. In contrast, the conversion rate was decreased when the methanol to oil molar ratio was used above 6:1. This is due to higher amount of methanol can dissolve the diglyceride, monoglyceride and glycerol during in the reaction, resulting in the mix of the methanol phase and glyceride phase to form homogenous phase. Therefore, the optimum methanol to oil molar ratio was used as 6:1.

### 4.8.6 Effect of reaction temperature on % conversion

Transesterification of vegetable oil with alkaline catalyst were normally performed under temperature ranging between 45 $^{o}$C to 65 $^{o}$C [73]. In this experimental section, effects of reaction temperature were studied by varying temperature in the range of 35 to 75 $^{o}$C in the synthesis of biodiesel. The condition used was 4 wt. % CaO-EGMShell catalyst with methanol to oil ratio of 6:1 for 2 h under constant agitation speed at 500 rpm. The results of this study showed that the % conversion of palm oil was increased when the temperature increased as shown in Figure 4.24. Therefore, the conversion of palm oil of 98.04 % was obtained at 65 $^{o}$C (64 ± 1$^{o}$C). However, the % conversion was decreased when temperature was above 65 $^{o}$C because methanol was easily evaporated under temperature above 65 $^{o}$C as the boiling point of methanol is approximate 65 $^{o}$C (64.7 $^{o}$C).

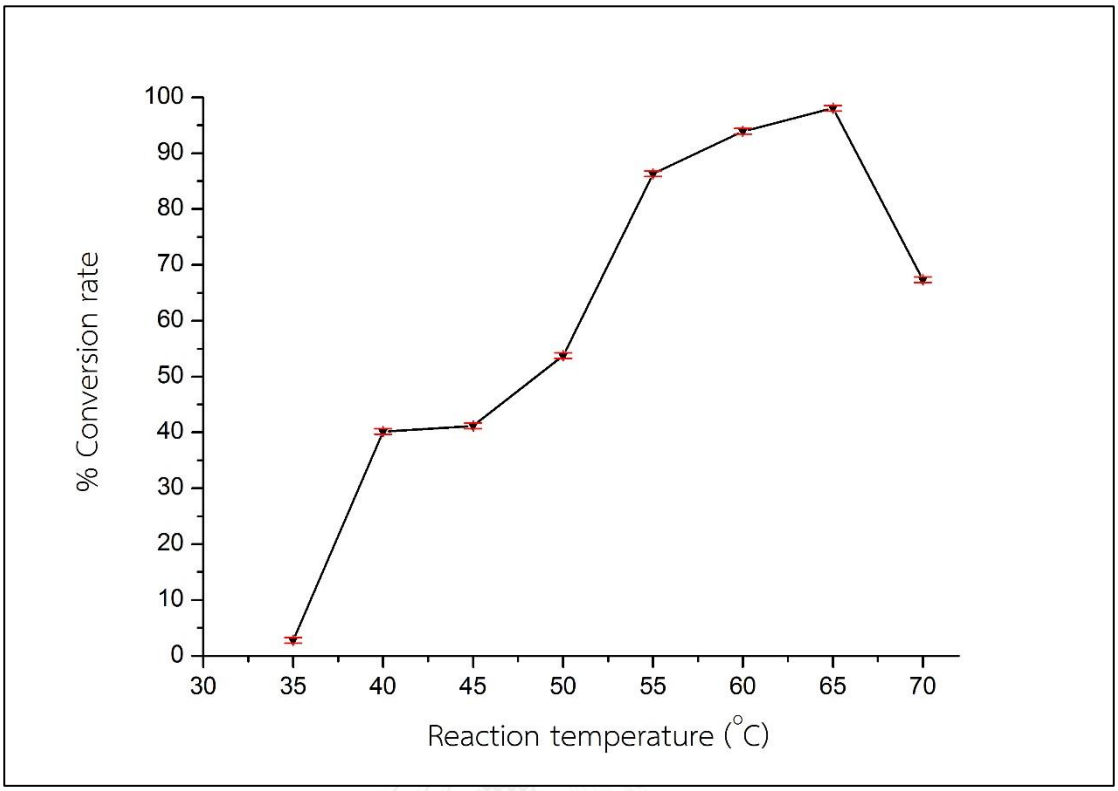


**Figure 4.24** Effect of reaction temperature on conversion of palm oil by using CaO-EGMShell catalyst. Reaction condition were 4 wt. % catalyst, methanol to oil molar ratio of 6:1, reaction time for 2 h and agitation speed at 500 rpm.

### 4.8.7 Effect of water loaded on % conversion

The effect of a small quantity of water is an important factor for biodiesel production. Water can quickly promoted the generation of methoxide anion as the real catalyst when the CaO catalyst react with methanol in transesterification leading to the higher yield of biodiesel within a short time [29, 74]. The results were illustrated in Figure 4.25.

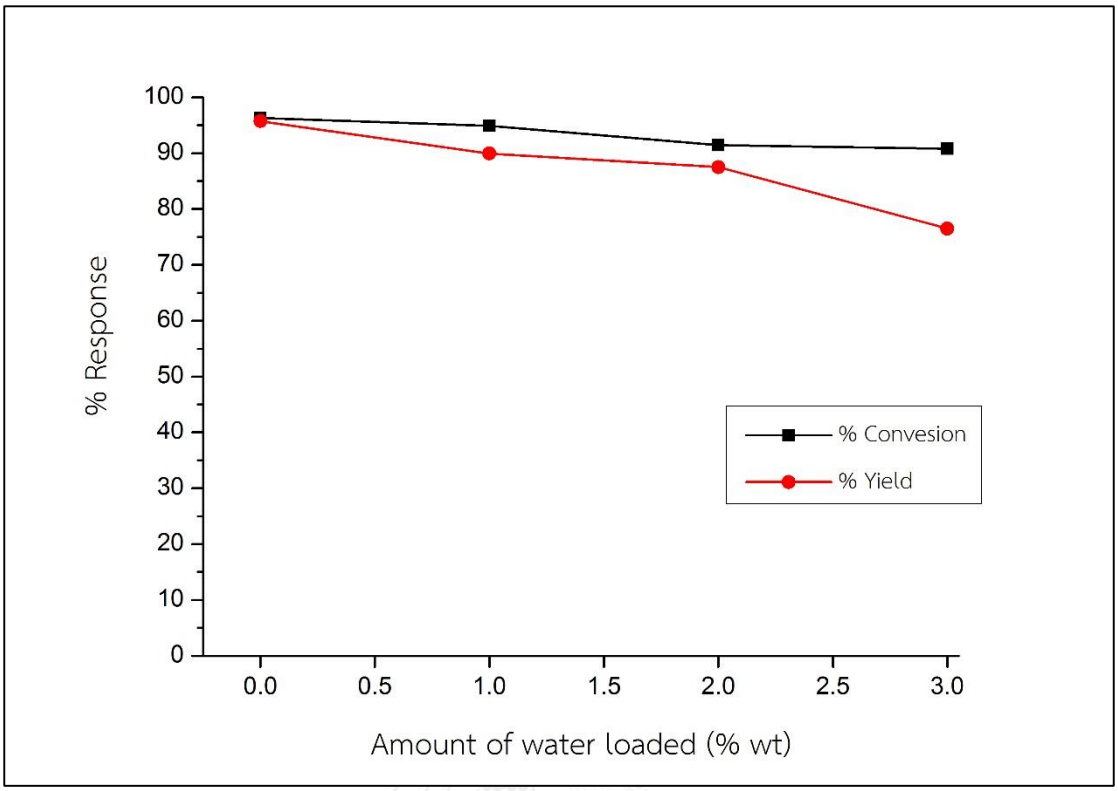


**Figure 4.25** Effect of amount of water loaded on conversion rate of palm oil using CaO-GMShell catalyst. Reaction condition were 4 wt. % catalyst, methanol to oil molar ratio of 6:1, reaction temperature at 64 ± 1 °C, reaction time for 2 h and agitation speed at 500 rpm.



In this experiment, percent conversion and yield of biodiesel decreased when larger amount of water were loaded in the reaction. The results were due to the fact that high amount of water can be hydrolysed methyl ester during in the transesterification and generated free fatty acids (FAA). Then, the soap was generated when the FAA reacted with CaO-EGMshell base catalyst from saponification reaction [75] as side reaction in this case. Moreover, the FAA can reduce catalytic activity of the catalyst in transesterification. These effects caused the decrease in the percent conversion and yield significantly.

### 4.8.8 Effect of agitation speed on % conversion

The effect of agitation speed or stirring speed is an important factor affecting percent conversion and yield in producing biodiesel. Several previous works have been studied to examine this effect. Vicente (2005) [76] and Jang (2010) [77] reported the agitation speed at 600 rpm as the optimum condition for synthesis biodiesel. In this experiment, the effect of agitation speed for mixing reactants such as triglyceride and methanol during the reaction with CaO-EGMShell catalyst in the transesterification reaction was investigated. The results showed in Figure 4.26.

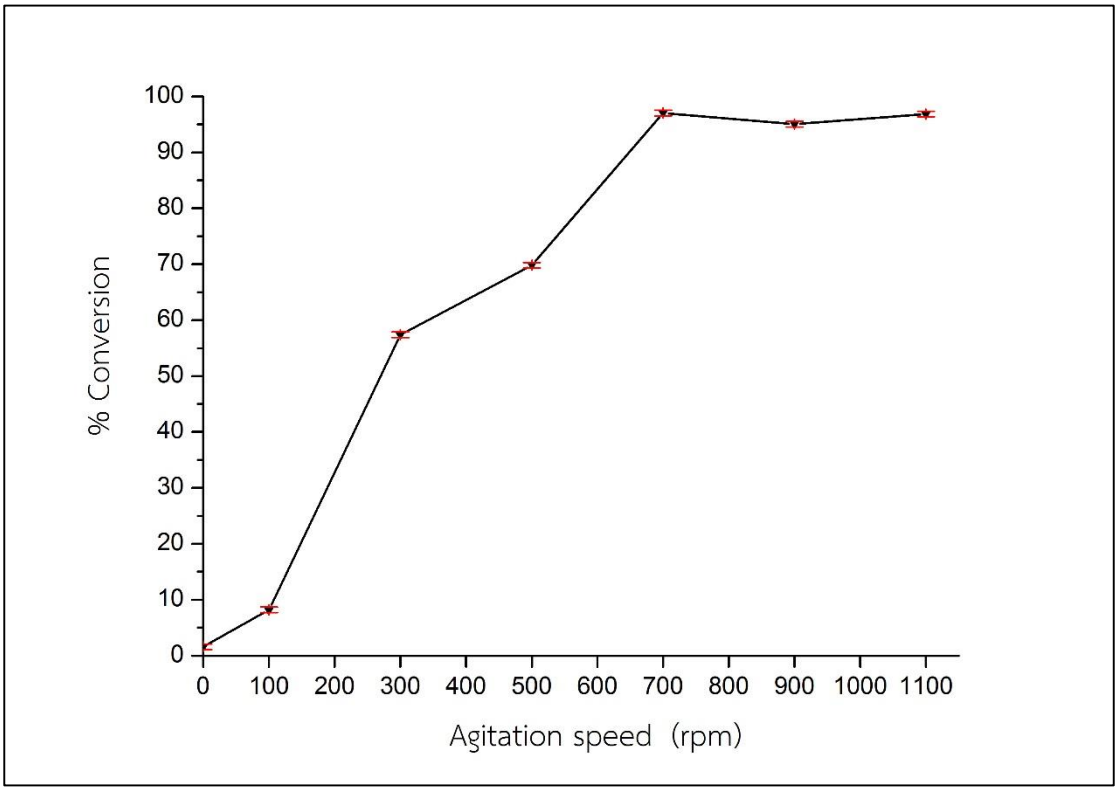


**Figure 4.26** Effect of agitation speed on conversion rate of palm oil using CaO-GMShell catalyst. Reaction condition were 4 wt. % catalyst, methanol to oil molar ratio of 6:1, reaction temperature at 64 ± 1 $^{o}$C, reaction time for 2 h.

The agitation speeds were varied from 0, 100, 300, 500, 700, 900 and 1100 rpm. The results clearly depicted in Figure 4.26 that the percent conversion increased when the stirring speed increased from 0 to 1100 rpm. At low agitation speeds (0 to 500

rpm), the two layers of mixture, upper layer of refined palm oil and methanol and lower layer of CaO-EGMShell catalyst, were found during transesterification reaction. In these conditions, it was observed that the reaction with low speed and without stirring speed could reduce the percent conversion rate of biodiesel because the two layer of mixture cannot mix completely. Therefore, reactions between reactants and catalyst were too slow. Also, soap was easily generated under the low agitation speed. These observations of soap formation were shown in Figure 4.27.

Moreover, the high percent conversion was obtained when the reaction stirred at above 500 rpm because it can reduce viscosity and promote homogenous phase of mixture. Therefore, the reaction shifted forward rapidly to obtain FAME as main product in biodiesel with maximum conversion rate of 97.04 % was obtained at 700 rpm.

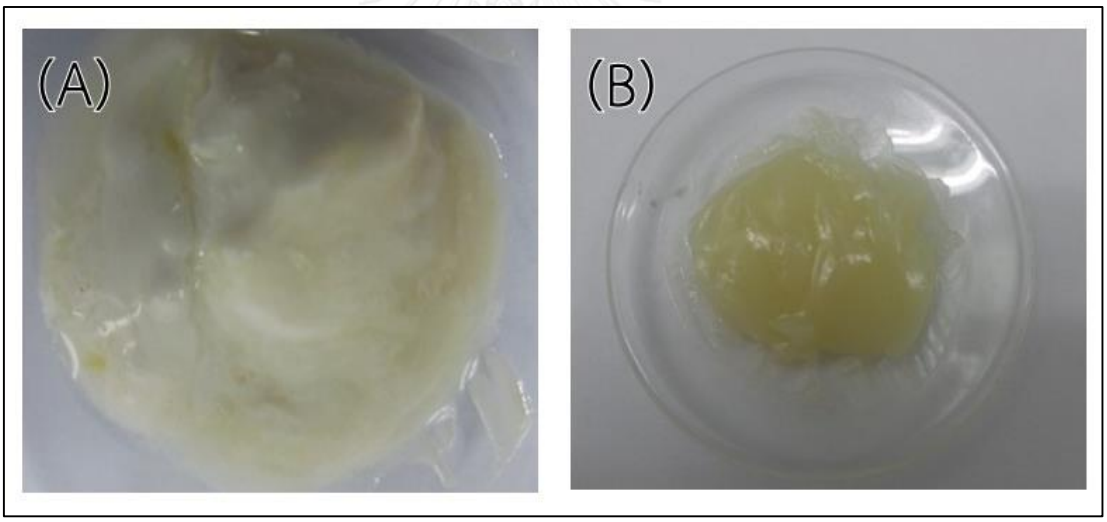


**Figure 4.27** Photograph of the mixtures of product and CaO-EGMShell catalyst after the reaction finished (A) before and (B) after the separation of CaO-EGMShell catalyst.

### 4.8.9 Effect of reaction time on % conversion

Duration of transesterification reaction has been designated as one of crucial parameters for synthesis biodiesel. To investigate the effect of reaction time for producing biodiesel in this experiment, the reaction time were varied from 30 to 240 minutes using optimal condition of 4 wt. % catalyst loaded, methanol to oil molar ratio of 6:1 at 64 ± 1 °C and constant agitation speed of 700 rpm. The percent conversion of biodiesel increased from 68.26 to 98.69 % when the reaction times from 30 to 150 minute were used. Besides, the higher percent conversion were observed at 150 minute and remained constant after reaction finished after 150 minute. The results were shown in Figure 4.28.

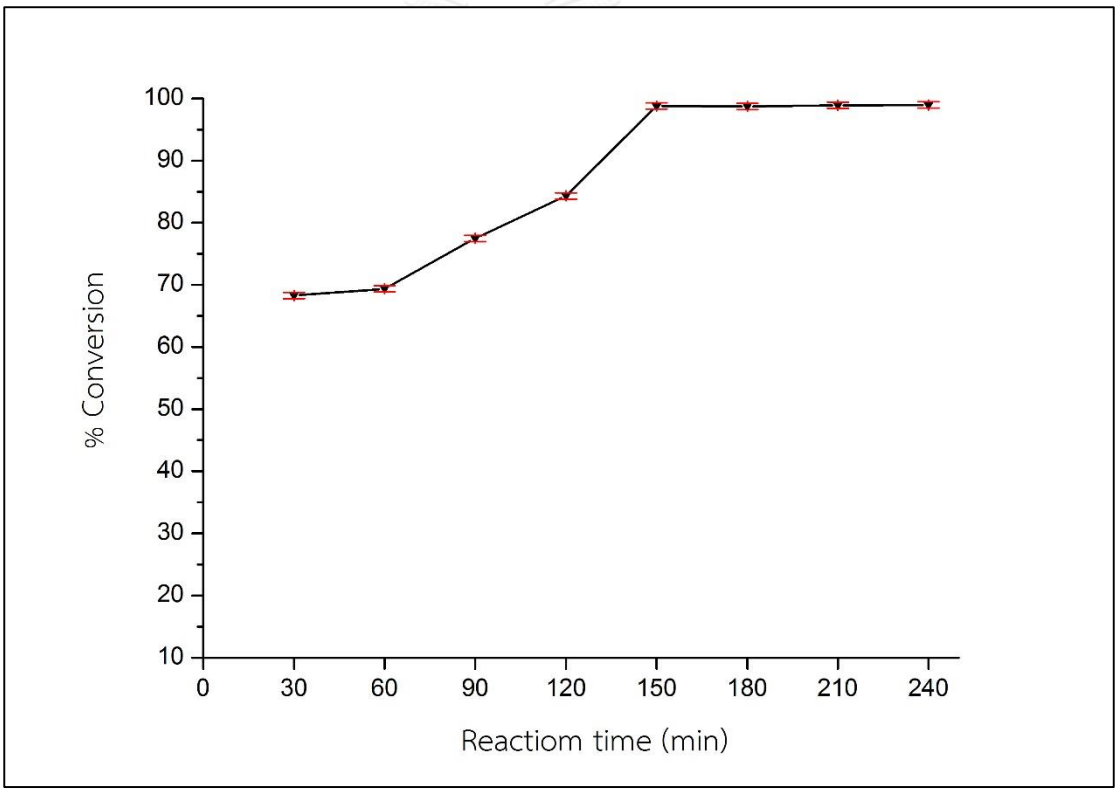


**Figure 4.28** Effect of reaction time on conversion rate of palm oil by using CaO-EGMShell catalyst. Reaction condition were 4 wt. % catalyst, methanol to oil molar ratio of 6:1, reaction temperature of 64 ± 1 °C and constant agitation speed at 700 rpm.

The percent conversion increased as the reaction time increased. During in transesterification, triglyceride from oil reacted with methanol and converted completely to FAME, thus the higher time were required for promoting the reaction to move forward significantly leading to higher conversion.

### 4.8.10 Reusability of CaO-EGMShell catalyst

In general, the reusability of heterogeneous catalysts are important factors for industry application [78] The stability of CaO-EGMShell catalyst were investigated under the optimal condition of amount of catalyst loaded, 4 wt. %, methanol to oil molar ratio, 1:6, reaction time 180 minute (2.5 h). The mixture was refluxed continuously at 64 ± 1 $^{o}$C for 2.5 h under 700 rpm. After the reaction finished, the CaO-EGMShell catalyst were separated by using centrifugation at 400 rpm for 10 minute and washing with a little amount of n-hexane and methanol for removed impurity. Finally, the CaO-EGMShell catalyst were removed excess solvent and moisture in electric oven until constant weight before use in the continuous cycle for produce biodiesel under the same condition. The number reused catalyst cycle were examined in the Figure 4.29.

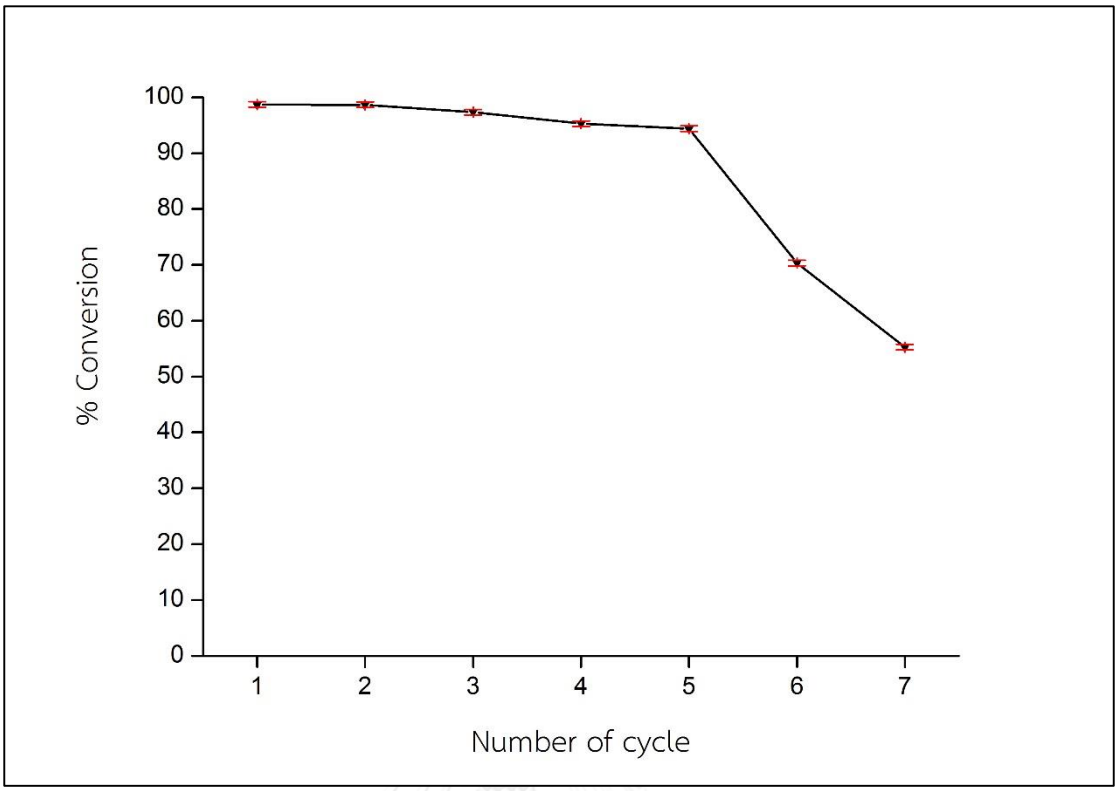


**Figure 4.29** Effect of reusing of catalyst on conversion of palm oil using CaO-GMShell catalyst. Reaction condition were 4 wt. % catalyst, methanol to oil molar ratio of 6:1, reaction temperature at 64 ± 1 °C, reaction time for 2 h and agitation speed at 700 rpm.



The high percent conversion of over 90 % was observed in the cycle No.1 to the cycle No.5 from 98.71 %, 98.65 %, 97.35 %, 95.27 % and 94.38 %, respectively. After the cycle 5, the percent conversion was significantly decreased most likely because of impurities that blocked pores and covered on CaO surface. Moreover, the CaO-EGMShell structure (CaO form) was converted to calcium diglyceroxide [79], the compound formed from the reaction between CaO and glycerol, as a byproduct during in the reaction. In this work, shape transformation of the catalyst and the decrease in surface area (due to effect of particle aggregation on its surface) can be confirmed for by Field emission scanning electron microscopy (FESEM) images as in Figure 4.30 for comparison between fresh CaO-EGMShell catalyst and reused CaO-EGMShell catalyst for 4 cycles.

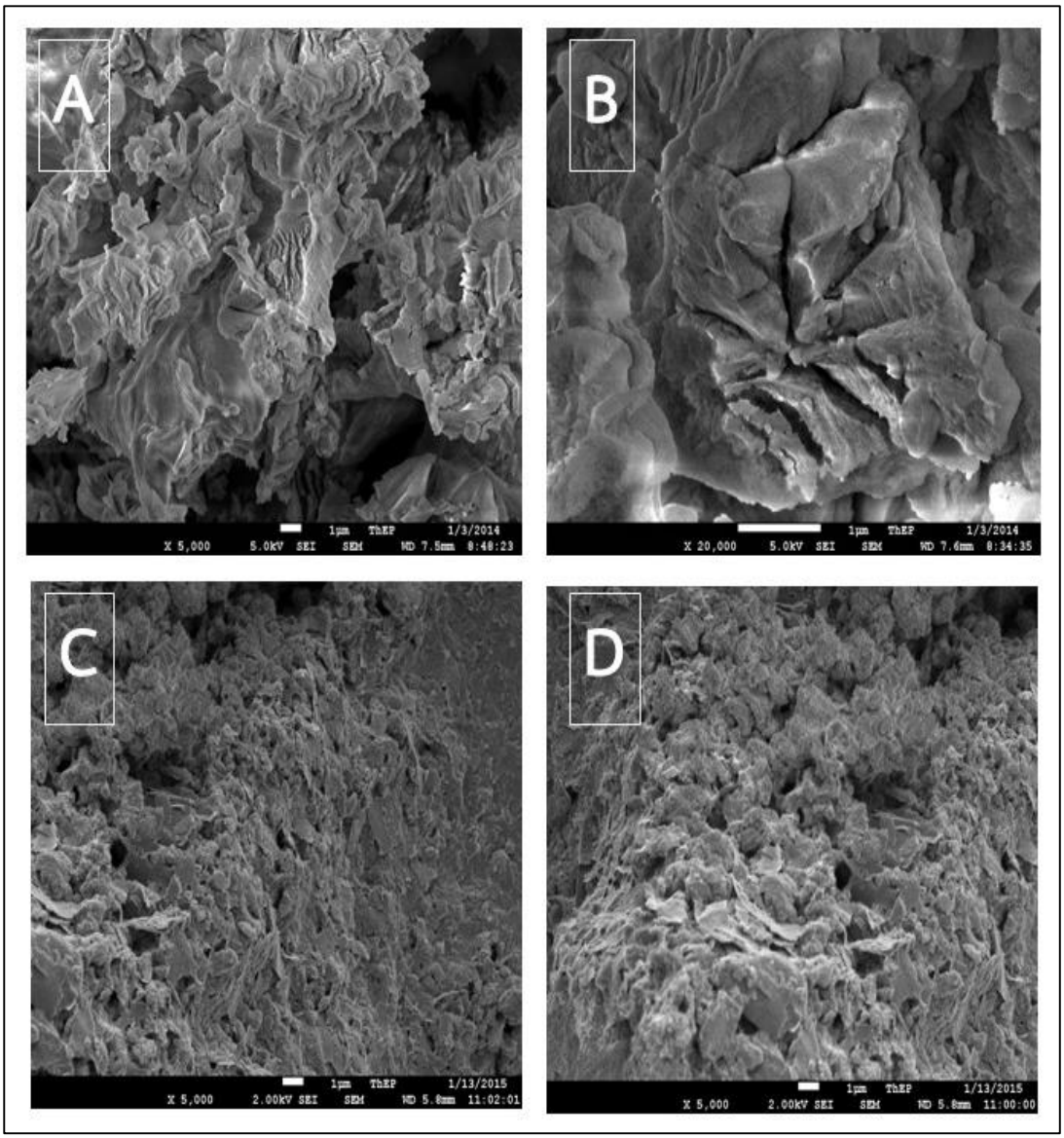


**Figure 4.30** FESEM images of (A) and (B) fresh CaO-EGMShell catalyst, (C) and (D) reused CaO-EGMShell catalyst for 4 cycles.

### 4.9 The chemical properties of the synthesized biodiesel using CaO-EGMShell catalyst

In this research, the biodiesel was successfully synthesized using CaO-EGMShell catalyst under the optimum condition of 4 wt. % catalyst, methanol to oil molar ratio of 6:1, reaction temperature of 64 ± 1 $^{o}$C, reaction time of 2.5 h and constant agitation speed of 700 rpm. The results in the Table 4.10 showed the maximum percent conversion and yield obtained using $^{1}$H-NMR and GC, respectively.

**Table 4.10** The optimal condition for biodiesel production

| Catalyst | Results of synthesized biodiesel production | | |
|---|---|---|---|
| | $^{1}$H-NMR technique | GC technique | |
| | % Conversion | % Purity | % Yield |
| CaO-EGMShell | 98.62 ± 0.52 | 97.65 ± 0.29 | 94.41 ± 0.33 |

Moreover, the ester content in the synthesized biodiesel was determined using GC technique and compared with European standard, EN 14103. From Table 4.10, the resulted 97.65 % m/m of ester content in synthesized biodiesel was higher than the standard, which required higher than 96.50 % m/m as minimum ester content. Therefore, the ester content in this work followed EN 14103. Moreover, the EN14105 was used to determine glyceride residue contents as showed in Table 4.11.

**Table 4.11** Properties of the synthesis biodiesel production

| Property | Unit | Specification | Results | Test method |
|---|---|---|---|---|
| Ester content | % (m/m) | 96.50 min | 97.65 | EN 14103 |
| Glycerol content | % (m/m) | 0.02 max | 0.04 | EN 14105 |
| Monoglyceride content | % (m/m) | 0.80 max | 0.26 | EN 14105 |
| Diglyceride content | % (m/m) | 0.20 max | 0.03 | EN 14105 |
| Triglyceride content | % (m/m) | 0.20 max | Not-detected | EN 14105 |
| Total glycerol content | % (m/m) | 0.25 max | 0.11 | EN 14105 |

### 4.10 Physical properties of modified $Ca(OH)_2$ from CaO precursor

From the XRD results (shown in Figure 4.31), it was found that the $Ca(OH)_2$ phase was obtained after CaO-EGMShell catalyst underwent a hydration method. We investigated this catalyst and found that the $Ca(OH)_2$ showed high basicity (H_) value from Hammett indicators method and high specific surface area by comparing to commercial $Ca(OH)_2$. The result shown in Table 4.12

**Table 4.12** Physical property of $Ca(OH)_2$ catalyst

| Catalyst | Basic strength (H_) | Specific surface area ($m^2/g$) | Total pore volume ($cm^3/g$) | Mean pore diameter (Å) |
|---|---|---|---|---|
| [a]$Ca(OH)_2$ | 15.0 < H_ < 18.4 | 110.20 | 0.2578 | 93.597 |
| [b]$Ca(OH)_2$ | 15.0 < H_ < 18.4 | 104.48 | 0.2443 | 93.535 |

[a]$Ca(OH)_2$, synthesized from CaO catalyst precursor by hydration method with DI water

[b]$Ca(OH)_2$, commercial used as standard

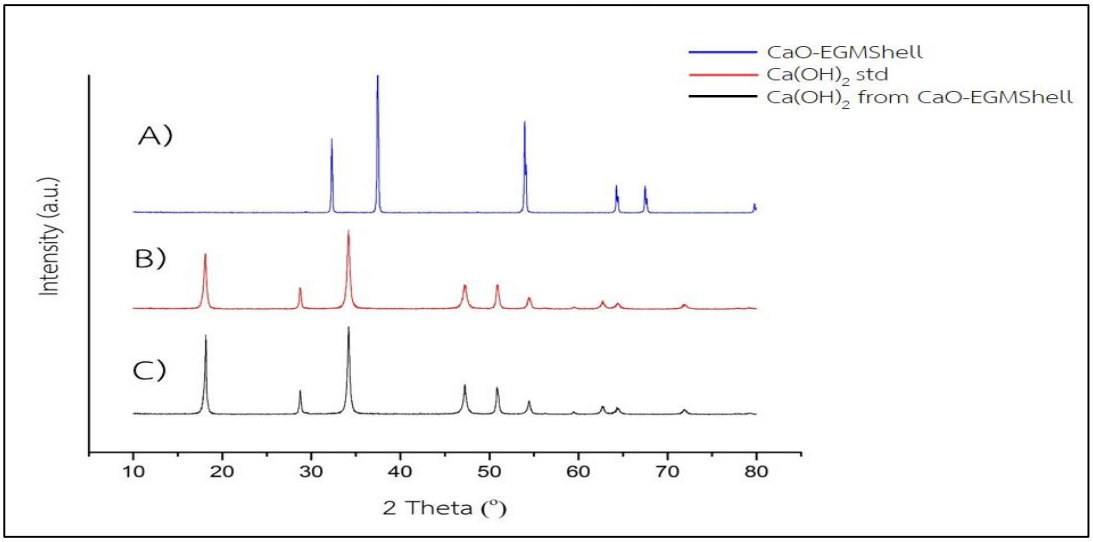


**Figure 4.31** XRD patterns of (A) CaO-EGMShell (B) Commercial $Ca(OH)_2$ used as standard and (C) $Ca(OH)_2$ from CaO-GMShell.

### 4.11 FESEM images of modified CaO-EGMShell catalyst

The fresh CaO-EGMShell catalyst was modified by hydration method with a small quantity of DI water and was removed of excess water at 105°C until reaching a constant weight. The results in Figure 4.32 showed the different morphologies of fresh CaO-EGMShell catalyst (Figure 4.32 (A)), and the catalyst after modification by wet impregnation (Figure 4.32 (B)). The high crystalline phases were formed after modification and some aggregated particles were when comparing with the morphologies of a fresh CaO-EGMShell catalyst.

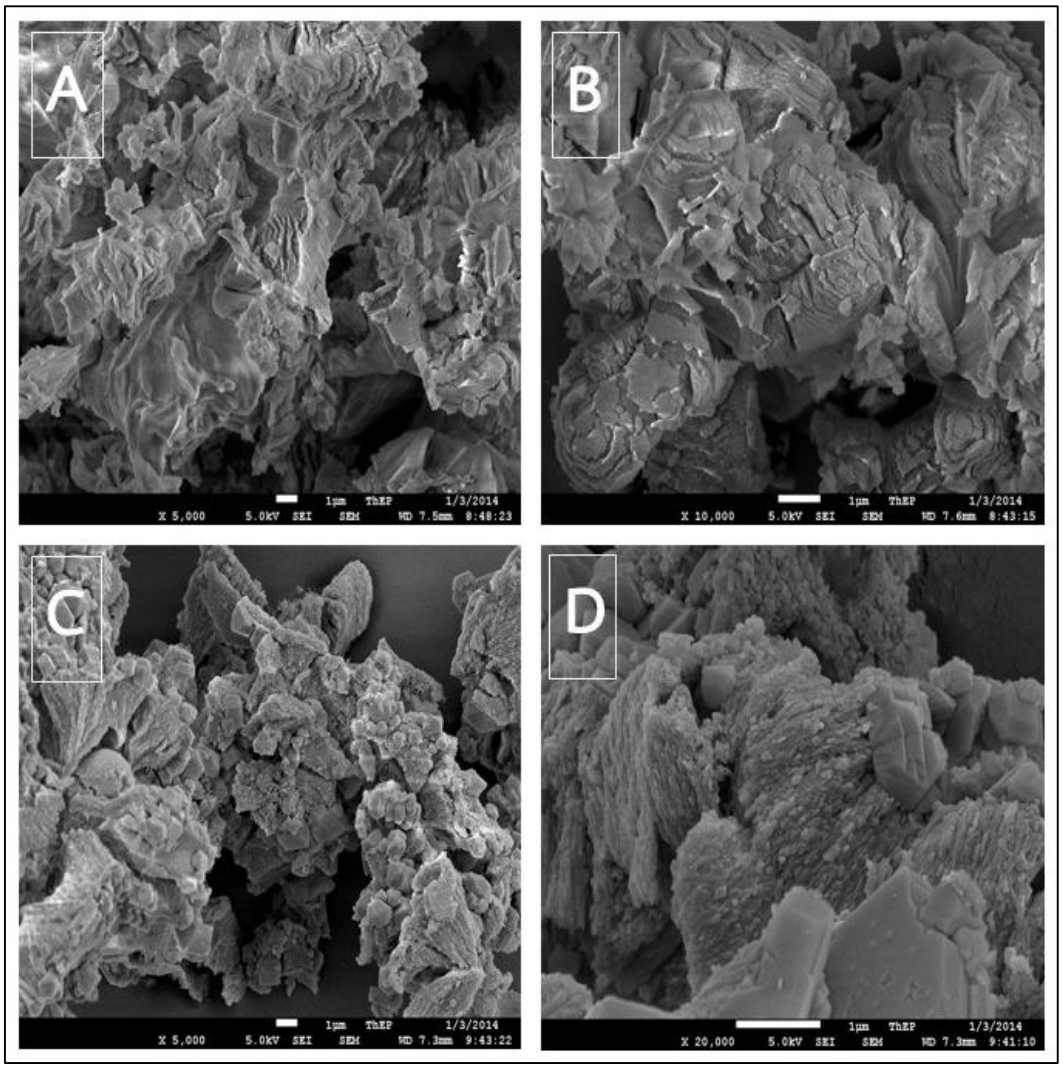


**Figure 4.32** FESEM images of (A) and (B) Fresh CaO-EGMShell catalyst, (C) and (D) $Ca(OH)_2$-EGMShell catalyst.

### 4.12 Transmission electron microscopy (TEM)

The fresh CaO-EGMShell and $Ca(OH)_2$-EGMShell were compared the morphologies before and after the CaO-EGMShell was modified with DI water using wet impregnation method. The morphology of fresh CaO-EGShell as large particles were similar to square prisms, as showed in Figure 4.33 (A) and (B). Besides, the particles of $Ca(OH)_2$-EGMShell were aggregated and its morphology was similar to honeycombs as showed in Figure 4.33 (C) and (D).

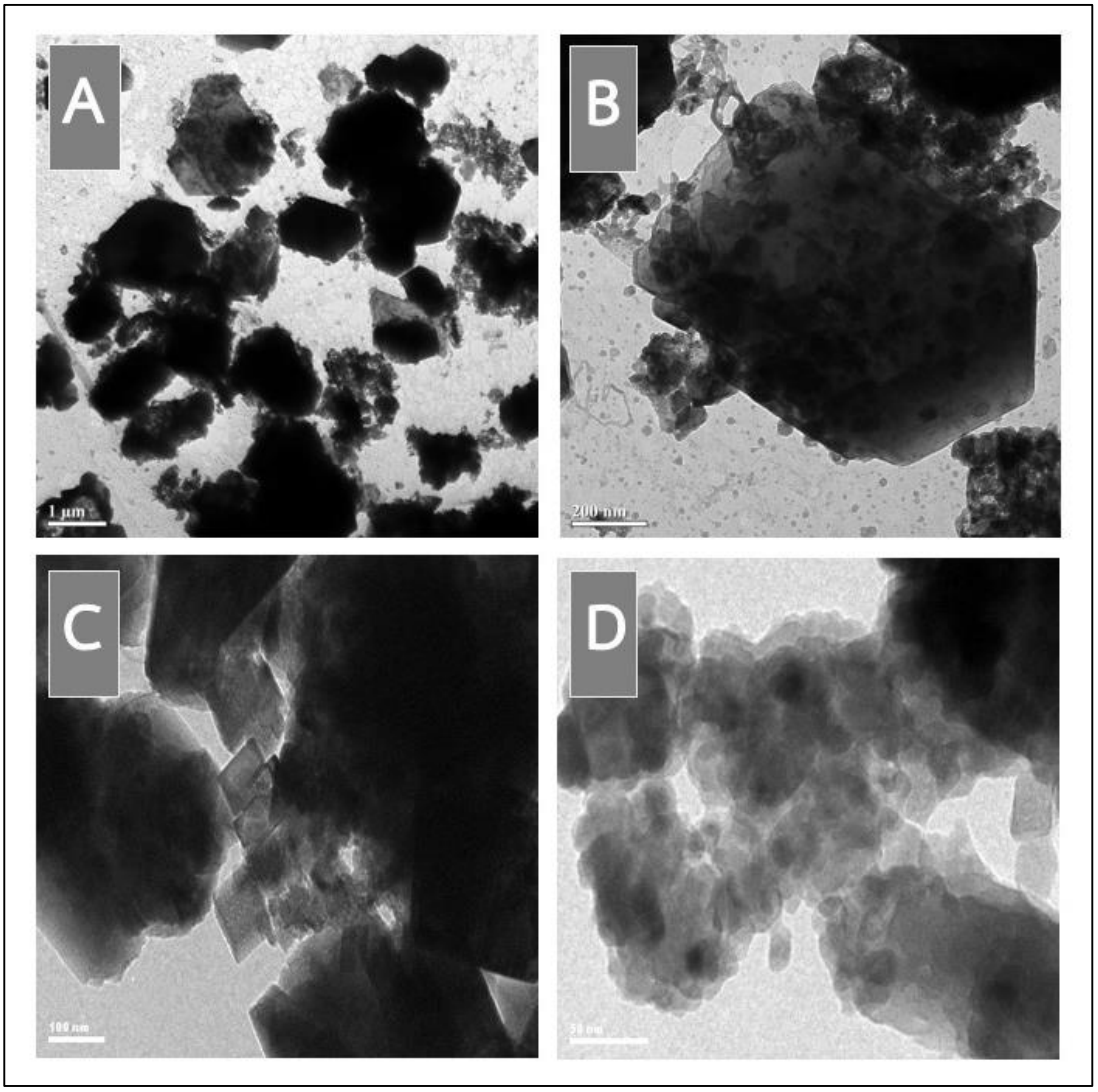


**Figure 4.33** TEM images of (A) and (B) fresh CaO-EGMShell catalyst; (C) and (D) $Ca(OH)_2$-EGMShell catalyst.

### 4.13 Catalyst activity of $Ca(OH)_2$-EGMShell catalyst in transesterification

In this experiment, $Ca(OH)_2$-EGMShell were used as catalyst in transesterification of refined palm oil with methanol under the same condition for CaO-EGMShell catalyst including the amount of catalyst loading, methanol to oil molar ratio, reaction temperature, agitation speed and reaction time.

### 4.13.1 Effect of amount of $Ca(OH)_2$-EGMShell catalyst loaded on % conversion

The quantity of $Ca(OH)_2$-CaO-EGMShell catalyst was varied from 1.0 to 5.0 wt. % for synthesis biodiesel using the previous condition. The results indicated that % conversion of palm oil increased when amount of catalyst increased from 1.0 to 3.0 wt. %. Furthermore, when catalyst was loaded for over 3.0 wt. % then % conversion rate decreased. The results were shown in Figure 4.34.

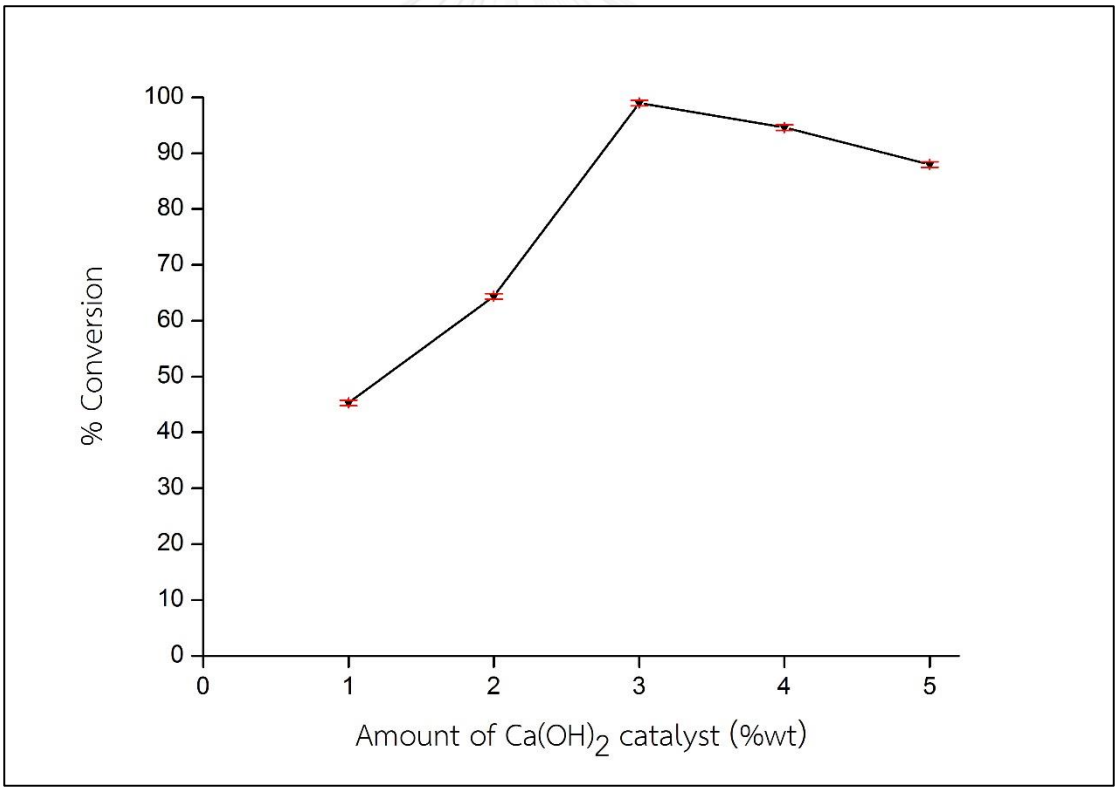


**Figure 4.34** Effect of amount of catalyst loaded on % conversion of palm oil using $Ca(OH)_2$-EGMShell catalyst. Reaction condition were methanol to oil molar ratio of 6:1, reaction temperature of 64 ± 1 °C, reaction time of 2.5 h and agitation speed at 700 rpm.

The effect of catalyst addition on the conversion was studied by varying the quantity of catalyst in transesterification. In the first step of transesterification process, the catalyst was continuously refluxed with methanol before oil was loaded in the system. The basic sites on surfaces of $Ca(OH)_2$-EGMShell catalyst will generate reactive methoxide ions as nucleophiles in the system. Therefore, highly available methoxide ions will react with the carbonyl carbon group of triglyceride molecules and convert to diglyceride and monoglyceride, respectively. Finally, the fatty acid methyl ester and glycerol as byproduct were generated in the transesterification. The result indicated that high percent conversion increased when the amount of catalyst loaded increase Therefore, the methoxide ions as available nucleophile active increase depend on amount of catalyst loaded. A maximum of 98.98 % conversion and 96.79 % of yield (as shown in Table 4.13.) for biodiesel production were achieved using 3 wt. % of $Ca(OH)_2$-EGMShell catalyst.

**Table 4.13** Effect of quantity of $Ca(OH)_2$-EGMShell catalyst on the yield of production

| **Catalyst** | **Quantity of catalyst (wt. %)** | **Yield (%)** |
|---|---|---|
| $Ca(OH)_2$-EGMShell | 1.0 | 98.28 |
| | 2.0 | 97.65 |
| | 3.0 | 96.79 |
| | 4.0 | 90.31 |
| | 5.0 | 88.26 |

However, above 3 wt. % of $Ca(OH)_2$-EGMShell catalyst, the conversion and yield significantly began to drop due to the high viscosity [80] and effect of mass transfer from slurry mixture of reactants during in transesterification reaction. Therefore, 3 wt. % $Ca(OH)_2$-EGMShell catalyst is the optimal condition for used in this experimental section.

### 4.13.2 Effect of methanol to palm oil molar ratio on the synthesis of biodiesel

The effect of methanol to oil molar ratio was investigated by varying the ratio from 3:1, 6:1, 9:1, 12:1 to 15:1, respectively. The experimental results indicated that maximum conversion of 98.23 % was obtained when using methanol to oil mole ratio of 6:1 as illustrated in Figure 4.35.

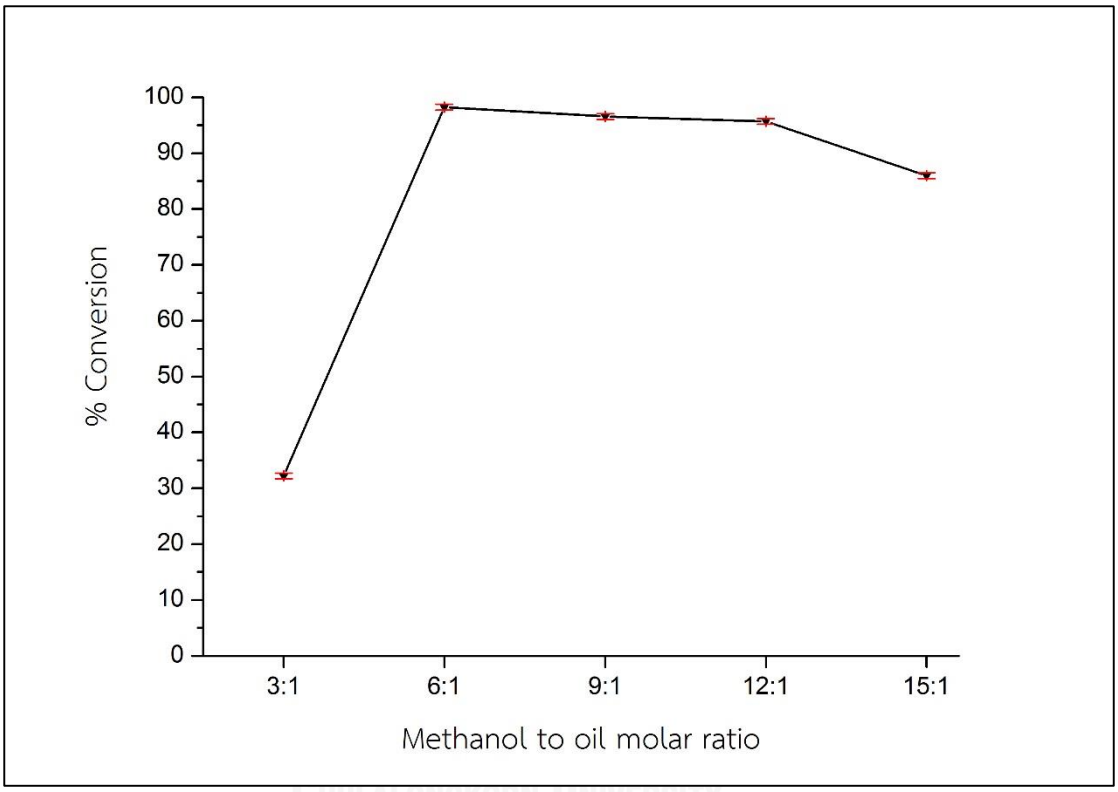




**Figure 4.35** Effect of methanol to oil molar ratio on conversion rate of palm oil using $Ca(OH)_2$-EGMShell catalyst. Reaction condition were 3 wt. % catalyst, reaction temperature of 64 ± 1 $^{o}$C, reaction time of 2.5 h and agitation speed at 700 rpm.

Theoretically, the stoichiometric ratio for transesterification required 3 moles of alcohol to react with 1 mole of triglyceride to yield 3 moles of FAME and 1 mole of glycerol. However, transesterification, as a reversible reaction, was motivated with excess amount of methanol for quickly shifting the equilibrium in forward pathway to drive all reactants as triglyceride, methanol and catalyst in the system toward maximum FAME production and attaining the high conversion and yield of FAME.

The conversion increased as methanol to oil molar ratio increased from 3:1 to 12:1. However, the conversion significantly decreased when excess methanol was used for more than 12:1 of methanol to oil molar ratio because by-product such as diglycreride, monoglyceride and glycerol can dissolved in a large amount of methanol [81]. The concentration of triglyceride was then decreased significantly, resulting in slower reaction with methanol and decrease in percent conversion. Moreover, the maximum yield of 96.45 % of product was obtained by using optimal condition with amount of catalyst loaded of 3 wt. %., methanol to oil molar ratio of 6:1 at 64 ± 1 $^{o}$C for 2.5 h as shown in Table 4.14 below. Therefore, the condition of methanol to oil molar ratio of 6:1 was used in the next experimental section for producing biodiesel because high conversion and yield of FAME were obtained.

**Table 4.14** Effect of methanol to oil molar ratio on the yield of production

| **Catalyst** | **Methanol to oil molar ratio (mole)** | **Yield (%)** |
|---|---|---|
| $Ca(OH)_2$-EGMShell | 3:1 | 31.86 |
| | 6:1 | 96.45 |
| | 9:1 | 94.83 |
| | 12:1 | 92.76 |
| | 15:1 | 54.85 |



### 4.13.3 Effect of reaction temperature on % conversion

In this experimental section, effect of reaction temperature was investigated by varying temperature from 35 $^{o}$C to 70 $^{o}$C for carrying out in transesterification with amount of $Ca(OH)_2$ catalyst of 3 wt. %, methanol to oil molar ratio of 6:1 for 2.5 h at constant agitation speed at 700 rpm. The results indicated that higher conversion was obtained when the temperature was increased from 35 $^{o}$C to 65 $^{o}$C (64 ± 1 $^{o}$C) as illustrated in Figure 4.36. However, the conversion started to decrease when the temperature exceeded the boiling point of methanol (65 $^{o}$C) due to the effect of

bubbles and high pressure of methanol vaporization in the system during the transesterification reaction. The maximum conversion of 98.84 % was reached at 65 °C. Therefore, it was concluded that the reaction temperature at 64 ± 1 °C was the suitable operating temperature in this experiment.

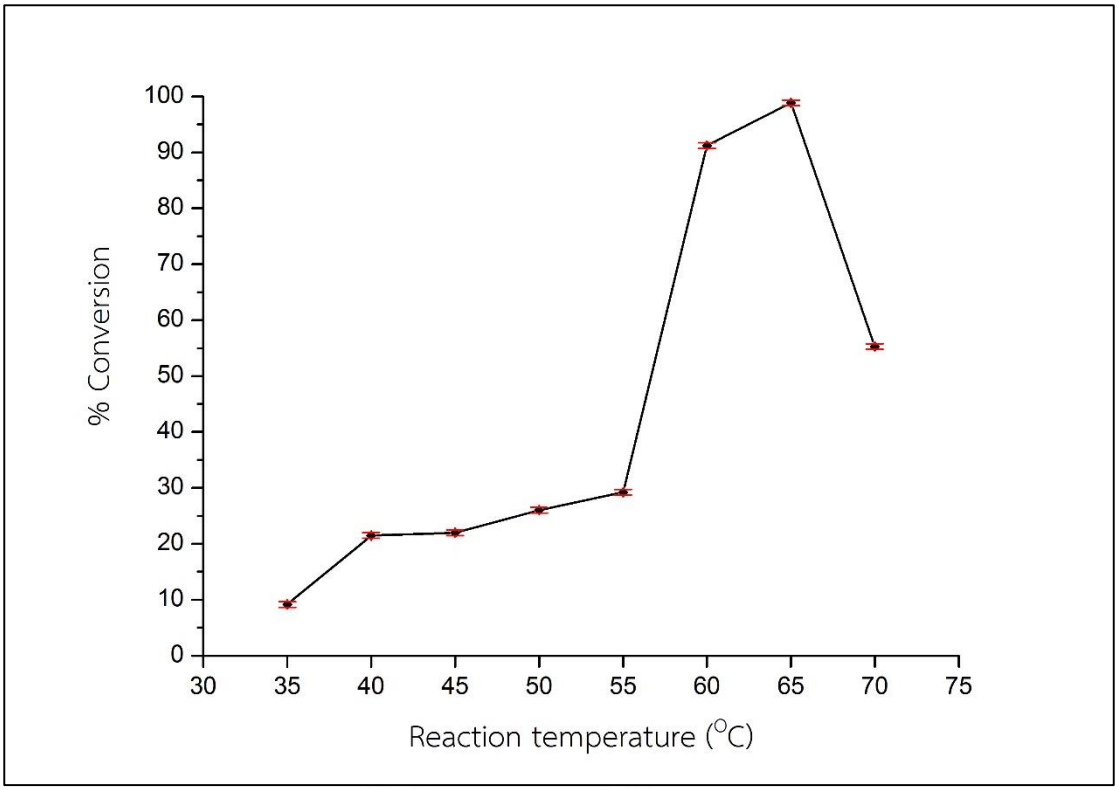




**Figure 4.36** Effect of reaction temperature on conversion of palm oil using $Ca(OH)_2$-EGMShell catalyst. Reaction condition were 3 wt. % catalyst, methanol to oil molar ratio of 6:1, reaction temperature of 64 ± 1 °C, reaction time of 2.5 h and agitation speed at 700 rpm.

### 4.13.4 Effect of agitation speed on % conversion

Due to mass transfer effect, the mixing rate may affect the conversion rate and yield of biodiesel during oil reacting with methanol using $Ca(OH)_2$-EGMShell as a catalyst in transesterification. Therefore, effects of agitation speed were investigated by varying the agitation speed from 0, 100, 300, 500, 700, 900 and 1100 rpm in this reaction under the condition of 3 wt. % $Ca(OH)_2$-EGMShell catalyst, methanol to oil molar ratio of 6:1 at 64 ± 1 °C for 2.5 h. The conversion was observed to be increased when the agitation speed increased from 0 to 700 rpm and decreased above 700 rpm. Additionally, maximum conversion of 98.72 % was obtained using mixing speed at 700 rpm. Therefore, the agitation speed at 700 rpm was selected for further studied to reduce immiscibility and mass transfer limitations in this process under the optimum condition. The result was shown in Figure 4.37.

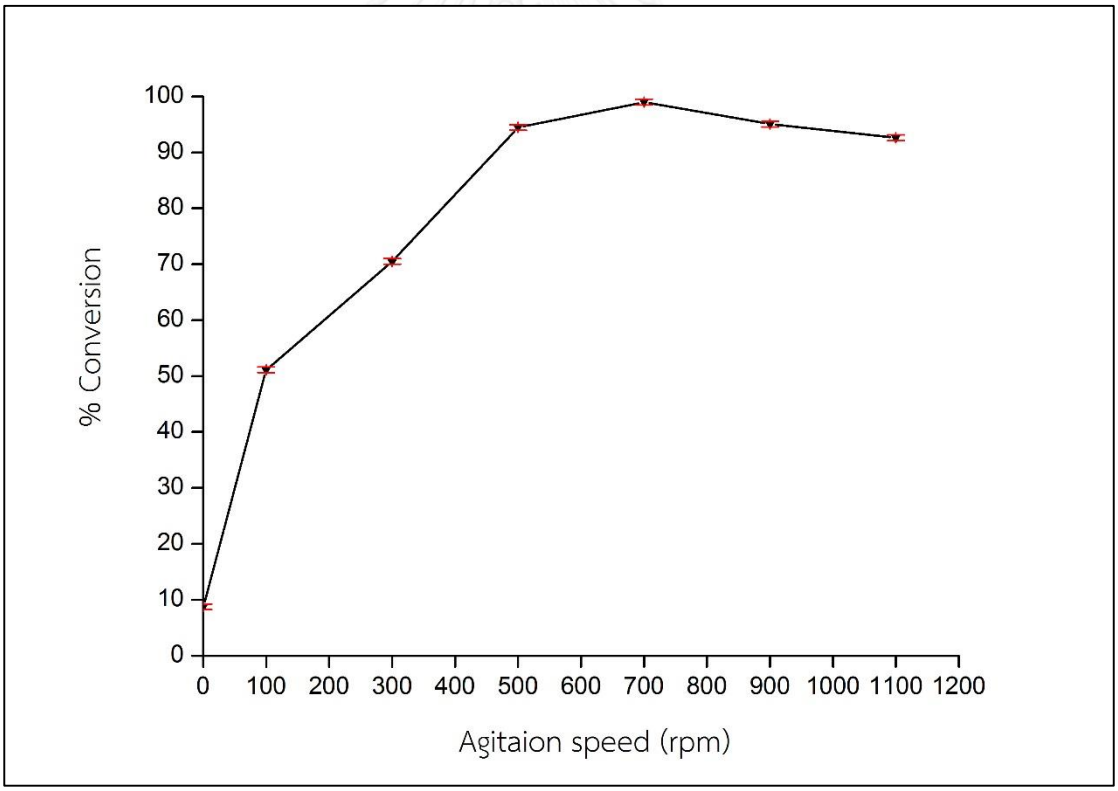


**Figure 4.37** Effect of agitation speed on conversion of palm oil using $Ca(OH)_2$-EGMShell catalyst. Reaction condition were 3 wt. % catalyst, methanol to oil molar ratio of 6:1, reaction temperature of 64 ± 1 °C, reaction time of 2.5 h.

### 4.13.5 Effect of reaction time on % conversion

The effect of reaction time was studied by varying time in the range from 30 to 210 minute for producing biodiesel under the condition of 3 wt. % $Ca(OH)_2$-EGMShell catalyst, methanol to oil molar ratio of 6:1 at 64 ± 1 °C. The results clearly indicated that when the reaction time increased, the percent conversion also increased. Therefore, the maximum conversion of 98.73 % was achieved at 150 minute or 2.5 h and unchanged after 150 minute as shown in Figure 4.38. Therefore, it required 2.5 h for higher conversion for this biodiesel production.

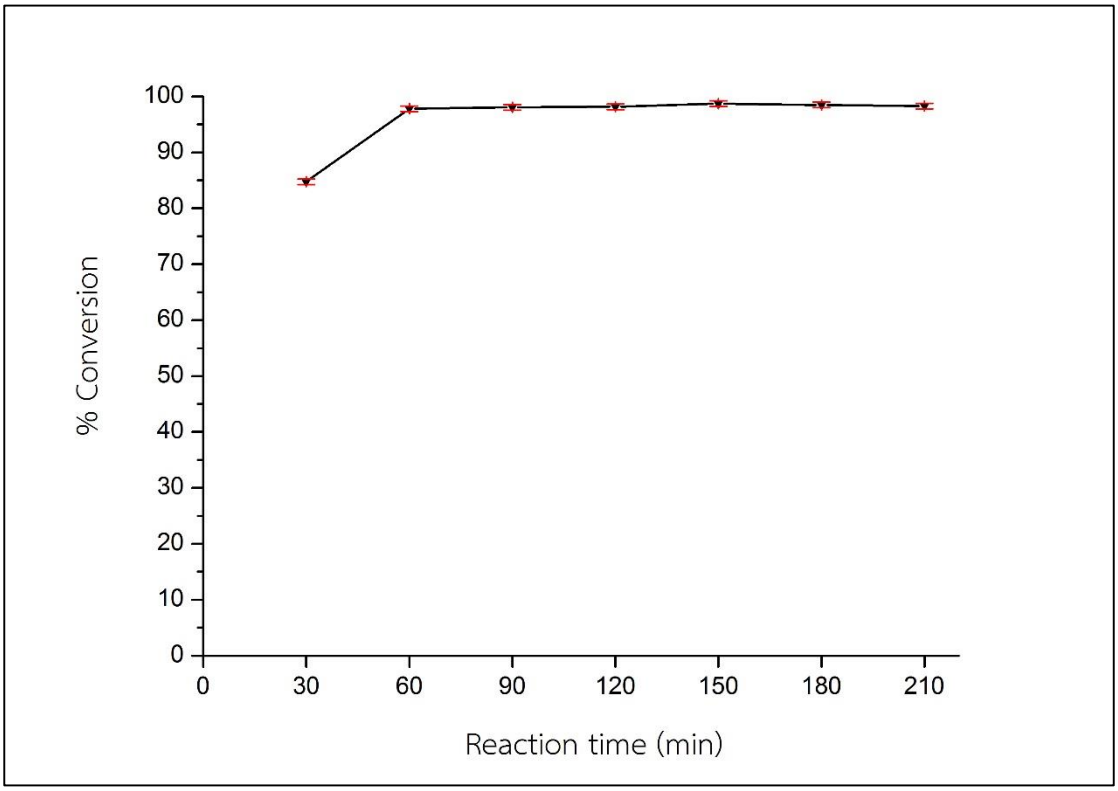


**Figure 4.38** Effect of reaction time on conversion of palm oil using $Ca(OH)_2$-EGMShell catalyst. Reaction condition were 3 wt. % catalyst, methanol to oil molar ratio of 6:1, reaction temperature of 64 ± 1 °C and agitation speed at 700 rpm.

### 4.13.6 Reusability of $Ca(OH)_2$-EGMShell catalyst

The important features of catalyst such as stability and reusability were investigated in transesterification for industrial applications. The reusability of the $Ca(OH)_2$-EGMShell catalyst was studied by carrying out repeating reaction cycles. After reaction finished, the $Ca(OH)_2$-EGMshell catalyst was carefully collected by separating from mixture of final product in the system and washed with a little amount of n-hexane and pure methanol. Residues and impurities of reactant and products such as soap from saponification as a competitive side reaction [82], glycerol, monoglyceride, diglyceride and biodiesel production were removed. The result was shown in Figure 4.39 that the conversion rate of more than 90 % was obtained after $Ca(OH)_2$-EGMShell catalyst was used for three cycle before the conversion rate decreased significantly after higher number of cycles for reusing of catalyst.

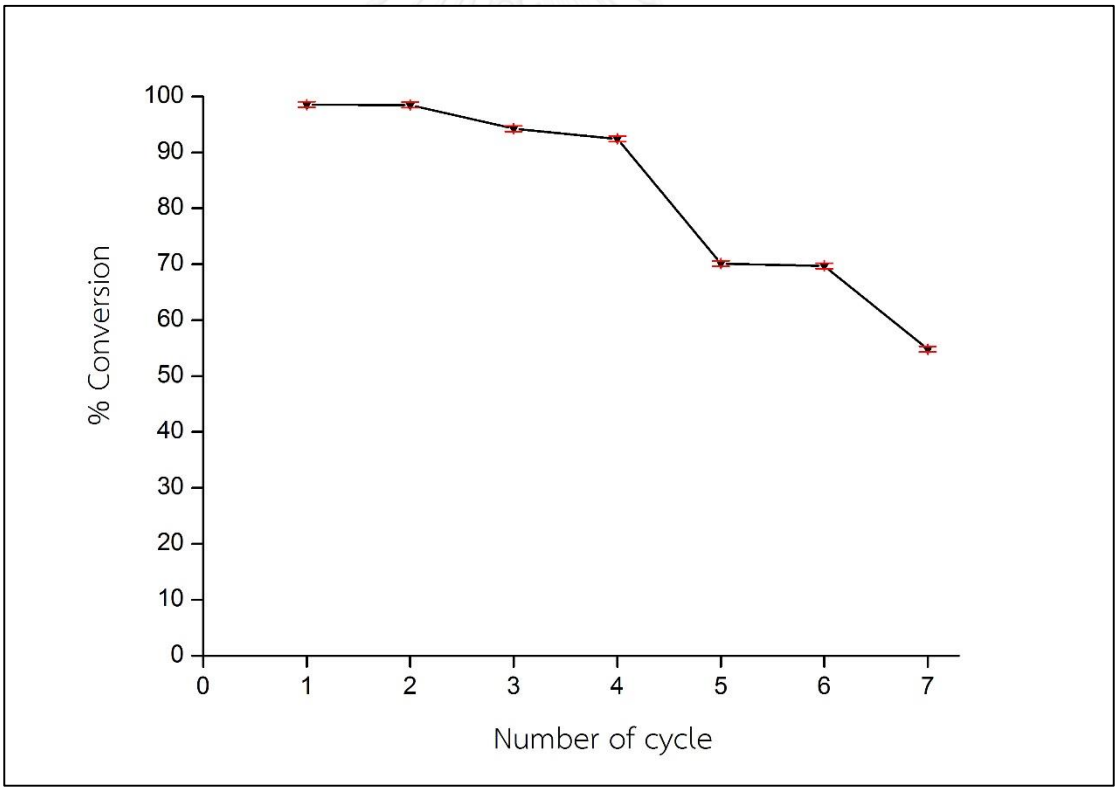


**Figure 4.39** Effect of reusing of catalyst on conversion rate of palm oil using $Ca(OH)_2$-EGMShell catalyst. Reaction condition were 3 wt. % catalyst, methanol to oil molar ratio of 6:1, reaction temperature of 64 ± 1 °C and agitation speed at 700 rpm.

From the results above, it was concluded that high yield of FAME of 90.37 % was achieved after the catalyst was reused for three times as illustrated in Table 4.15.

**Table 4.15** The yield of production of the reused $Ca(OH)_2$-EGMShell catalyst

| **Catalyst** | **Number of reaction cycles for the reused catalyst** | **Yield (%)** |
|---|---|---|
| $Ca(OH)_2$-EGMShell | 1 | 95.50 |
| | 2 | 94.23 |
| | 3 | 90.37 |
| | 4 | 86.28 |
| | 5 | 66.04 |
| | 6 | 59.88 |
| | 7 | 46.26 |

The decrease in conversion and yield for biodiesel in this experimental section were observed from physical properties of the catalyst after reused for more than three cycles. The table 4.16 showed the decrease in specific surface area of the reused catalyst before being used in transesterification of the next cycles.

**Table 4.16** Surface properties of $Ca(OH)_2$-EGMShell catalyst

| Number of cycles the $Ca(OH)_2$ catalyst reused | Specific surface area ($m^2/g$) | Total pore volume ($cm^3/g$) | Mean pore diameter (Å) |
|---|---|---|---|
| 1 | 110.20 | 0.26 | 93.60 |
| 2 | 101.08 | 0.25 | 100.86 |

**Table 4.16** Surface properties of $Ca(OH)_2$-EGMShell catalyst (continued)

| Number of cycles the $Ca(OH)_2$ catalyst reused | Specific surface area ($m^2/g$) | Total pore volume ($cm^3/g$) | Mean pore diameter (Å) |
|---|---|---|---|
| 3 | 82.80 | 0.24 | 116.84 |
| 4 | 75.72 | 0.24 | 128.36 |
| 5 | 45.48 | 0.18 | 156.46 |

Moreover, the bulk $Ca(OH)_2$-EGMShell catalyst was obtained after reaction finished because the residues and impurities were covered on catalyst surface with difficulty in separation. Reduced catalytic activity of $Ca(OH)_2$-EGMShell catalyst and the resulted deactivation of surface area and pore blockage were due to the loss of active sites on its surface. The catalyst transformation of its structure was observed as shown in Figure 4.40.

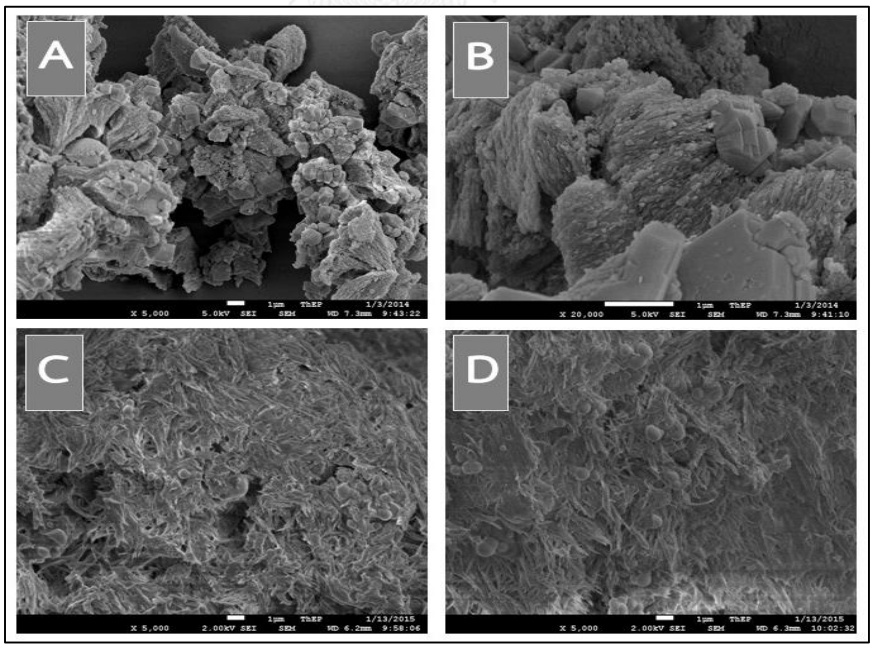


**Figure 4.40** SEM image of A), B) fresh $Ca(OH)_2$-EGMShell catalyst and C), D) reused $Ca(OH)_2$-EGMShell catalyst at cycle 5 after separated from the reaction mixtures.

### 4.13.7 Comparison of catalytic activities in transesterification of different catalysts.

In this experimental section, the catalytic activities of different catalysts were studied under the identical condition of 3 wt. % catalyst, methanol to oil molar ratio of 6:1, reaction temperature of 64 ± 1 °C and constant agitation speed at 700 rpm for 2.5 h. The results indicated that catalytic activity of catalyst can be ranked as follows: CaO-EGMShell << commercial $Ca(OH)_2$ as standard < $Ca(OH)_2$-EGMShell which was modified from CaO-EGMShell under the same condition of transesterification. The $Ca(OH)_2$-EGMShell catalyst can generate methoxide ions more efficiently than CaO-EGMShell catalyst when both catalysts were refluxed in methanol under the same condition. The possible of mechanism pathways for $Ca(OH)_2$-EGMShell and CaO-EGMShell were proposed in appendix C.

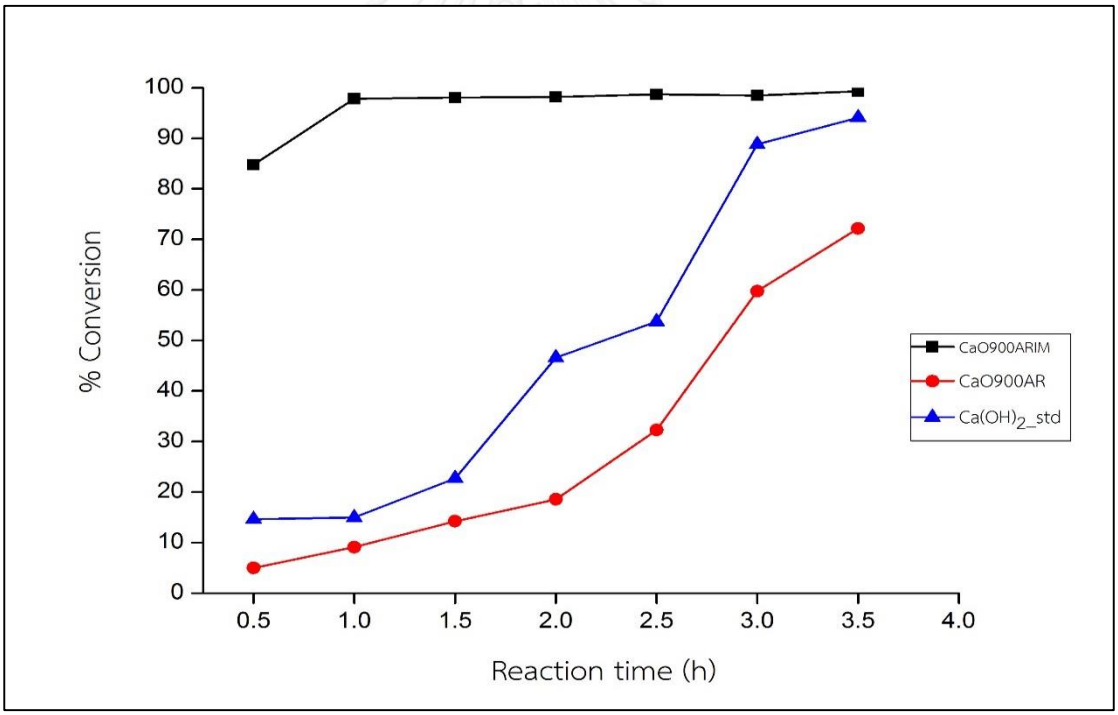


**Figure 4.41** Comparison of catalyst activities with the reaction condition of 3 wt. % catalyst, methanol/ oil molar ratio of 6:1, reaction temperature of 64 ± 1 °C and agitation speed of 700 rpm for 2.5 h.

### 4.14 The chemical properties of the synthesized biodiesel using $Ca(OH)_2$-EGMShell catalyst

In this research, the biodiesel was successfully synthesized using $Ca(OH)_2$-EGMShell catalyst under the optimum condition of 3 wt. % catalyst, methanol to oil molar ratio of 6:1, reaction temperature of 64 ± 1 $^{o}$C, reaction time of 2.5 h and constant agitation speed of 700 rpm. Table 4.17 summarized the ester content in synthesized biodiesel in the form of %yield and % conversion determined by $^{1}$H-NMR and GC technique.

**Table 4.17** Analyses of the biodiesel obtained at the optimal condition

| Catalyst | Analyses of synthesized biodiesel | | |
|---|---|---|---|
| | $^{1}$H-NMR technique | GC technique | |
| | % Conversion | % Purity | % Yield |
| $Ca(OH)_2$-EGMShell | 98.55 ± 0.48 | 97.32 ± 0.51 | 94.56 ± 0.45 |

Moreover, the EN 14105 was used to determine the amount of impurities such as monoglyceride, diglyceride, triglyceride and total glycerol content in the synthesized biodiesel. As shown in Table 4.18, the results indicated that the synthesized biodiesel is in accordance with EN1403 and EN 1405.



**Table 4.18** Properties of the synthesis biodiesel production

| Properties | Unit | Specification | Results | Test method |
|---|---|---|---|---|
| Ester content | % (m/m) | 96.50 min | 97.32 | EN 14103 |
| Glycerol content | % (m/m) | 0.02 max | 0.04 | EN 14105 |
| Monoglyceride content | % (m/m) | 0.80 max | 0.25 | EN 14105 |
| Diglyceride content | % (m/m) | 0.20 max | 0.03 | EN 14105 |
| Triglyceride content | % (m/m) | 0.20 max | Not-detected | EN 14105 |
| Total glycerol content | % (m/m) | 0.25 max | 0.11 | EN 14105 |

# CHAPTER V

# CONCLUSION

## 5.1 Conclusion

In this research, the CaO-EGMShell as heterogeneous base catalyst was successfully synthesized from waste green-mussel shells. The results form FESEM can preliminary observe the different morphologies of the $CaCO_3$-EGMShell and CaO-EGMShell. In addition, The XRD results clearly confirmed that the $CaCO_3$-EGMShell was completely transformed to CaO-EGMShell after calcination at 900 $^{o}$C for 5 h. The CaO-EGMShell showed high catalytic activities under the optimal condition for the synthesis of biodiesel via transesterification using 4 wt. % catalyst loaded with 6:1 ratio of methanol to oil at 64 ± 1 $^{o}$C for 2.5 h with agitation speed of 700 rpm. The highest percent conversion and yield of synthesized biodiesel obtained were 98.62 % and 94.41 %, respectively, under the optimal condition. Moreover, the purity of synthesized biodiesel determined from methyl ester content was achieved 97.65 % in accordance with EN 14103 method of European standard.

Furthermore, the fresh CaO-EGMShell catalyst was further modified using wet impregnation method by addition of a small quantity of DI water for cleanup and removal of impurities after calcination. The XRD patterns showed that CaO-EGMShell was converted to calcium hydroxide ($Ca(OH)_2$) phase after modification as observed the 2θ at 34.180 degree as the characteristic peak of $Ca(OH)_2$. The results from BET surface area analysis indicated high surface area (110.20 $m^2/g$) of the $Ca(OH)_2$, and the absorption-desorption isotherm indicated mesoporous character of this catalyst. Therefore, the transesterification with $Ca(OH)_2$-EGMShell as catalyst was carried out under optimal condition determined from CaO-EGMShell catalyst. The high conversion rate and yield of biodiesel of 98.55 % and 94.56 %, respectively, were obtained when 3 wt. % $Ca(OH)_2$-EGMShell was used with methanol to oil ratio of 6:1 at 64 ± 1 $^{o}$C for 2.5 h under agitation speed of 700 rpm. Moreover, the $Ca(OH)_2$-EGMShell exhibited higher catalytic activities than the commercial $Ca(OH)_2$ in transesterification under the

same condition for synthesis of biodiesel. High stability of $Ca(OH)_2$-EGMShell catalyst was likely due to a small quantity of organic matrix in its structure as can be confirmed by the results from FTIR. Moreover, the result from Hammett indicator method supported the high catalytic activities of $Ca(OH)_2$-EGMShell catalyst when compared with commercial $Ca(OH)_2$. Besides, the purity of biodiesel reached 97.32 % when $Ca(OH)_2$-EGMShell was used as catalyst in transesterification.

CaO-EGMShell and $Ca(OH)_2$-EGMShell can be reused for 5 cycles and 3 cycles, respectively, without significant decrease in catalytic activities and structures. The advantages of this research are not only the reduction of high quantity of waste from green-mussel shells, but also the addition to the value of waste to highly active catalysts and decrease the expenditure for synthesis of biodiesel.

## 5.2 Suggestion

1. The activation of catalysts in the biodiesel synthesis should be of concern and further study. The transesterification reaction required methoxide species ($CH_3O^-$), as the real catalyst, that generated on the surface of CaO-EGMShell and $Ca(OH_2)$-EGMShell catalysts. Therefore, the catalyst must be promoted with methanol by refluxing for several times before addition of triglyceride to react with methanol in the system.

2. The $Ca^{2+}$ ion content (residues from CaO-EGMShell and $Ca(OH_2)$-EGMShell catalysts) in biodiesel is one of important factors that acts as a hindrance in motor of engines. Therefore, the synthesized biodiesel after separated from catalysts should be determined for $Ca^{2+}$ ion content in biodiesel before use to check whether it meets the standard of lower than 5 mg/kg as set in EN 14214 [83]

## REFERENCES


[1] Lucarelli, C., et al. Catalyst deactivation in on-board H2 production by fuel dehydrogenation. International Journal of Hydrogen Energy 39(3) (2014): 1336-1349.

[2] de Llobet, S., Pinilla, J.L., Lázaro, M.J., Moliner, R., and Suelves, I. Catalytic decomposition of biogas to produce H2-rich fuel gas and carbon nanofibers. Parametric study and characterization. International Journal of Hydrogen Energy 37(8) (2012): 7067-7076.

[3] Roberts, J.J., Cassula, A.M., Osvaldo Prado, P., Dias, R.A., and Balestieri, J.A.P. Assessment of dry residual biomass potential for use as alternative energy source in the party of General Pueyrredón, Argentina. Renewable and Sustainable Energy Reviews 41 (2015): 568-583.

[4] Kumar, V., Shrivastava, R.L., and Untawale, S.P. Solar Energy: Review of Potential Green & Clean Energy for Coastal and Offshore Applications. Aquatic Procedia 4 (2015): 473-480.

[5] Asress, M.B., Simonovic, A., Komarov, D., and Stupar, S. Wind energy resource development in Ethiopia as an alternative energy future beyond the dominant hydropower. Renewable and Sustainable Energy Reviews 23 (2013): 366-378.

[6] Zimny, J., Michalak, P., Bielik, S., and Szczotka, K. Directions in development of hydropower in the world, in Europe and Poland in the period 1995–2011. Renewable and Sustainable Energy Reviews 21 (2013): 117-130.

[7] Power, C., McNabola, A., and Coughlan, P. Development of an evaluation method for hydropower energy recovery in wastewater treatment plants: Case studies in Ireland and the UK. Sustainable Energy Technologies and Assessments 7 (2014): 166-177.

[8] de Almeida, V.F., García-Moreno, P.J., Guadix, A., and Guadix, E.M. Biodiesel production from mixtures of waste fish oil, palm oil and waste frying oil: Optimization of fuel properties. Fuel Processing Technology 133 (2015): 152-160.

[9] Shahir, S.A., Masjuki, H.H., Kalam, M.A., Imran, A., and Ashraful, A.M. Performance and emission assessment of diesel–biodiesel–ethanol/bioethanol blend as a fuel in diesel engines: A review. Renewable and Sustainable Energy Reviews 48 (2015): 62-78.

[10] Mohsin, R., Majid, Z.A., Shihnan, A.H., Nasri, N.S., and Sharer, Z. Effect of biodiesel blends on engine performance and exhaust emission for diesel dual fuel engine. Energy Conversion and Management 88 (2014): 821-828.

[11] Cho, Y.B., Seo, G., and Chang, D.R. Transesterification of tributyrin with methanol over calcium oxide catalysts prepared from various precursors. Fuel Processing Technology 90(10) (2009): 1252-1258.

[12] Adewale, P., Dumont, M.-J., and Ngadi, M. Recent trends of biodiesel production from animal fat wastes and associated production techniques. Renewable and Sustainable Energy Reviews 45 (2015): 574-588.

[13] de Mendonça, D.R., da Silva, J.P.V., de Almeida, R.M., Wolf, C.R., Meneghetti, M.R., and Meneghetti, S.M.P. Transesterification of soybean oil in the presence of diverse alcoholysis agents and Sn(IV) organometallic complexes as catalysts, employing two different types of reactors. Applied Catalysis A: General 365(1) (2009): 105-109.

[14] Vicente, G., Martínez, M., and Aracil, J. Optimisation of integrated biodiesel production. Part II: A study of the material balance. Bioresource Technology 98(9) (2007): 1754-1761.

[15] Semwal, S., Arora, A.K., Badoni, R.P., and Tuli, D.K. Biodiesel production using heterogeneous catalysts. Bioresource Technology 102(3) (2011): 2151-2161.

[16] Almerindo, G.I., et al. Magnesium oxide prepared via metal–chitosan complexation method: Application as catalyst for transesterification of soybean oil and catalyst deactivation studies. Journal of Power Sources 196(19) (2011): 8057-8063.

[17] Zhao, L., Qiu, Z., and Stagg-Williams, S.M. Transesterification of canola oil catalyzed by nanopowder calcium oxide. Fuel Processing Technology 114 (2013): 154-162.

[18] Yan, S., Mohan, S., DiMaggio, C., Kim, M., Ng, K.Y.S., and Salley, S.O. Long term activity of modified ZnO nanoparticles for transesterification. Fuel 89(10) (2010): 2844-2852.

[19] Wang, Y.-B. and Jehng, J.-M. Hydrotalcite-like compounds containing transition metals as solid base catalysts for transesterification. Chemical Engineering Journal 175 (2011): 548-554.

[20] Bello Bugallo, P.M., Stupak, A., Cristóbal Andrade, L., and Torres López, R. Material Flow Analysis in a cooked mussel processing industry. Journal of Food Engineering 113(1) (2012): 100-117.

[21] Mussel shells treat wastewater. Focus on Catalysts (10) (2013): 6.

[22] Boro, J., Thakur, A.J., and Deka, D. Solid oxide derived from waste shells of Turbonilla striatula as a renewable catalyst for biodiesel production. Fuel Processing Technology 92(10) (2011): 2061-2067.

[23] Chakraborty, R., Bepari, S., and Banerjee, A. Application of calcined waste fish (Labeo rohita) scale as low-cost heterogeneous catalyst for biodiesel synthesis. Bioresource Technology 102(3) (2011): 3610-3618.

[24] Meyers, M.A., Chen, P.-Y., Lopez, M.I., Seki, Y., and Lin, A.Y.M. Biological materials: A materials science approach. Journal of the Mechanical Behavior of Biomedical Materials 4(5) (2011): 626-657.

[25] Weiner, S. and Wagner, H.D. THE MATERIAL BONE: Structure-Mechanical Function Relations. Annual Review of Materials Science 28(1) (1998): 271-298.

[26] Rodriguez, N., Alonso, M., Grasa, G., and Abanades, J.C. Heat requirements in a calciner of CaCO3 integrated in a CO2 capture system using CaO. Chemical Engineering Journal 138(1–3) (2008): 148-154.

[27] Boey, P.-L., Maniam, G.P., and Hamid, S.A. Performance of calcium oxide as a heterogeneous catalyst in biodiesel production: A review. Chemical Engineering Journal 168(1) (2011): 15-22.

[28] Kouzu, M., Kasuno, T., Tajika, M., Sugimoto, Y., Yamanaka, S., and Hidaka, J. Calcium oxide as a solid base catalyst for transesterification of soybean oil and its application to biodiesel production. Fuel 87(12) (2008): 2798-2806.

[29] Liu, X., He, H., Wang, Y., Zhu, S., and Piao, X. Transesterification of soybean oil to biodiesel using CaO as a solid base catalyst. Fuel 87(2) (2008): 216-221.

[30] Ferrero, G.O., Almeida, M.F., Alvim-Ferraz, M.C.M., and Dias, J.M. Water-free process for eco-friendly purification of biodiesel obtained using a heterogeneous Ca-based catalyst. Fuel Processing Technology 121 (2014): 114-118.

[31] Nakatani, N., Takamori, H., Takeda, K., and Sakugawa, H. Transesterification of soybean oil using combusted oyster shell waste as a catalyst. Bioresource Technology 100(3) (2009): 1510-1513.

[32] Boey, P.-L., Maniam, G.P., Hamid, S.A., and Ali, D.M.H. Utilization of waste cockle shell (Anadara granosa) in biodiesel production from palm olein: Optimization using response surface methodology. Fuel 90(7) (2011): 2353-2358.

[33] Hu, S., Wang, Y., and Han, H. Utilization of waste freshwater mussel shell as an economic catalyst for biodiesel production. Biomass and Bioenergy 35(8) (2011): 3627-3635.

[34] Nair, P., Singh, B., Upadhyay, S.N., and Sharma, Y.C. Synthesis of biodiesel from low FFA waste frying oil using calcium oxide derived from Mereterix mereterix as a heterogeneous catalyst. Journal of Cleaner Production 29–30 (2012): 82-90.

[35] Boro, J., Konwar, L.J., Thakur, A.J., and Deka, D. Ba doped CaO derived from waste shells of T striatula (TS-CaO) as heterogeneous catalyst for biodiesel production. Fuel 129 (2014): 182-187.

[36] Lee, S.L., Wong, Y.C., Tan, Y.P., and Yew, S.Y. Transesterification of palm oil to biodiesel by using waste obtuse horn shell-derived CaO catalyst. Energy Conversion and Management 93 (2015): 282-288.

[37] Li, F.-J., Li, H.-Q., Wang, L.-G., and Cao, Y. Waste carbide slag as a solid base catalyst for effective synthesis of biodiesel via transesterification of soybean oil with methanol. Fuel Processing Technology 131 (2015): 421-429.

[38] Sirisomboonchai, S., et al. Biodiesel production from waste cooking oil using calcined scallop shell as catalyst. Energy Conversion and Management 95 (2015): 242-247.

[39] Zhu, S., Zhang, Y., Zhang, Y., and Zhang, C. Effect of CaCO3/LiCO3 on the HCl generation of PVC during combustion. Polymer Testing 22(5) (2003): 539-543.

[40] Killner, M.H.M., Garro Linck, Y., Danieli, E., Rohwedder, J.J.R., and Blümich, B. Compact NMR spectroscopy for real-time monitoring of a biodiesel production. Fuel 139 (2015): 240-247.

[41] Margaretha, Y., Prastyo, H., Ayucitra, A., and Ismadji, S. Calcium oxide from Pomacea sp. shell as a catalyst for biodiesel production. International Journal of Energy and Environmental Engineering 3(1) (2012): 1-9.

[42] Suryaputra, W., Winata, I., Indraswati, N., and Ismadji, S. Waste capiz (Amusium cristatum) shell as a new heterogeneous catalyst for biodiesel production. Renewable Energy 50 (2013): 795-799.

[43] Chen, A., Luo, Z., and Akbulut, M. Ionic liquid mediated auto-templating assembly of CaCO3-chitosan hybrid nanoboxes and nanoframes. Chemical Communications 47(8) (2011): 2312-2314.

[44] Yacob, A.R., Noordin, N.P., Sulaiman, N.F., and Mustajab, M.K.A.A. Single Step Transesterification of Palm Oil Using Prepared Calcium Oxide.

[45] Granados, M.L., et al. Biodiesel from sunflower oil by using activated calcium oxide. Applied Catalysis B: Environmental 73(3–4) (2007): 317-326.

[46] Birla, A., Singh, B., Upadhyay, S.N., and Sharma, Y.C. Kinetics studies of synthesis of biodiesel from waste frying oil using a heterogeneous catalyst derived from snail shell. Bioresource Technology 106 (2012): 95-100.

[47] Heinemann, F., Launspach, M., Gries, K., and Fritz, M. Gastropod nacre: Structure, properties and growth — Biological, chemical and physical basics. Biophysical Chemistry 153(2–3) (2011): 126-153.

[48] Checa, A.G., Cartwright, J.H.E., and Willinger, M.-G. Mineral bridges in nacre. Journal of Structural Biology 176(3) (2011): 330-339.

[49] Meyers, M.A., Chen, P.-Y., Lin, A.Y.-M., and Seki, Y. Biological materials: Structure and mechanical properties. Progress in Materials Science 53(1) (2008): 1-206.

[50] Chen, P.Y., et al. Structure and mechanical properties of selected biological materials. Journal of the Mechanical Behavior of Biomedical Materials 1(3) (2008): 208-226.

[51] Chen, G., Shan, R., Li, S., and Shi, J. A biomimetic silicification approach to synthesize CaO–SiO2 catalyst for the transesterification of palm oil into biodiesel. Fuel 153 (2015): 48-55.

[52] Anderson, M.W. and Klinowski, J. Use of Hammett indicators for the study of acidity of zeolite catalysts. Zeolites 6(3) (1986): 150-153.

[53] Staples, P.J. A series of transition metal complex ion indicators for the measurement of Hammett acidity functions. Journal of Inorganic and Nuclear Chemistry 28(10) (1966): 2209-2213.

[54] Maniam, G.P., Hindryawati, N., Nurfitri, I., Manaf, I.S.A., Ramachandran, N., and Rahim, M.H.A. Utilization of waste fat from catfish (Pangasius) in methyl esters preparation using CaO derived from waste marine barnacle and bivalve clam as solid catalysts. Journal of the Taiwan Institute of Chemical Engineers 49 (2015): 58-66.

[55] Maneerung, T., Kawi, S., and Wang, C.-H. Biomass gasification bottom ash as a source of CaO catalyst for biodiesel production via transesterification of palm oil. Energy Conversion and Management 92 (2015): 234-243.

[56] Chen, G., Shan, R., Shi, J., and Yan, B. Ultrasonic-assisted production of biodiesel from transesterification of palm oil over ostrich eggshell-derived CaO catalysts. Bioresource Technology 171 (2014): 428-432.

[57] Bhargava, S.K. and Akolekar, D.B. Adsorption of NO and CO over transition-metal-incorporated mesoporous catalytic materials. Journal of Colloid and Interface Science 281(1) (2005): 171-178.

[58] Vujicic, D., Comic, D., Zarubica, A., Micic, R., and Boskovic, G. Kinetics of biodiesel synthesis from sunflower oil over CaO heterogeneous catalyst. Fuel 89(8) (2010): 2054-2061.

[59] Obadiah, A., Swaroopa, G.A., Kumar, S.V., Jeganathan, K.R., and Ramasubbu, A. Biodiesel production from Palm oil using calcined waste animal bone as catalyst. Bioresource Technology 116 (2012): 512-516.

[60] Choudhury, H.A., Chakma, S., and Moholkar, V.S. Mechanistic insight into sonochemical biodiesel synthesis using heterogeneous base catalyst. Ultrasonics Sonochemistry 21(1) (2014): 169-181.

[61] Yoosuk, B., Udomsap, P., Puttasawat, B., and Krasae, P. Modification of calcite by hydration–dehydration method for heterogeneous biodiesel production process: The effects of water on properties and activity. Chemical Engineering Journal 162(1) (2010): 135-141.

[62] Lertpanyapornchai, B. and Ngamcharussrivichai, C. Mesostructured Sr and Ti mixed oxides as heterogeneous base catalysts for transesterification of palm kernel oil with methanol. Chemical Engineering Journal 264 (2015): 789-796.

[63] Geist, J., Auerswald, K., and Boom, A. Stable carbon isotopes in freshwater mussel shells: Environmental record or marker for metabolic activity? Geochimica et Cosmochimica Acta 69(14) (2005): 3545-3554.

[64] Meyers, M.A., et al. The role of organic intertile layer in abalone nacre. Materials Science and Engineering: C 29(8) (2009): 2398-2410.

[65] Xu, J. and Zhang, G. Unique morphology and gradient arrangement of nacre's platelets in green mussel shells. Materials Science and Engineering: C 52 (2015): 186-193.

[66] Song, F., Soh, A.K., and Bai, Y.L. Structural and mechanical properties of the organic matrix layers of nacre. Biomaterials 24(20) (2003): 3623-3631.

[67] Yang, L., Zhang, A., and Zheng, X. Shrimp Shell Catalyst for Biodiesel Production. Energy & Fuels 23(8) (2009): 3859-3865.

[68] Viriya-empikul, N., Krasae, P., Nualpaeng, W., Yoosuk, B., and Faungnawakij, K. Biodiesel production over Ca-based solid catalysts derived from industrial wastes. Fuel 92(1) (2012): 239-244.

[69] Yu, J., Ge, Q., Fang, W., and Xu, H. Influences of calcination temperature on the efficiency of CaO promotion over CaO modified Pt/γ-Al2O3 catalyst. Applied Catalysis A: General 395(1–2) (2011): 114-119.

[70] Nikulshina, V., Gebald, C., and Steinfeld, A. CO2 capture from atmospheric air via consecutive CaO-carbonation and CaCO3-calcination cycles in a fluidized-bed solar reactor. Chemical Engineering Journal 146(2) (2009): 244-248.

[71] Zhu, Y., Wu, S., and Wang, X. Nano CaO grain characteristics and growth model under calcination. Chemical Engineering Journal 175 (2011): 512-518.

[72] Esipovich, A., Danov, S., Belousov, A., and Rogozhin, A. Improving methods of CaO transesterification activity. Journal of Molecular Catalysis A: Chemical 395 (2014): 225-233.

[73] Gnanaprakasam, A., Sivakumar, V.M., Surendhar, A., Thirumarimurugan, M., and Kannadasan, T. Recent Strategy of Biodiesel Production from Waste Cooking Oil and Process Influencing Parameters: A Review. Journal of Energy 2013 (2013): 10.

[74] 04/02862 Effects of water on biodiesel fuel production bysupercritical methanol treatment: Kusdiana, D. and Saka, S. Bioresource Technology, 2004, 91, (3), 289–295. Fuel and Energy Abstracts 45(6) (2004): 404.

[75] Atadashi, I.M., Aroua, M.K., Abdul Aziz, A.R., and Sulaiman, N.M.N. Production of biodiesel using high free fatty acid feedstocks. Renewable and Sustainable Energy Reviews 16(5) (2012): 3275-3285.

[76] Vicente, G., Martínez, M., Aracil, J., and Esteban, A. Kinetics of Sunflower Oil Methanolysis. Industrial & Engineering Chemistry Research 44(15) (2005): 5447-5454.

[77] Jung, S.-M., Park, Y.-C., and Park, K. Effects of environmental conditions and methanol feeding strategy on lipase-mediated biodiesel production using soybean oil. Biotechnology and Bioprocess Engineering 15(4) (2010): 614-619.

[78] Tang, Y., Xu, J., Zhang, J., and Lu, Y. Biodiesel production from vegetable oil by using modified CaO as solid basic catalysts. Journal of Cleaner Production 42 (2013): 198-203.

[79] Kouzu, M., Kasuno, T., Tajika, M., Yamanaka, S., and Hidaka, J. Active phase of calcium oxide used as solid base catalyst for transesterification of soybean oil with refluxing methanol. Applied Catalysis A: General 334(1–2) (2008): 357-365.

[80] Knothe, G. and Steidley, K.R. Kinematic viscosity of biodiesel fuel components and related compounds. Influence of compound structure and comparison to petrodiesel fuel components. Fuel 84(9) (2005): 1059-1065.

[81] Mahajan, S., Konar, S., and Boocock, D.B. Variables Affecting the Production of Standard Biodiesel. Journal of the American Oil Chemists' Society 84(2) (2007): 189-195.

[82] Cunha Jr, A., Feddern, V., De Prá, M.C., Higarashi, M.M., de Abreu, P.G., and Coldebella, A. Synthesis and characterization of ethylic biodiesel from animal fat wastes. Fuel 105 (2013): 228-234.

[83] Melero, J.A., Vicente, G., Morales, G., Paniagua, M., and Bustamante, J. Oxygenated compounds derived from glycerol for biodiesel formulation: Influence on EN 14214 quality parameters. Fuel 89(8) (2010): 2011-2018.

[84] ASTM D5555-Standard Test Method for Determination of Free Fatty Acids Contained in Animal, Marine, and Vegetable Fats and Oils Used in Fat Liquors and Stuffing Compounds. 15.04 (2011).

[85] ASTM D5558- Standard Test Method for Determination of the Saponification Value of Fats and Oils. 15.04 (2011).

[86] Shirazi, M.M.A., et al. Acceleration of biodiesel–glycerol decantation through NaCl-assisted gravitational settling: A strategy to economize biodiesel production. Bioresource Technology 134 (2013): 401-406.

# APPENDIX A

# $^{1}$H-NMR, $^{13}$C-NMR SPECTRUM AND GC CHOMATOGRAMS OF REFINED PALM OIL AND BIODIESEL (METHYL ESTER)

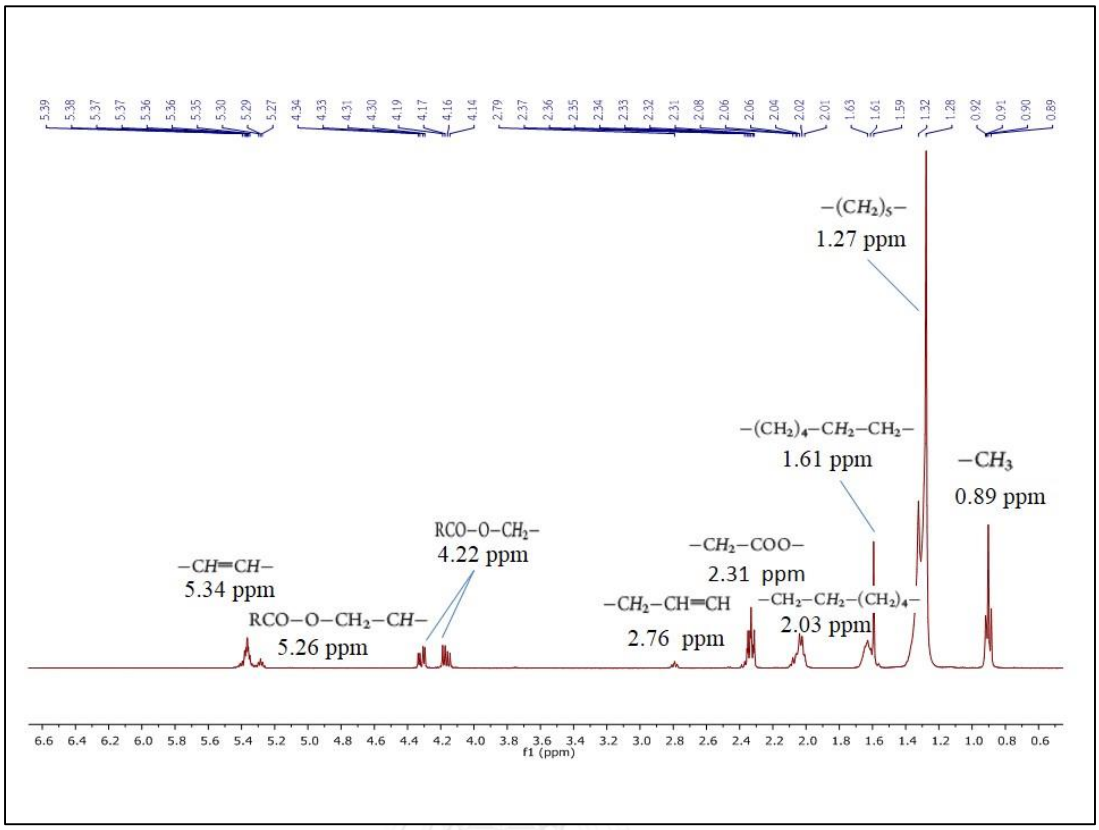


**Figure A1** $^{1}$H-NMR spectrum of triglyceride from refined palm oil.

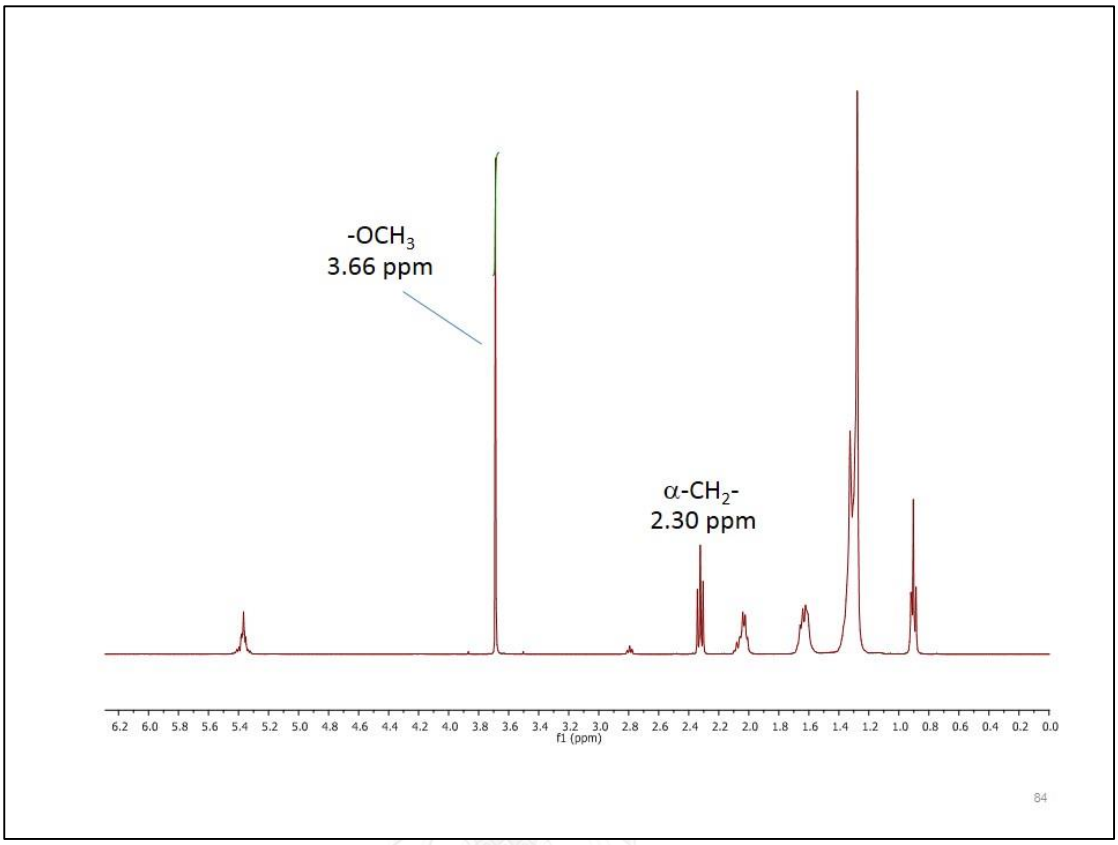


**Figure A2** $^{1}$H-NMR spectrum of fatty acid methyl ester (FAME) from refined palm oil**.**

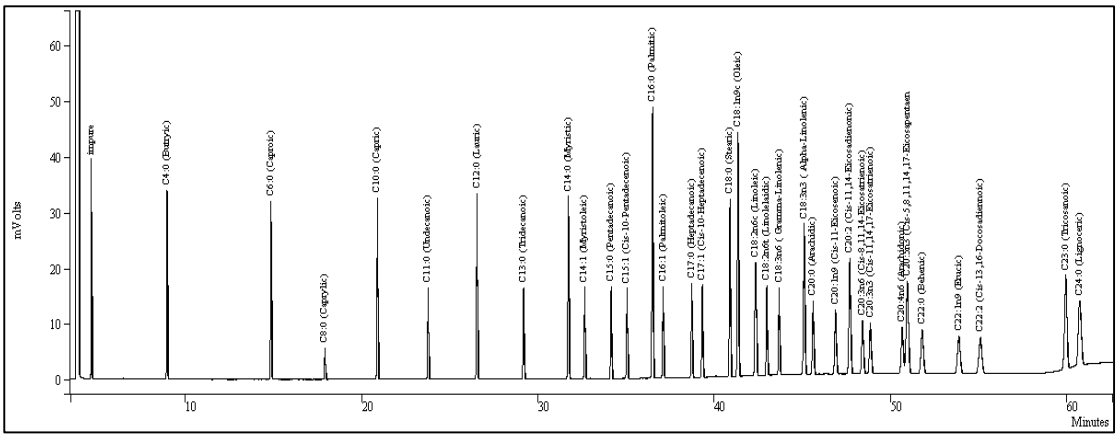


| Peak No | Peak Name | Result () | Ret Time (min) | Time Offset (min) | Peak Area (counts) | Rel Ret Time | Sep. Code | Width 1/2 (sec) | Status Codes | Group |
|---|---|---|---|---|---|---|---|---|---|---|
| 1 | impure | 2.2697 | 4.637 | -0.000 | 78226 | 0.00 | BB | 1.8 | | 0 |
| 2 | C4:0 (Butryic) | 2.7498 | 8.931 | -0.000 | 94774 | 0.00 | BB | 2.6 | | 0 |
| 3 | C6:0 (Caproic) | 3.1322 | 14.830 | -0.000 | 107956 | 0.00 | BB | 3.2 | | 0 |
| 4 | C8:0 (Caprylic) | 0.6165 | 17.894 | 0.000 | 21249 | 0.00 | BB | 3.5 | | 0 |
| 5 | C10:0 (Capric) | 3.5082 | 20.876 | -0.000 | 120914 | 0.00 | BB | 3.5 | | 0 |
| 6 | C11:0 (Undecanoic) | 1.8114 | 23.753 | -0.000 | 62431 | 0.00 | BB | 3.6 | | 0 |
| 7 | C12:0 (Lauric) | 3.7958 | 26.526 | -0.000 | 130825 | 0.00 | BB | 3.7 | | 0 |
| 8 | C13:0 (Tridecanoic) | 1.9202 | 29.168 | 0.000 | 66181 | 0.00 | BB | 3.8 | | 0 |
| 9 | C14:0 (Myristic) | 3.9527 | 31.714 | -0.000 | 136235 | 0.00 | BB | 3.9 | | 0 |
| 10 | C14:1 (Myristoleic) | 1.9769 | 32.640 | -0.000 | 68135 | 0.00 | BP | 3.9 | | 0 |
| 11 | C15:0 (Pentadecanoic) | 2.0181 | 34.139 | 0.000 | 69557 | 0.00 | BB | 4.0 | | 0 |
| 12 | C15:1 (Cis-10-Pentadecenoic) | 2.0018 | 35.044 | -0.000 | 68995 | 0.00 | BB | 4.0 | | 0 |
| 13 | C16:0 (Palmitic) | 6.1738 | 36.490 | 0.000 | 212786 | 0.00 | BB | 4.1 | | 0 |
| 14 | C16:1 (Palmitoleic) | 2.0735 | 37.090 | -0.000 | 71464 | 0.00 | BB | 4.1 | | 0 |
| 15 | C17:0 (Heptadecanoic) | 2.1447 | 38.716 | 0.000 | 73919 | 0.00 | BB | 4.1 | | 0 |
| 16 | C17:1 (Cis-10-Heptadecenoic) | 2.1090 | 39.312 | -0.000 | 72687 | 0.00 | BB | 4.1 | | 0 |
| 17 | C18:0 (Stearic) | 4.2376 | 40.885 | -0.000 | 146051 | 0.00 | BB | 4.3 | | 0 |
| 18 | C18:1n9c (Oleic) | 6.3372 | 41.339 | 0.000 | 218416 | 0.00 | BB | 4.7 | | 0 |
| 19 | C18:2n6c (Linoleic) | 4.1562 | 42.339 | 0.000 | 143248 | 0.00 | BP | 6.9 | | 0 |
| 20 | C18:2n6t (Linolelaidic) | 2.0821 | 42.974 | 0.000 | 71762 | 0.00 | VB | 4.2 | | 0 |
| 21 | C18:3n6 ( Gramma-Linolenic) | 2.1318 | 43.674 | -0.000 | 73475 | 0.00 | BB | 4.3 | | 0 |
| 22 | C18:3n3 ( Alpha-Linolenic) | 4.4137 | 45.097 | -0.000 | 152122 | 0.00 | BB | 5.3 | | 0 |
| 23 | C20:0 (Arachidic) | 2.1830 | 45.603 | 0.000 | 75241 | 0.00 | BP | 5.4 | | 0 |
| 24 | C20:1n9 (Cis-11-Eicosenoic) | 2.1410 | 46.875 | 0.000 | 73792 | 0.00 | BB | 6.0 | | 0 |
| 25 | C20:2 | 4.2043 | 47.685 | 0.000 | 144903 | 0.00 | BB | 6.6 | | 0 |
| 26 | C20:3n6 | 2.0262 | 48.411 | -0.000 | 69835 | 0.00 | BV | 6.8 | | 0 |
| 27 | C20:3n3 | 1.9834 | 48.852 | -0.000 | 68361 | 0.00 | VB | 7.0 | | 0 |
| 28 | C20:4n6 (Arachidonic) | 2.0424 | 50.661 | -0.000 | 70394 | 0.00 | BV | 7.9 | | 0 |
| 29 | C20:5n3 | 4.4978 | 50.958 | 0.000 | 155020 | 0.00 | VB | 8.8 | | 0 |
| 30 | C22:0 (Behenic) | 2.2171 | 51.795 | -0.000 | 76415 | 0.00 | BB | 9.1 | | 0 |
| 31 | C22:1n9 (Erucic) | 2.1608 | 53.876 | 0.000 | 74474 | 0.00 | BB | 10.4 | | 0 |
| 32 | C22:2 | 2.2696 | 55.102 | -0.000 | 78223 | 0.00 | BB | 11.3 | | 0 |
| 33 | C23:0 (Tricosanoic) | 4.3861 | 59.946 | -0.000 | 151170 | 0.00 | BV | 9.2 | | 0 |
| 34 | C24:0 (Lignoceric) | 4.2754 | 60.729 | 0.000 | 147355 | 0.00 | VV | 12.6 | | 0 |
| | **Totals** | **100.0000** | | **0.000** | **3446591** | | | | | |

**Figure A3** GC chromatogram of 37 FAME stand.

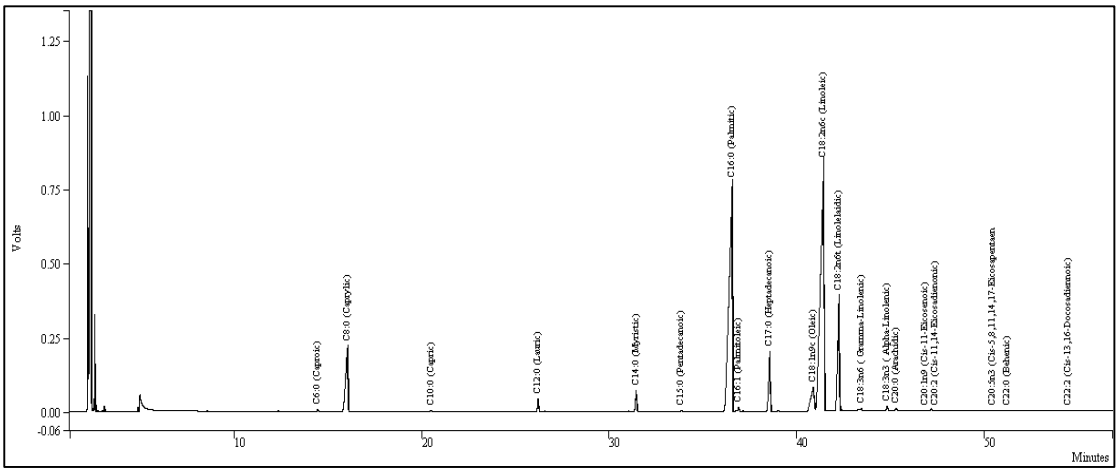


| Peak No | Peak Name | Result () | Ret Time (min) | Time Offset (min) | Peak Area (counts) | Rel Ret Time | Sep. Code | Width 1/2 (sec) | Status Codes | Group |
|---|---|---|---|---|---|---|---|---|---|---|
| 1 | C6:0 (Caproic) | 0.0729 | 14.452 | 0.011 | 20688 | 0.00 | BB | 3.3 | | 0 |
| 2 | C8:0 (Caprylic) | 7.1835 | 16.058 | 0.002 | 2039776 | 0.00 | PB | 9.1 | | 0 |
| 3 | C10:0 (Capric) | 0.0483 | 20.506 | 0.002 | 13705 | 0.00 | BB | 3.7 | | 0 |
| 4 | C12:0 (Lauric) | 0.5966 | 26.199 | 0.021 | 169405 | 0.00 | PB | 3.8 | | 0 |
| 5 | C14:0 (Myristic) | 1.1041 | 31.429 | 0.040 | 313501 | 0.00 | VP | 4.1 | | 0 |
| 6 | C15:0 (Pentadecanoic) | 0.0433 | 33.843 | 0.017 | 12281 | 0.00 | BV | 4.1 | | 0 |
| 7 | C16:0 (Palmitic) | 33.6955 | 36.554 | 0.010 | 9567981 | 0.00 | BP | 12.2 | | 0 |
| 8 | C16:1 (Palmitoleic) | 0.1943 | 36.901 | 0.116 | 55181 | 0.00 | TF | 0.0 | | 0 |
| 9 | C17:0 (Heptadecanoic) | 4.0464 | 38.553 | 0.131 | 1149000 | 0.00 | BV | 5.4 | | 0 |
| 10 | C18:1n9c (Oleic) | 3.5689 | 40.874 | -0.172 | 1013415 | 0.00 | VV | 12.0 | | 0 |
| 11 | C18:2n6c (Linoleic) | 38.8567 | 41.429 | 0.012 | 11033540 | 0.00 | VV | 12.7 | | 0 |
| 12 | C18:2n6t (Linolelaidic) | 9.3619 | 42.244 | 0.000 | 2658351 | 0.00 | VB | 6.2 | | 0 |
| 13 | C18:3n6 ( Gramma-Linolenic) | 0.1782 | 43.443 | 0.050 | 50587 | 0.00 | TF | 0.0 | | 0 |
| 14 | C18:3n3 ( Alpha-Linolenic) | 0.3248 | 44.815 | 0.041 | 92221 | 0.00 | TF | 0.0 | | 0 |
| 15 | C20:0 (Arachidic) | 0.2357 | 45.302 | 0.034 | 66942 | 0.00 | TF | 0.0 | | 0 |
| 16 | C20:1n9 (Cis-11-Eicosenoic) | 0.0529 | 46.840 | 0.336 | 15025 | 0.00 | TF | 0.0 | | 0 |
| 17 | C20:2 | 0.0545 | 47.397 | 0.108 | 15487 | 0.00 | TF | 0.0 | | 0 |
| 18 | C20:5n3 | 0.1072 | 50.448 | -0.005 | 30441 | 0.00 | VV | 10.1 | | 0 |
| 19 | C22:0 (Behenic) | 0.1220 | 51.207 | -0.062 | 34629 | 0.00 | VV | 9.8 | | 0 |
| 20 | C22:2 | 0.1524 | 54.493 | 0.026 | 43275 | 0.00 | PV | 12.3 | | 0 |
| | **Totals** | **100.0001** | | **0.718** | **28395432** | | | | | |

**Figure A4** GC chromatogram of palm oil methyl ester.

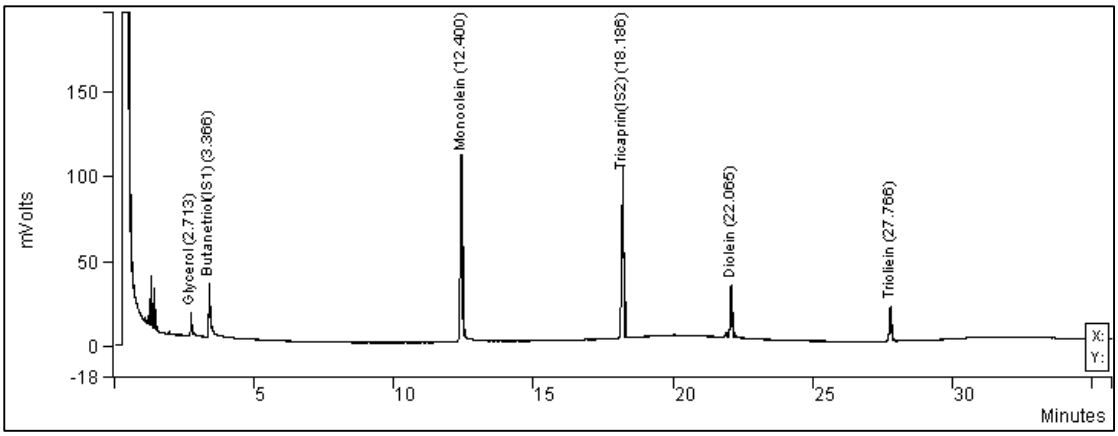


| Peak No | Peak Name | Result () | Ret Time (min) | Time Offset (min) | Peak Area (counts) | Rel Ret Time | Sep. Code | Width 1/2 (sec) | Status Codes | Group |
|---|---|---|---|---|---|---|---|---|---|---|
| 1 | Glycerol | 2.7003 | 2.713 | -0.002 | 37959 | 0.00 | BB | 2.1 | | 0 |
| 2 | Butanetriol(IS1) | 7.8658 | 3.366 | -0.001 | 110574 | 0.00 | BB | 2.5 | | 0 |
| 3 | Monoolein | 38.1313 | 12.400 | -0.001 | 536031 | 0.00 | BB | 4.4 | | 0 |
| 4 | Tricaprin(IS2) | 34.9182 | 18.186 | -0.001 | 490864 | 0.00 | BB | 4.5 | | 0 |
| 5 | Diolein | 9.6609 | 22.065 | 0.002 | 135809 | 0.00 | VB | 4.1 | | 0 |
| 6 | Triolein | 6.7235 | 27.766 | -0.002 | 94516 | 0.00 | BB | 4.4 | | 0 |
| | **Totals** | **100.0000** | | **-0.005** | **1405753** | | | | | |

**Figure A5** GC chromatogram of standard for EN 14105 methid.

# APPENDIX B

## VALUES OF FREE FATTY ACID, SAPONIFICATION NUMBER AND METHYL ESTER CONTAINT

**B1. Calculation of the % free fatty acid (ASTM D5555) [84]**

**Reagents**

1. Ethanol ($CH_3CH_2OH$)
2. Phenolphthalein indicator
3. 0.25 N Sodium hydroxide solution (NaOH)

The 1 g of refined palm oil sample and 75 mL of ethanol were loaded into a 250 mL of Erlenmeyer flask. The mixture was stirred by magnetic bar at room temperature until homogeneous mixture was obtained. The approximately 2 mL of 1 wt. % phenolphthalein as indicator was added before the homogeneous mixture was carried to titrate with 0.25 N sodium hydroxide (NaOH) solution until the pink colour appeared in the system. The volume (mL) of sodium hydroxide solution used was recorded.

The percentage of free fatty acids was calculated as follows:

% free fatty acids (% FFA) = (Volume (mL) of NaOH solution x *N* x 28.2) / weight of sample

*N* = normality of NaOH solution

**Table B1** Value of free fatty acids contain in refined palm oil.

| Sample | Weight of sample (g) | Volume of titrant (mL) | Concentration of NaOH (N) | Average free fatty acid (%FFA) |
|---|---|---|---|---|
| Refined palm oil | 1.0018 | 0.10 | 0.248 | 0.69 |
| | 1.0010 | 0.10 | 0.248 | |
| | 1.0012 | 0.10 | 0.248 | |

**B2. Determination of the Saponification value (ASTM D5558) [85]**

**Reagents**

1. Phenolphthalein
2. Alcoholic KOH solution
3. 0.5 N hydrochloric acid (HCl)

The 1 g of refined palm oil sample, 25 mL of alcoholic potassium hydroxide solution and 1 mL of 1 wt. % phenolphthalein indicator was loaded into a 250 mL of Erlenmeyer flask and stirred at room temperature until the homogenous mixture was obtained. The homogenous mixture was subject to titrate with 0.5 N of hydrochloric acid (HCl) solution until the pink colour has vanished from the system. Next, the blank was prepared for determination and carried out under condition with the identical sample. Finally, the volume (mL) of 0.5 N HCl solution used was recorded.

The saponification value was calculated as follows:

Saponification value = $56.1 \times N \times (A - B) /$ weight of sample

$A$ = titration of blank (mL)

$B$ = titration of sample (mL)

$N$ = normality of hydrochloric acid solution

Alcoholic KOH = 40 g of potassium hydroxide dissolved in 1 L of ethanol

**Table B2** Saponification value of refined palm oil.

| Sample | Weight of sample (g) | Volume of titrant (mL) | Volume of blank (mL) | SN[a] |
|---|---|---|---|---|
| Refined palm oil | 1.0026 | 21.75 | 28.95 | 196.59 |
| | 1.0021 | 21.75 | 28.95 | |
| | 1.0023 | 21.75 | 28.95 | |

a = 0.4892 N

**B3.** Calculation of % methyl ester contain in synthesized biodiesel by using chromatogram GC data [86].

The % methyl ester content in synthesized biodiesel, by using heterogeneous CaO-EGMShell and $Ca(OH)_2$-EGMShell catalyst via transesterification, were calculated as follow below:

$$\%C = \frac{(\Sigma A - Ai)}{Ai} x \frac{(CixVi)}{m} x\ 100\%$$

When the parameter is;

| | | |
|---|---|---|
| C | = | Methyl ester content in biodiesel |
| $\sum$A | = | Total area of fatty acid methyl esters |
| Ai | = | Area of methyl heptadecanoate as internal standard (IS) |
| Ci | = | Concentration of methyl ester heptadecanoate solution (mg/mL) |
| Vi | = | Volume of methyl heptadecanoate solution (mL) |
| m | = | Mass of biodiesel sample |



**B4.** Example for calculation of % methyl ester contain in synthesized biodiesel.

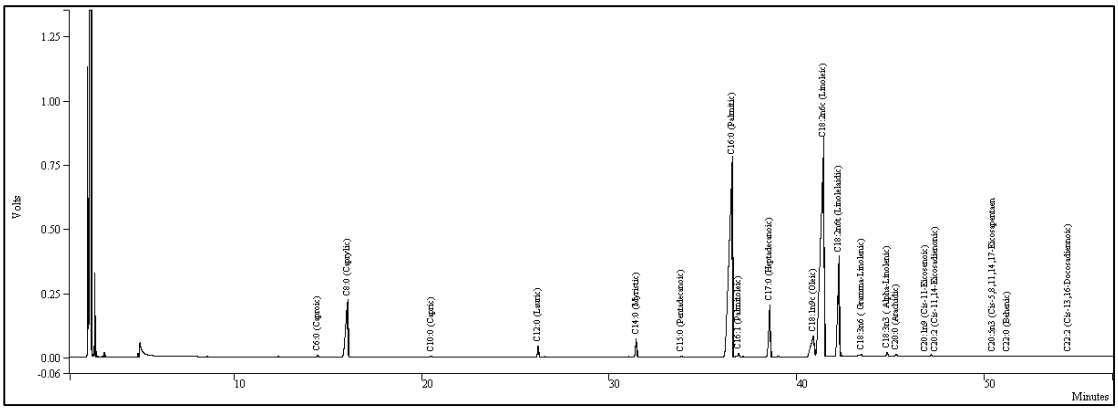

| Peak No | Peak Name | Result () | Ret Time (min) | Time Offset (min) | Peak Area (counts) | Rel Ret Time | Sep. Code | Width 1/2 (sec) | Status Codes | Group |
|---|---|---|---|---|---|---|---|---|---|---|
| 1 | C6:0 (Caproic) | 0.0729 | 14.452 | 0.011 | 20688 | 0.00 | BB | 3.3 | | 0 |
| 2 | C8:0 (Caprylic) | 7.1835 | 16.058 | 0.002 | 2039776 | 0.00 | PB | 9.1 | | 0 |
| 3 | C10:0 (Capric) | 0.0483 | 20.506 | 0.002 | 13705 | 0.00 | BB | 3.7 | | 0 |
| 4 | C12:0 (Lauric) | 0.5966 | 26.199 | 0.021 | 169405 | 0.00 | PB | 3.8 | | 0 |
| 5 | C14:0 (Myristic) | 1.1041 | 31.429 | 0.040 | 313501 | 0.00 | VP | 4.1 | | 0 |
| 6 | C15:0 (Pentadecanoic) | 0.0433 | 33.843 | 0.017 | 12281 | 0.00 | BV | 4.1 | | 0 |
| 7 | C16:0 (Palmitic) | 33.6955 | 36.554 | 0.010 | 9567981 | 0.00 | BP | 12.2 | | 0 |
| 8 | C16:1 (Palmitoleic) | 0.1943 | 36.901 | 0.116 | 55181 | 0.00 | TF | 0.0 | | 0 |
| 9 | C17:0 (Heptadecanoic) | 4.0464 | 38.553 | 0.131 | 1149000 | 0.00 | BV | 5.4 | | 0 |
| 10 | C18:1n9c (Oleic) | 3.5689 | 40.874 | -0.172 | 1013415 | 0.00 | VV | 12.0 | | 0 |
| 11 | C18:2n6c (Linoleic) | 38.8567 | 41.429 | 0.012 | 11033540 | 0.00 | VV | 12.7 | | 0 |
| 12 | C18:2n6t (Linolelaidic) | 9.3619 | 42.244 | 0.000 | 2658351 | 0.00 | VB | 6.2 | | 0 |
| 13 | C18:3n6 (Gramma-Linolenic) | 0.1782 | 43.443 | 0.050 | 50587 | 0.00 | TF | 0.0 | | 0 |
| 14 | C18:3n3 (Alpha-Linolenic) | 0.3248 | 44.815 | 0.041 | 92221 | 0.00 | TF | 0.0 | | 0 |
| 15 | C20:0 (Arachidic) | 0.2357 | 45.302 | 0.034 | 66942 | 0.00 | TF | 0.0 | | 0 |
| 16 | C20:1n9 (Cis-11-Eicosenoic) | 0.0529 | 46.840 | 0.336 | 15025 | 0.00 | TF | 0.0 | | 0 |
| 17 | C20:2 | 0.0545 | 47.397 | 0.108 | 15487 | 0.00 | TF | 0.0 | | 0 |
| 18 | C20:5n3 | 0.1072 | 50.448 | -0.005 | 30441 | 0.00 | VV | 10.1 | | 0 |
| 19 | C22:0 (Behenic) | 0.1220 | 51.207 | -0.062 | 34629 | 0.00 | VV | 9.8 | | 0 |
| 20 | C22:2 | 0.1524 | 54.493 | 0.026 | 43275 | 0.00 | PV | 12.3 | | 0 |
| | **Totals** | **100.0001** | | **0.718** | **28395432** | | | | | |

**Example for calculation**

$$\% \text{ Ester content} = \frac{(28395432-1149000)}{1149000} \times \frac{(102.65 \text{ mg} \times 1 \text{ mL})}{10 \text{ mL} \times 250.12 \text{ mg}} \times 100$$

% Ester content = 97.32 %

**B4.** Calculation of % methyl ester contain in synthesized biodiesel by using $^{1}$H-NMR spectrum [40].

The % conversion of palm oil convert to biodiesel using heterogeneous CaO-EGMShell and $Ca(OH)_2$-EGMShell catalyst via transesterification, was calculated as follow:

$$\% \text{ Conversion} = [(2A_{Me})/ (3A_{CH2})] \times 100 \%$$

Where $A_{Me}$ is the integration of the area under the curve at 3.6-3.7 ppm, which is corresponding to the methoxy protons of the FAMEs or biodiesel, and $A_{CH2}$ is the integration of the area under the curve at 2.2-2.3 ppm, which is corresponding to $\alpha$-methylene protons from triglycerides in the starting oil.

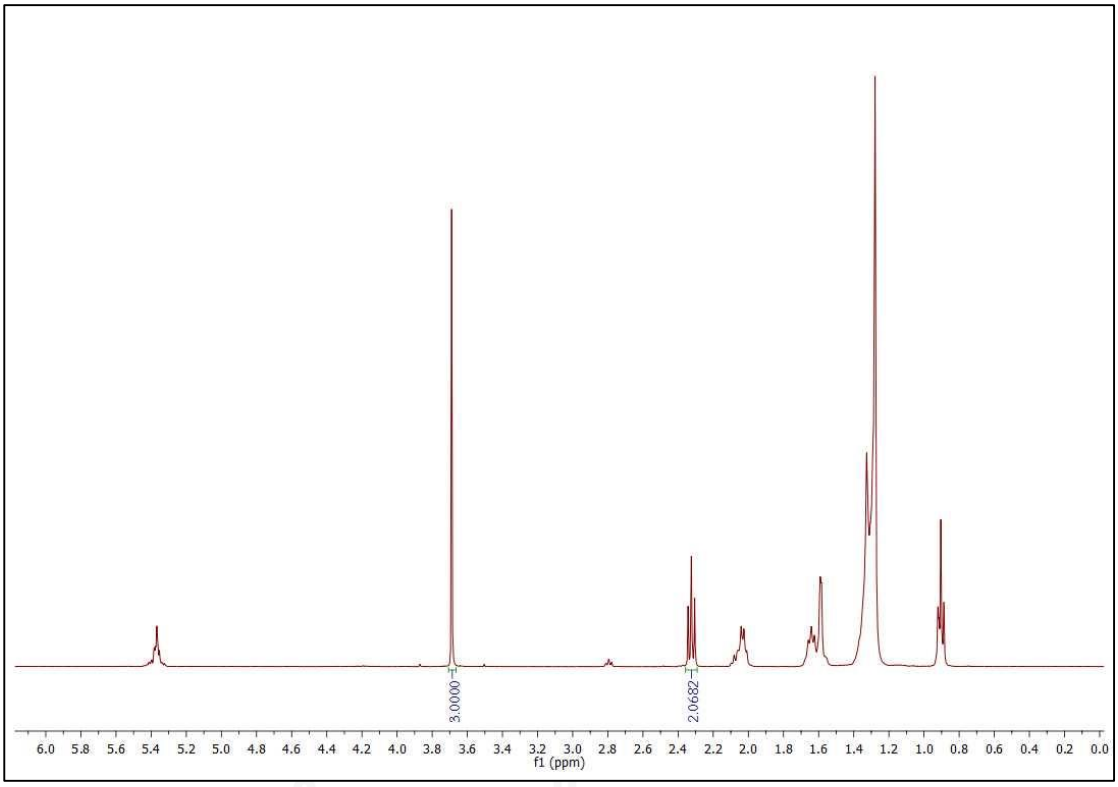




**Example for calculation**

$$\% \text{ Conversion} = \frac{2A_{\text{CH3 at 3.65 ppm}}}{3A_{\alpha\text{-CH2 at 2.31 ppm}}} \times 100$$

$$\% \text{ Conversion rate} = \frac{2 \times (3.000)}{3 \times (2.0499)} \times 100\ \%$$

$$\% \text{ Conversion rate} = 97.57\ \%$$

# APPENDIX C

## MECHANISM OF TRANSESTERIFICATION BY USING CaO-EGMShell AND $Ca(OH)_2$-EGMShell FOR SYNTHESIZED BIODIESEL

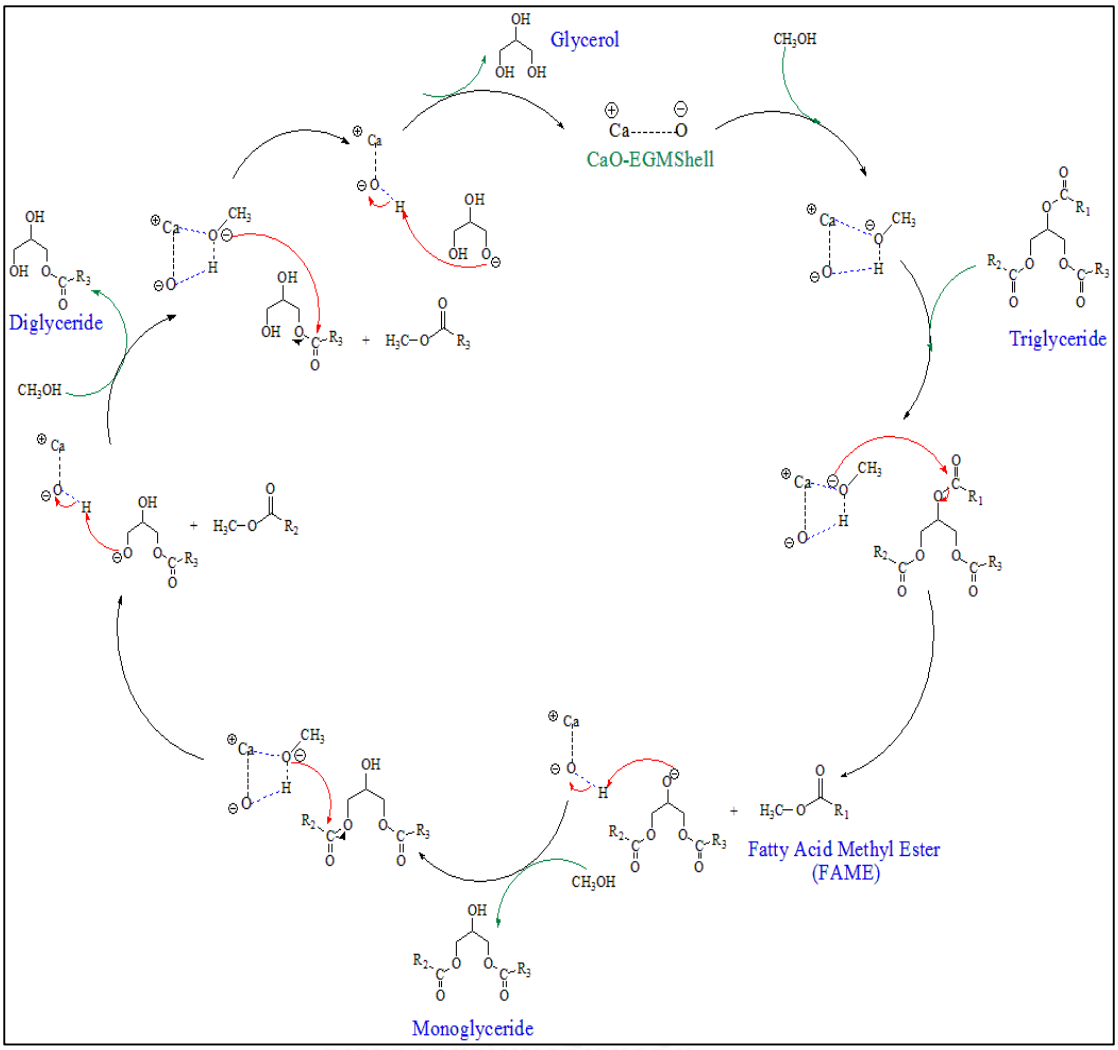




**Figure C1** Mechanism between triglyceride and methanol in transesterification using CaO-EGMshell as catalyst.

**Step 1**: The $Ca(OH)_2$-EGMShell catalyst were refluxed with methanol then the methoxide ions ($CH_3O^-$) were generated on surface of $Ca(OH)_2$-EGMShell catalyst catalyst.

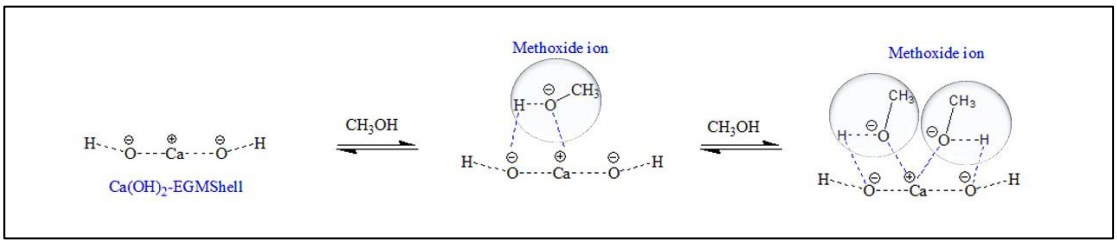


**Step 2**: The triglyceride reacts with methoxide ions in the system. After the reaction finished, the fatty acid methyl ester (FAME) and the glycerol as by-product were generated.

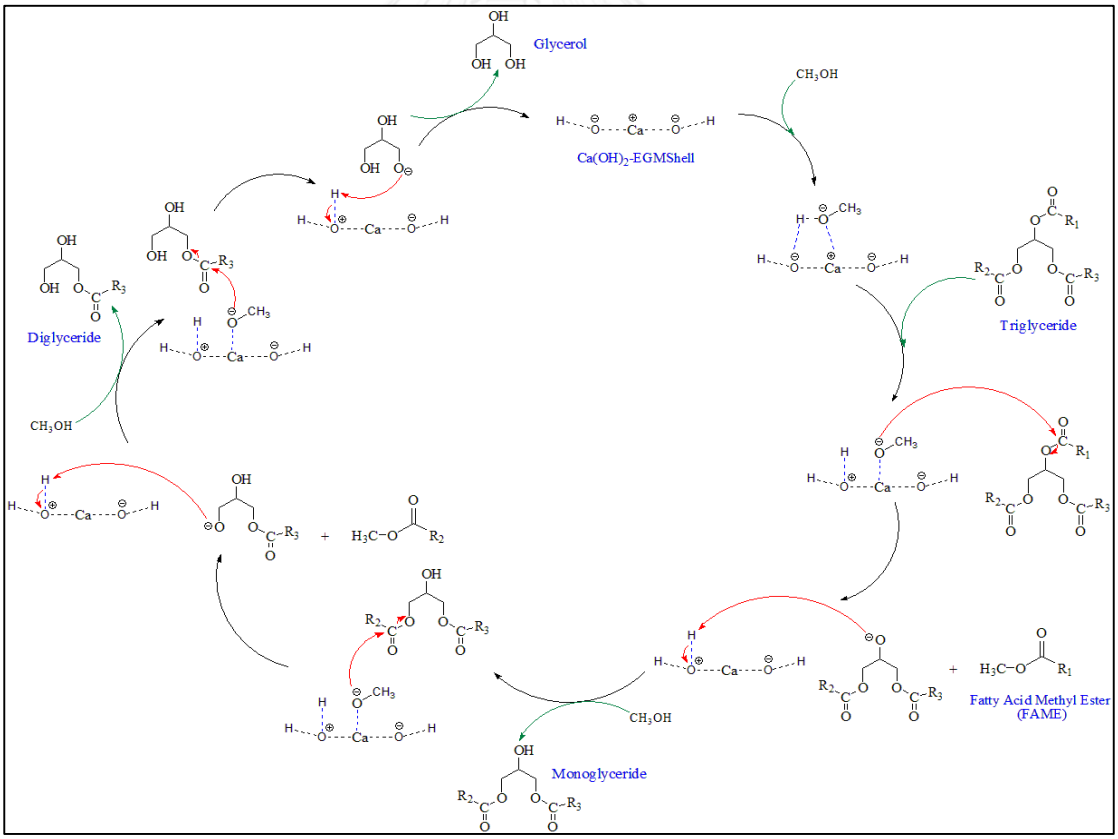


**Figure C2** Mechanism between triglyceride and methanol in transesterification using $Ca(OH)_2$-EGMshell as catalyst.

# VITA

Mr. Korakot Niyomsat was born on Apirl 8th, 1988 in Chanthaburi, Thaland. He graduated with High School degree at Benjamanusorn School in 2007. He received the Bachelor of Science degree from the Department of Chemistry, Faculty of Science, Burapha University, Chonburi in 2011. In 2012, he started studying in in a Master degree program, majoring in Inorganic Chemistry at the Department of Chemistry, Faculty of Science, Chulalongkorn University, Bangkok. He received scholarship from the 90th Anniversary of Chulalongkorn University Fund (Ratchadaphiseksomphot Endowment Fund). He successfully graduated with M.Sc. Degree in Chemistry in the academic year 2015.

Conferences attended;

1). Oral presentation, 12-14 November 2014 in the topic “Innovative Processes for the Production of Calcium Oxide Catalyst for Biodiesel Production from Wasted Green-Mussel Shell” at the Congress on the 7th Thailand Renewable Energy for Community Conference (TREC-7) at Rajamangala University of Technology Rattanakosin, Wangkraikangwon Campus, Amphoe Hua Hin, Prachuap Khiri Khan, Thailand.

2). Poster presentation, 15-16 December 2014, in the topic of “High Performance Calcium Hydroxide Catalyst from Waste Green-mussel Shell for Biodiesel Production” at the Congress on the 8th International Conference on Materials Science and Technology (MSAT-8) at Swissotel Le Concorde, Bangkok, Thailand.